

Design and Implementation of Anti-collision Algorithms for Dense RFID Systems

**Der Technischen Fakultät der Universität Erlangen-Nürnberg
zur Erlangung des Grades**

DOKTOR-INGENIEUR

vorgelegt von

Hazem Abdelaal Ahmed Elsaid Ibrahim

Supervisor

Prof. Dr.-Ing. Albert Heuberger

February 4, 2018

Abstract

Radio Frequency Identification (RFID) is a rapidly emerging technology that wirelessly transmits the identification of transponders (tags) attached to an object or a person. The RFID technology attracted more attention since the adoption of the EPCglobal Class 1 Gen 2 standard in 2005. It has replaced other automatic identification systems like barcodes in some applications, e.g., logistics. In such applications, the identification time is a very critical performance parameter. Currently, developments are underway in various areas of RFID to decrease the total identification time for a massive number of tags. This thesis focuses on passive Ultra High Frequency (UHF) RFID, whose transmission on the Medium Access Control (MAC) layer is scheduled by Framed Slotted Aloha (FSA). Conventional FSA regards only the reply of a single tag as a successful slot. Empty and collided slots are considered as losses. Therefore, the reading efficiency is limited due to empty and collided slots. Modern physical layer systems have the capability of converting part of the collided slots into successful slots. This capability is called “Collision Recovery”. Moreover, modern RFID readers can identify the type of slot, e.g., successful, collided, or empty. In addition, the readers are able to terminate a slot earlier upon recognizing that it is empty. This capability is called “Time-Aware”. The performance of the FSA depends strongly on two main parameters, the precise estimation of the number of tags in the reading area, and the optimizations of the FSA frame length.

In this thesis, a new tag estimation method is introduced, taking into consideration the collision recovery capability of modern RFID systems. The proposed method provides the advantage of giving a novel closed form solution for the tag population estimator, which considers the collision recovery probability of the used system. Simulation results indicate that the proposed solution is more accurate when it is compared to state-of-the-art.

Apart from that, closed form solutions for the optimum FSA frame length using different scenarios are calculated. The first scenario is the Time-Aware Framed Slotted ALOHA. It considers the differences in slots durations without collision recovery capability. The second scenario is the Time-Aware with constant collision recovery coefficients system. The proposed method provides a new closed form equation for the frame length considering the different slot durations and the collision recovery capability with equal coefficients. Moreover, a new calculation method of the collision recovery probability per frame is presented. In the third scenario, the multiple collision recovery coefficients system is introduced. There, the differences in the collision recovery probability coefficients are examined with equal slots durations. In this regard, the values of the collision recovery coefficients are extracted from the physical layer parameters. Finally, a Time-aware and multiple collision recovery system is

proposed. It considers the multiple collision recovery probability coefficients in addition to the different slot durations. For each scenario, timing comparisons between the proposed formulas and the state-of-the-art are presented.

This thesis focuses on the EPCglobal C1 G2 standard. Therefore, the tags cannot be modified, and all the improvements are done only on the reader side. However, due to the limitation of the EPCglobal C1 G2, there is still a room of improvement between the proposed solutions and the theoretical lower bound of the identification time. Accordingly, compatible improvements of the EPCglobal C1 G2 standard are proposed. This proposal includes compatible modifications in the UHF RFID tags/readers, to be capable of acknowledging more than a single tag per slot. Finally, the obtained results demonstrate that the proposed system optimizations lead to tags identification in a significantly shorter time, which is crucial for time-sensitive applications.

Contents

1	Introduction	1
1.1	Motivation	1
1.2	Thesis Contribution	3
1.3	Document Outline	4
2	Background and Literature Review	7
2.1	Historical Development of RFID	7
2.2	System Components	8
2.3	Frequency Bands	10
2.4	Collision Problems	11
3	RFID Anti-collision Protocols	15
3.1	PHY-Layer Anti-collision Protocols	15
3.2	MAC-Layer Anti-collision Protocols	16
3.3	DFSA with EPCglobal C1G2	23
3.4	Cross Layer Anti-Collision Protocol	25
4	Estimation of the Tag Population	31
4.1	State-of-the-Art Estimation Algorithms	31
4.2	Novel Collision Recovery Aware Tag Estimation	37
5	Frame Length Optimization	49
5.1	Time Aware System	50
5.2	Time and Collision Recovery System	58
5.3	Multiple Collision Recovery System	63
5.4	Time and Multiple Collision Recovery System	70
5.5	Comparison of the Proposed Algorithms	76
6	Improvements of the EPCglobal C1 G2	81
6.1	EPCglobal C1 G2 Reading Process	82
6.2	Proposed System Description	83
6.3	Performance Analysis	88
6.4	Measurement and Simulation Results	90

7 Conclusions and Future Work	95
7.1 Conclusions	96
7.2 Open Issues and Future Work	97
Bibliography	107

Chapter 1

Introduction

Radio Frequency Identification (RFID) is a technology that uses communication through radio waves to transfer data between a reader and electronic tags attached to an object, either to be identified or tracked. The RFID technology has benefits in reference to other identification technologies [1], such as no line-of-sight connection, fully automotive identification process, robustness, identification speed, and secured communication. Thus, RFID became the optimum solution for several applications where other identification technologies like bar-codes are unsuitable, e.g. inventory tracking, supply chain management, automated manufacturing, etc. [2–4]. Due to the crucial significance of the RFID system in different real-world applications, they have received large attention from both research groups and industry. Recently, a lot of work has been published in the area of RFID systems whether in hardware and software design, or in protocols and applications [5–7]. This chapter presents the research motivation along with the contributions and the outline of the thesis.

1.1 Motivation

During the past few years, the number of applications that use RFID has increased, and will potentially further grow in the near future. One of these applications is logistics, where, for example, many tags (transponders) are closely placed on pallets. Thus, in such systems, we have a single RFID reader that is responsible for identifying an unknown number of tags in the reading area as shown in figure 1.1. This naturally requires fast RFID readers (interrogators) in order not to slow down the delivery process of the actual goods. According to [8–10], the EPCglobal C1 G2 [11] is the most commonly used RFID standard in logistics. It is based on Time Division Multiple Access (TDMA), which leads to a certain probability of tag-collisions on the communication channel. Owing to their low price and simple design, tags can neither sense the channel nor communicate with the other tags. Hence, the readers are responsible for co-

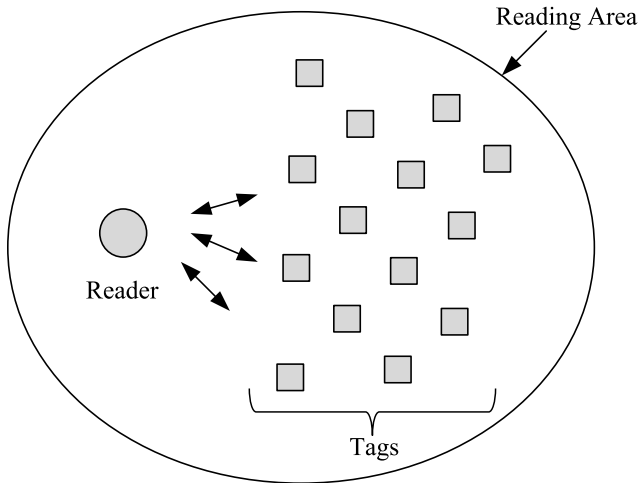


Figure 1.1: Dense RFID network with single RFID reader.

ordinating the network, and avoiding collisions using anti-collision algorithms.

According to the previously published RFID work, Frame Slotted ALOHA (FSA) [12, 13] is the most widely used Medium Access Control (MAC) anti-collision protocol for RFID systems due to its simplicity and robustness. In FSA, the communication timing between the reader and the tags is divided into TDMA frames, each frame includes a specific number of slots. The frame length is a function of the existing number of tags in the reading area. During the reading process, each active tag randomly assigns itself to one of the available slots in a frame. Therefore, each slot can take one of three different states: 1) Successful Slot: Only single tag chooses this slot and identified. It is then muted by the reader until the end of the reading process. 2) Collided Slot: Multiple tags reply, resulting in a collision. The collided tags normally remain in their active state and retry their transmission in the next frame. 3) Empty Slot: No tag responds and the slot remains unused. Therefore, the reading efficiency is limited by the effect of two main parameters:

1. The robustness of the number of tags estimation: The optimum FSA frame length strongly depends on the actual number of tags in the reading area. However, in real-world applications, the number of tags of the reading area is unknown. Therefore, the more precise the number of tags estimation, the better the reading efficiency.
2. The accuracy of the FSA frame length: If the frame length is higher than the optimum value, many empty slots exist in this frame, which reduces the reading efficiency. If the frame length is lower than the optimum value, this will produce many collided slots, which again reduces the reading

efficiency. Thereby, choosing the optimum value in FSA frame length is the most crucial optimization parameter in such applications.

Recent research groups have focused upon using the PHY layer properties, in the so-called Collision Recovery phenomena, to convert part of the collided slots into successful ones [14, 15]. This decreases the losses which result from collisions. Moreover, modern RFID readers have the ability to identify the type of the slot (successful, collided, or empty). Thus, the RFID readers are able to terminate the slot earlier as soon as they recognize the absence of a tag reply [16, 17], which reduces the effects of empty slots.

Based on the previous discussion, the number of tags estimation algorithm and the optimum FSA frame length strongly depend on the PHY layer properties of the system being used.

1.2 Thesis Contribution

This thesis aims to improve the performance of existing UHF RFID systems, mainly by minimizing the total identification delay. The accomplished work focuses on optimizing the FSA frame length and the number of tags estimation algorithm for dense RFID networks, taking into consideration MAC/PHY-layer parameters. All modifications are on the reader side, as the improved system has to follow the EPCglobal C1 G2 standard [11]. Moreover, results are compared to the theoretical lower limit for this standard. Finally, compatible upgrades of the EPCglobal C1 G2 standard are proposed, thus granting additional improvements for the overall performance. The main contributions of this thesis can be summarized as follows:

1. A method for number of tags estimation is developed, considering the collision recovery capability of the PHY layer. The main advantage of the proposed method is that it provides a new closed-form solution for the tag population estimator, which considers the collision recovery probability of the used system. Simulation results indicate that the proposed solution is more precise compared to the state-of-the-art. Timing comparisons presented in the simulation results show the reduced identification delay of the proposed estimation method compared to other proposals.
2. A closed-form solution of the optimum frame length for FSA is provided by optimizing the Time-Aware Framed Slotted ALOHA reading efficiency, which considers the differences in the slot durations. The simulation results indicate that the proposed solution gives the most accurate results with respect to the exact solution.
3. An additional closed-form solution for the optimum frame length for FSA is found by optimizing the time and constant collision recovery coefficients

aware reading efficiency. The proposed solution gives a new closed form equation for the frame length considering the different slot durations and the collision recovery capability with equal coefficients. Moreover, a new method is introduced to calculate the capture probability per frame. Simulations indicate that the proposed solution gives accurate results for all relevant parameter configurations without the need for multi-dimensional look-up tables.

4. A new closed-form solution for the optimal FSA frame length is established, which considers the differences in the collision recovery probabilities. The values of the collision recovery coefficients are extracted from the PHY layer parameters. Timing comparisons are presented in the simulation results to show the mean reduction in reading time using the proposed frame length compared to other proposals.
5. Further, a new closed-form solution for the optimal Frame Slotted ALOHA (FSA) frame length is created. The new solution considers the multiple collision recovery probability coefficients, and the different slot durations. Timing comparisons are presented in the simulation results to show the reading time reduction using the proposed frame length compared to the state-of-the-art algorithms.
6. Finally, compatible improvements of the EPCglobal C1 G2 standard are proposed. They require some compatible modifications in the UHF RFID tags/readers, to be capable of acknowledging more than a single tag per slot.

1.3 Document Outline

A brief outline of this document is presented as follows. Chapter 2 introduces the historical background and literature review of RFID systems. Chapter 3 presents the RFID collision problem and the existing anti-collision algorithms. Moreover, the concept of the proposed cross-layer anti-collision algorithm is defined. Chapter 4 reports the most commonly used number of RFID tags estimation algorithms. Afterwards, the proposed collision recovery aware maximum likelihood estimation algorithm is discussed. In this part, a closed-form solution for the estimated number of tags in the reading area is suggested taking into consideration the collision recovery capability of the used system. Chapter 5 shows different case studies for FSA frame optimization. Each case depends on the PHY-layer parameters. Hence, in every case, a closed-form solution for the optimum FSA frame length is an analytically derived function of the estimated number of tags and the PHY-layer parameters. Chapter 6 provides compatible improvements of the EPCglobal C1 G2 standard. In this system,

such modifications to tags/readers, can acknowledge more than a single tag per slot. Finally, chapter 7 sums up the thesis by highlighting the main issues addressed in this thesis and outlining some of the future research aspects.

Chapter 2

Background and Literature Review

This chapter provides an overview of the historical development of RFID. In addition, it describes the basic principles and the major technical aspects related to the RFID technology and its standardization. At the end of this chapter, the major issues in dense networks are presented.

In section 1 an overview is given about the historical development of RFID. Secondly, section 2 presents the main components of the system followed by section 3, in which the operating frequency bands in RFID are shown. Finally, section 4 describes the RFID collision problem.

2.1 Historical Development of RFID

In the year 1935, the first notion of RFID systems was invented by a Scottish physicist called Robert Alexander for detecting aircrafts [18]. Next, in 1950, the British government developed the first prototype of the RFID system, which is known as Identification Friend or Foe (IFF) system [19]. This system was designed for aeronautical applications. Between the 1950s and the 1960s, there was a big development in the area of RFID for different applications, e.g. the application of microwave [20] and radio transmission systems that modulate passive responders [18]. In the 1970s, RFID was intensively applied to logistics, transportation, vehicle tracking, livestock tracking as well as industrial automation. The first US patent in this field was published in 1973 for the invention of an active RFID tag with re-writable memory [19]. In 2008, the US Department of Defense have announced that they plan to use Electronic Product Code (EPC) [1] technology to track goods in their supply chain. In Europe, RFID is intended to improve industrial applications and to enable short-range systems for animal control [20]. In Japan, RFID is used for contact-less payments in transportation systems [18].

2.2 System Components

As shown in figure 2.1, the conventional RFID system consists of three main components: First, RFID tag or transponder which is attached to the object requested to be identified or tracked. Second, the RFID reader or interrogator, which controls data transmission and the whole identification process. Finally, the processing device, which is commonly called “Middleware”. It is always a software processing device. All the external processing depending on the application is done through this device using the EPC code which is identified by the reader from the tag. In the following sections, each component is described in detail.

2.2.1 Tag

The tag is the device, which is attached to the object. It stores information and might be incorporated to sensors. This information includes its unique EPC, which is a standardized identification code. When tags are within the reading range of the reader, they receive a command from the reader asking them for their EPC. They reply with their identification data to the reader, which processes the information according to the current application. Generally, RFID tags are divided into the following categories:

Active tags They have a fully autonomous power source [21, 22]. The approximate price for a single tag is $\simeq 10$ Euro, because they incorporate circuits with a microprocessor and a memory to read, write, rewrite, or erase data from an external device. There are several advantages of active tags: First, they support long reading distance, i.e. more than 100 meters. In addition, they also support immunity to multi-path fading, especially in harsh environment with excessive amounts of metals, such as shipping containers. Owing to their power supply property, they can be easily connected with sensors, thus, monitoring the environment depending on the application e.g. food or drug shipments. However, such tags are not suitable for applications which require dense RFID network, due to their cost.

Semi-passive tags In semi-passive tags, batteries are used on-board to power the controller or the chip. They may contain additional devices such as sensors [23, 24]. The signals generated by the reader are only used to activate tags in coverage. Then, the tag’s reply is generated using the energy emitted from the internal batteries. Semi-passive tags can communicate over longer distances than the normal passive tags. Moreover, the circuitry activation of the semi-passive tags is faster than in passive tags. However, the approximate price for

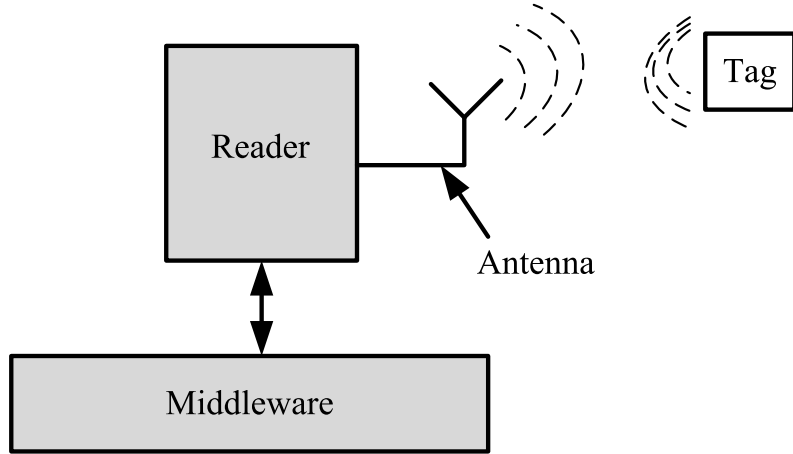


Figure 2.1: Main UHF RFID system components with single reader and back-scatter UHF tag

the semi-passive tags is \simeq 4 Euro, which makes such tags not suitable for dense RFID applications with hundreds or thousands of tags.

Passive tags Passive tags are the most commonly used in tracking and supply chain markets [25, 26]. They are extremely simple and inexpensive devices. The approximate price of such tags is less than 0.10 Euro. Passive tags do not contain any power source, so they derive all of the required energy for their operation from the signals emitted by the reader. This energy activates the circuit of the tags. Then, they send a reply signal that includes their information. The maximum communication range is up to a few meters. The aim of this thesis is to improve the identification efficiency for dense RFID applications. Thus, passive tags are the focus of this thesis.

2.2.2 Reader

The RFID reader is the most important element in an RFID system [21], because it is responsible of accessing the tag information and coordinate the complete reading process. The reader decodes the received data from the tags and then sends this information to the middleware. The reader performance depends strongly on two factors: First, the decoder architecture, and second, the antenna design.

Decoder architecture According to the previous discussion, this thesis focuses on passive RFID tags. Thus, the reader's transmission power must be sufficient to feed the surrounding passive tags [13]. These tags obtain energy

from the transmitted signal using the back-scattering technique. The back-scattering technique uses the reflection of the reader's carrier wave where the tag modulates the signal which includes its data. Then, the reader detects the tag's response, processes the signal and reads the information sent by the tag.

Antennas The polarization of the used antenna is one of the most critical issues which controls the identification performance [27]. In RFID systems, there are two types of antenna polarization: First, linearly polarized antennas, where the electrical field component of the transmitted signal is propagated in a plane (either vertically or horizontally). They must have a known RFID tag orientation and the RFID tag must be fixed upon the same plane as the antenna in order to get a consistent reading performance [28]. Second, circularly polarized antennas, where the electromagnetic fields are emitted in a corkscrew-like fashion. They broadcast electromagnetic waves on two planes making one complete revolution in a single wavelength. Compared to linearly polarized antennas of the same gain, circularly polarized antennas have a shorter read range because they lose about 3 dB splitting their power across two separate planes. [29, 30]. When deciding which type of antenna to choose for a RFID system, it depends on how the RFID tags should be oriented with respect to the antennas. If all the tags, which are needed to be identified, are on the same plane and about the same height, then a linearly polarized antenna should be considered. If the tag orientation is something that is not reliable or consistent, then a circularly polarized antenna is a better choice.

2.2.3 Middleware

Middleware is a layer of software created to connect other components together, e.g. hardware components, software programs, enterprise applications, databases, etc. Middleware gives software developers the ability to communicate and manage data throughout an entire system, rather than on each individual application. RFID middleware goes beyond simply connecting devices; rather, it allows users to collect, manipulate, and disseminate data with ease. The EPCglobal standards [11] define specifications that standardize the interfaces between RFID tags, RFID readers and enterprise systems.

2.3 Frequency Bands

Similar to how a radio must be tuned to different frequencies to hear different channels, RFID tags and readers have to be tuned to the same frequency in order to communicate. There are several different frequencies can be employed by a RFID system. First, RFID systems use the Low Frequency (LF) band [31].

Table 2.1: Frequency Bands for RFID Systems [32]

Frequency Band	Range	Common Frequencies
Low Frequency (LF)	0.5 m	125 kHz, 134 kHz
High Frequency (HF)	1 – 3 m	13.56 MHz
Ultra High Frequency (UHF)	10 m	866 MHz Europe 915 MHz USA
Microwave (μ W)	> 10 m	2.45 GHz, 5.8 GHz

The LF tags have a long wave-length and are better to penetrate thin metallic substances. Additionally, the LF RFID systems are ideal for reading objects with high-water content, such as fruits or vegetables. However, the LF RFID systems have a limited reading range with 0.5 m. Second, RFID systems use the High Frequency (HF) band [32]. The HF tags work well on objects made of metal and can work around goods with medium to high water content. However, they have 1 m as a maximum reading range. Third, RFID systems use the Ultra High Frequency (UHF) band [33]. UHF tags typically offer much better reading range (approximate 10 m) and can transfer data faster, i.e., read many more tags per second than the low/high-frequency tags. However, the UHF radio waves have a shorter wavelength, which makes their signal more likely to be attenuated (or weakened) and they cannot pass through metal or water. Due to their high data transfer rate, the UHF RFID tags are well suited for dense applications, such as boxes of goods as they pass through a gate. Finally, the microwave tags are usually smaller than the UHF tags and have a larger reading range. The microwave tags are more expensive than the UHF tags due to low demand, but they share the same advantages and disadvantages [25]. Table 2.1 presents the most common frequencies as well as the maximum communication range for each band.

2.4 Collision Problems

In RFID systems, both readers and tags communicate using the same frequency. Thus, simultaneous transmission can happen which leads to collisions. Collisions destroy the identification number EPC of the tag and may also interfere control commands of the readers. Thereby, the collision problem is the main source of delays in the identification process. There are two types of collisions, reader collisions and tag collisions. The following sections describe both types and their effects on the system performance.

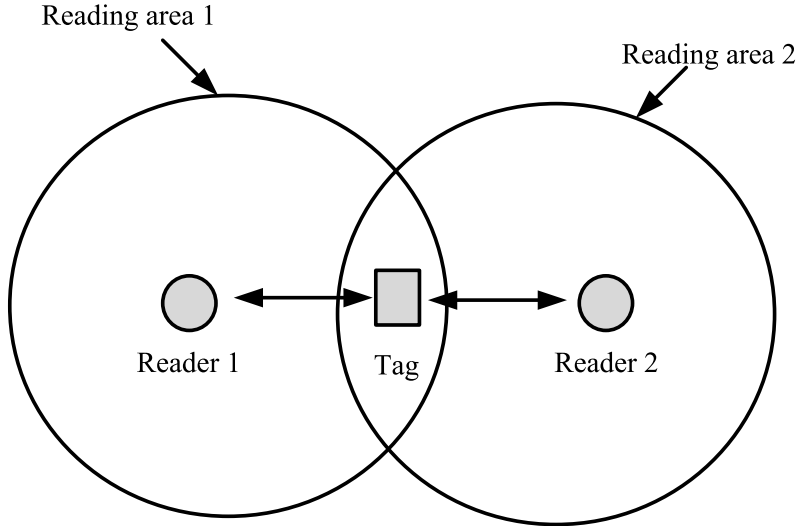


Figure 2.2: Multiple readers to a single tag collision.

2.4.1 Readers Collisions

There are two main types of readers collisions or interferences in RFID systems: multiple readers-to-tag collision and reader-to-reader collision.

Multiple Readers-to-Tag Collision Multiple readers-to-tag collision occurs when one tag is simultaneously located in an overlapped area between two neighbor reading areas [34, 35], and both readers communicate simultaneously with the shared tag as shown in figure 2.2. In this situation, the tag will not be able to determine such communication, due to the interference between the two readers commands. Therefore, the tag most likely will not respond to any reader. Finally, this slot would be an empty one leading to losses in the total identification time.

Reader-to-Reader Collision Reader-to-reader collision or interference, occurs when the signal generated by a reader acts as a jamming signal for a neighbor reader as shown in figure 2.3. This signal might prevent the second reader from communicating with its tags in its reading area [36, 37]. This interference affects the total identification time of the interfered system.

2.4.2 Tag Collisions

Tag collisions are common in dense RFID systems [38–41]. In such systems, there is a single RFID reader and multiple tags as shown in figure 2.4. The main objective is to identify all tags in the reading area in the minimum possible

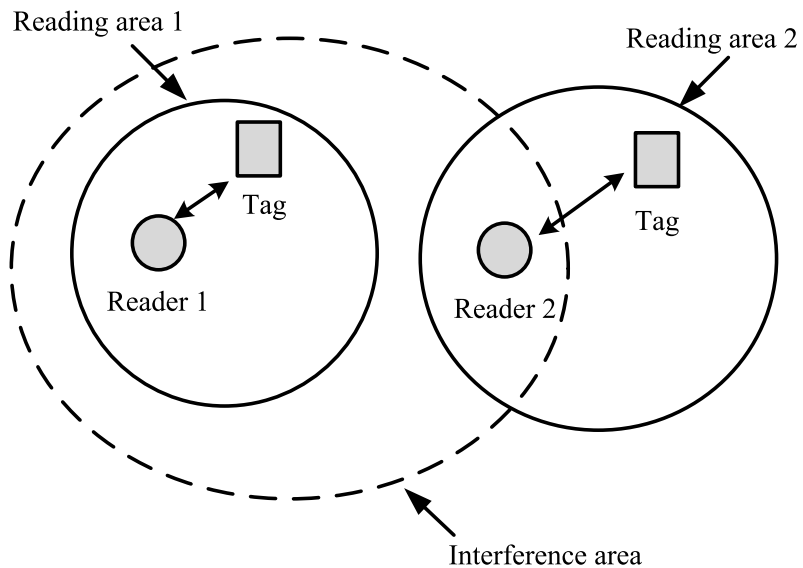


Figure 2.3: Multiple readers interference.

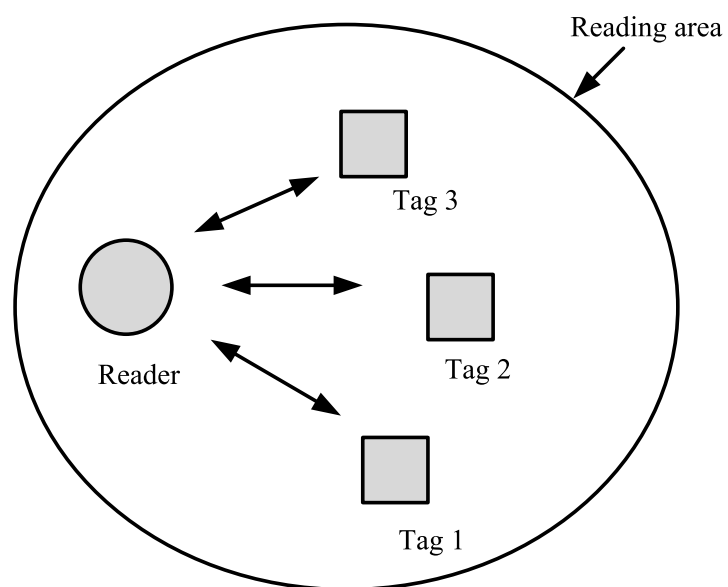


Figure 2.4: Multiple tags to a single reader collision.

time. However, in dense networks, the number of tag collisions increases, which decreases the reading efficiency, and hence increases the reading time.

Tags anti-collision protocols can be classified into two main types, PHY layer protocols and MAC layers protocols. The main motivation of this thesis is to minimize the total identification time for a dense and passive RFID network. Therefore, in the following chapters, there are different proposals to enhance the MAC layer anti-collision protocols taking into consideration the PHY layer parameters.

Chapter 3

RFID Anti-collision Protocols

This chapter presents the most common anti-collision protocols for passive RFID systems, either using the PHY layer or the MAC layer. It emphasizes the anti-collision algorithms which are compatible with the EPCglobal C1 G2 standard, as it is the main focus of this thesis, because it is the most suitable standard for the dense passive RFID applications.

This chapter is organized as follows. Section 1 gives an overview about the PHY layer anti-collision algorithms. In section 2, different MAC-layer anti-collision algorithms are presented. Afterwards, a brief description for the EPCglobal C1 G2 reading process is presented in section 3. Section 4 gives an introduction about the main PHY-layer parameters, e.g., the collision recovery and the slots duration in modern RFID readers. Then, the effect of these parameters on the MAC-layer anti-collision algorithm, which is the main focus of the remaining part of this thesis, is presented.

3.1 PHY-Layer Anti-collision Protocols

Different PHY layer anti-collision protocols have been developed to separate colliding tag signals on the PHY layer. Figure 3.1 shows the most common PHY layer anti-collision protocols, which are Frequency Division Multiple Access (FDMA), Space Division Multiple Access (SDMA), Code Division Multiple Access (CDMA), and Time Division Multiple Access (TDMA). These algorithms are discussed in the following paragraphs:

FDMA [42]: In this protocol, the frequency band is divided into different sub-frequency bands and tags are distributed among them. However, this technique adds complexity to the system, because readers should be able to decode different frequencies at the same time. Moreover, tags should be able to select its desirable sub-channel, which is incompatible with EPCglobal C1 G2. Only active tags can do such a function.

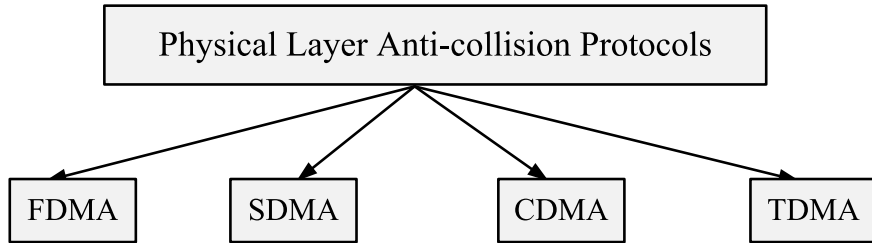


Figure 3.1: Common existing PHY-Layer anti-collision protocols.

SDMA [43]: This technique makes use of spreading tags over the reading area. It provides a high increase in the reading efficiency. The main drawback is the cost of implementing the RFID reader with multiple antennas. Moreover, in dense applications, the distances between tags are very small in order to be distributed on the reading area.

CDMA [44]: This protocol uses spread-spectrum modulation techniques to transmit the data over the entire spectrum. CDMA is the ideal procedure for many applications, e.g., navigation systems. However, the cost of the tags severely increases. Thereby, it is not an optimum protocol for dense RFID applications.

TDMA [45]: In this protocol, a single frequency band is divided into time slots and assigned to the tags. In this technique, each tag must be synchronized with the time slots and sends its information at the beginning of the selected slot. This technique can be directly applied on passive RFID systems. In such systems, the simplicity of tags transfers the complexity to the readers, where the reader has to control the time synchronization. However, in active RFID systems, synchronization can be either centralized or distributed to the tags.

3.2 MAC-Layer Anti-collision Protocols

PHY anti-collision proposals are not cost effective for the market challenges of the passive RFID technologies, because they require additional modifications of the tags. Therefore, solutions, that resolve tag collisions, are commonly implemented at the MAC-layer. This section discusses the most common MAC-layer anti-collision protocols.

Figure 3.2 presents the main classification of the most common MAC-layer anti-collision protocols. MAC-layer anti-collision protocols are classified into two main categories, deterministic protocols and probabilistic protocols. Deterministic or “Tree-based” protocols are used in systems with known number of tags to be identified in the reading area, because these protocols identify the

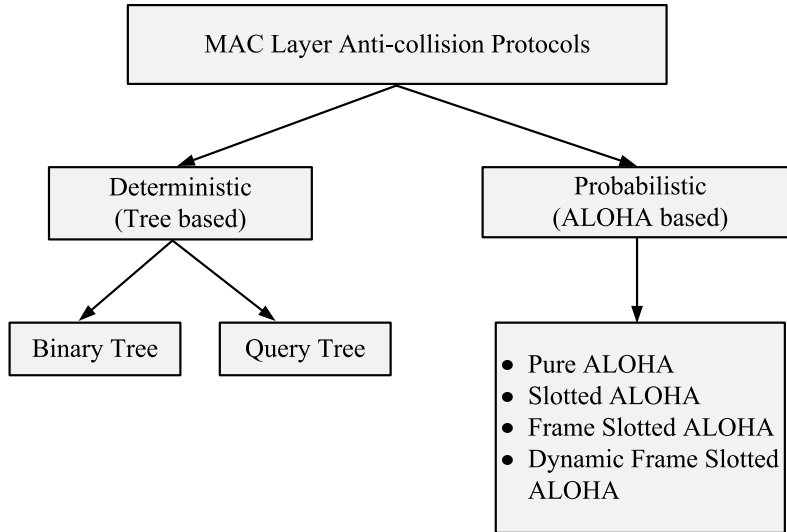


Figure 3.2: Common existing MAC-Layer anti-collision protocols.

depth of the tree by knowing the number of tags. Probabilistic or “ALOHA-based” protocols are used in systems with unknown number of tags. The following sections discusses the most commonly used anti-collision algorithms.

3.2.1 Deterministic Anti-collision Protocols

These protocols are commonly named tree-based anti-collision protocols. Using these algorithms, the reader aims to identify a set of tags in the coverage area in subsequent time slots [46]. Each time slot contains a “Query” command transmitted from the reader, and the response of tags in the reading area. If there are more than a single tag reply in one slot, a collision occurs and the reader tries to split the tags into two subgroups. The reader repeats the splitting procedure until it receives a single tag reply. Tree-based anti-collision protocols can be classified into two groups as follows.

Binary Tree: The binary tree algorithm [47] is commonly used in tree-based anti-collision protocols. Using this algorithm, if a collision occurs in a time slot, each collided tag selects randomly ‘0’ or ‘1’. Thus, the colliding tags are separated into two subgroups. Tags, which selected ‘0’, always transmit their IDs to the reader first. If a collision occurs again, collided tags are splitted again by selecting ‘0’ or ‘1’. Tags, which have selected ‘1’, have to wait until all other tags which have selected ‘0’ are successfully identified by the reader. This procedure continues recursively until the subset is reduced to one tag, that is identified without collisions.

Figure 3.3 shows an example of the binary tree algorithm resolving the

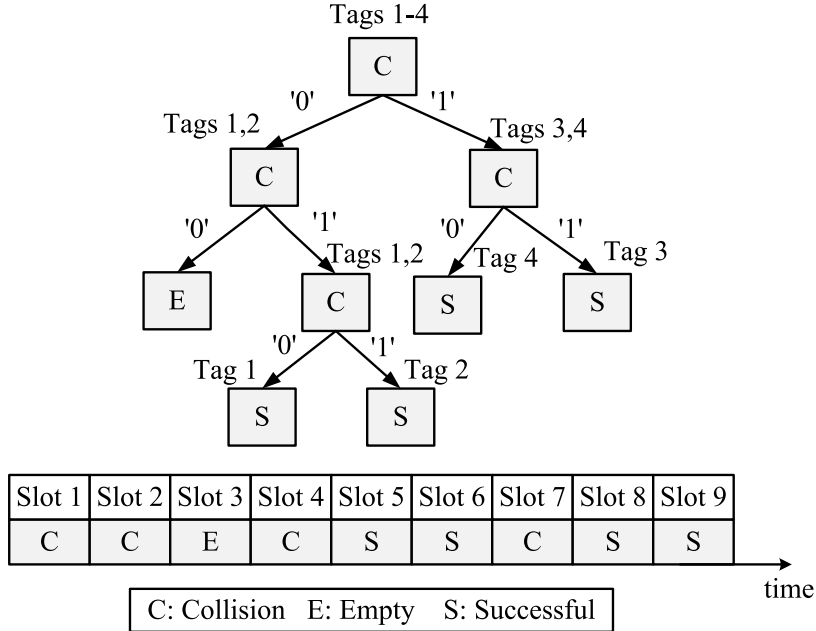


Figure 3.3: Binary tree anti-collision algorithm example.

collision of four tags in a reading area. Thus, there is a collided time slot at the beginning. At time slot 2, each collided tag chooses '0' or '1' randomly. In the shown example, tags 1 and 2 select '0' and tags 3 and 4 select '1'. According to the binary tree algorithm, tags 3 and 4 have to wait until tags 1 and 2 are successfully identified. Therefore, time slot 2 is a collided slot due to the collision between tags 1 and 2. Due to this collision, both tags 1 and 2 choose either '0' or '1'. In this example, both tags 1 and 2 select '1'. This results in an empty slot in time slot 3 and a collided slot in time slot 4. Afterwards, tag 1 selects '0' and tag 2 selects '1'. This random selection separates them into two successive successful slots (5 and 6). At this moment, tags 3 and 4 started their identification process. The reader repeats the previous process until identifying all tags in the reading area.

Query Tree: Another tree algorithm category is the query tree algorithm [48]. It is also commonly used in tree-based anti-collision algorithms. Using this algorithm, the broadcast is a query signal asking the tags for a reply. If there is a collision, the reader starts splitting the collided tags into two groups by sending a new query signal with a single bit '0' or '1' randomly. Tags in the reading area receive this signal and match this bit with their ID. If this bit matches their ID, they transmit their ID. If a collision took place again, the reader adds another random bit '0' or '1' to its next query signal. This process is repeated until the reader receives a successful single tag reply.

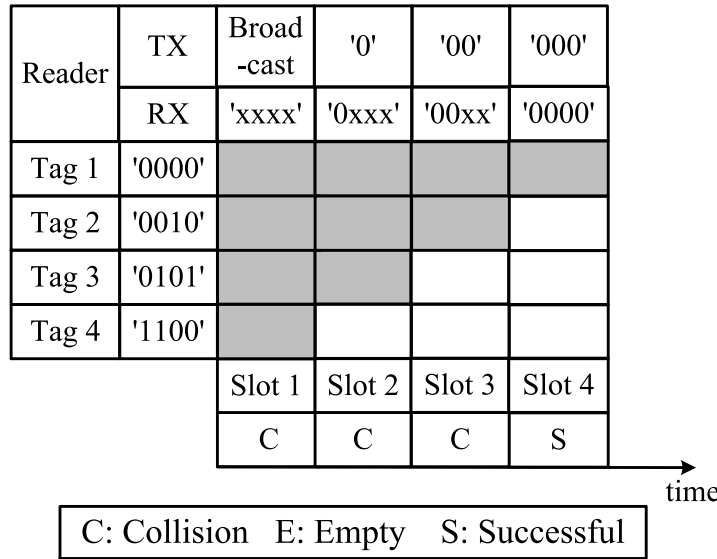


Figure 3.4: Query tree anti-collision algorithm example.

Figure 3.4 presents an example for the query tree algorithm resolving the collision of 4 tags in a reading area. At time slot 1, the reader broadcasts a query signal asking the tags for a reply. Thus, a collision between the four tags is taken place. The reader sends a '0' in a new query signal at time slot 2. However, there are three tags sharing this bit, so a new collision between the three tags is happening. Thereby, the reader sends a '00' in its next query signal in time slot 3. At this time, there is a collision between two tags, leads the reader to send '000' in time slot 4. At last, the reader receives a single successful reply from tag 1. This process is repeated until the reader identify all the tags in the reading area.

3.2.2 Probabilistic Anti-collision Protocols

The main disadvantage of using tree-based protocols is that they are not efficient in dense networks, due to the increase in identification time [49]. Therefore, in such networks, ALOHA-based anti-collision protocols are more suitable [49]. ALOHA anti-collision protocols are therefore the most commonly used in UHF active and passive RFID. ALOHA anti-collision protocols can be classified into the following four groups.

Basic ALOHA: Basic ALOHA [50] is the simplest anti-collision protocol for passive read-only-memory RFID tags. This protocol works as follows, the reader sends a query signal to power the tags. Then, tags send their ID randomly in time. The reader can only recognize the single tag reply case, without

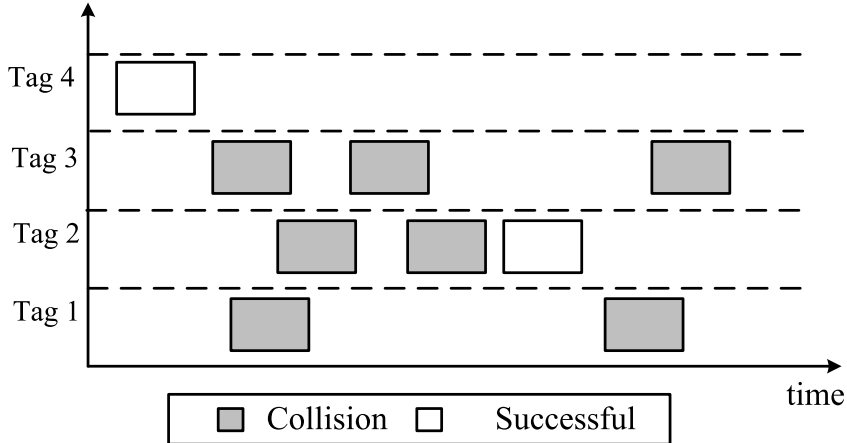


Figure 3.5: Example of pure ALOHA protocol.

any ability to handle the collision. When every tag replies to the reader without checking whether the channel is free or not there is always the possibility of the collision. In case of collision, the collided tags wait for a random duration of time and transmit again till it transmits successfully. According to [50], the maximum available reading efficiency is 18.4 %. Figure 3.5 shows an example of basic ALOHA for a single reader identifying four tags.

Slotted ALOHA: The second ALOHA anti-collision protocol is the slotted ALOHA protocol [51]. As shown in figure 3.6, slotted ALOHA is based on basic ALOHA. However, the time is divided into slots. In this protocol, the reader broadcasts a query signal which includes the beginning of each slot. Each tag chooses randomly if it will transmit in this slot or wait for a coming slot. Each tag is allowed only to start transmission at the beginning of each time slot. Therefore, the maximum possible collided time is a single complete slot. However, in the basic ALOHA protocol, the possible collided time is two slots. Thus, the maximum available reading efficiency using slotted ALOHA is 36.8 % [51].

Framed Slotted ALOHA (FSA): The third group is Framed Slotted ALOHA (FSA) protocol [49]. It uses a fixed frame length. Thus, the frame length is fixed during the complete tag identification process. At the beginning of each frame, the reader broadcasts a query signal to all tags. This signal includes the frame size. Each tag has to choose a random number between 0 and $L - 1$, where L is the frame length. If a collision happens, the colliding tags have to retry in the next frame.

Figure 3.7 presents an example for the identification process of four tags using FSA. In this example, the frame length is selected to be four slots. Ac-

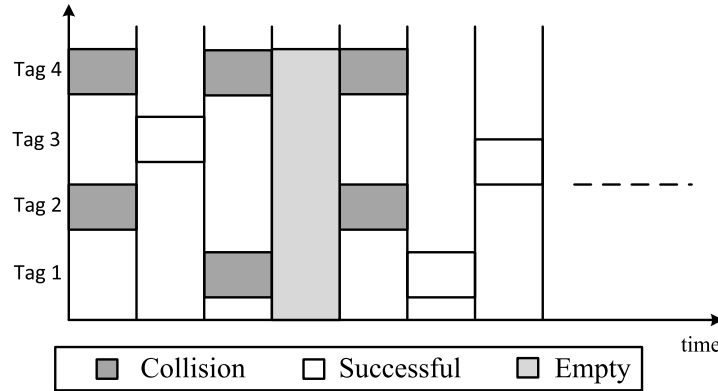


Figure 3.6: Example of slotted ALOHA.

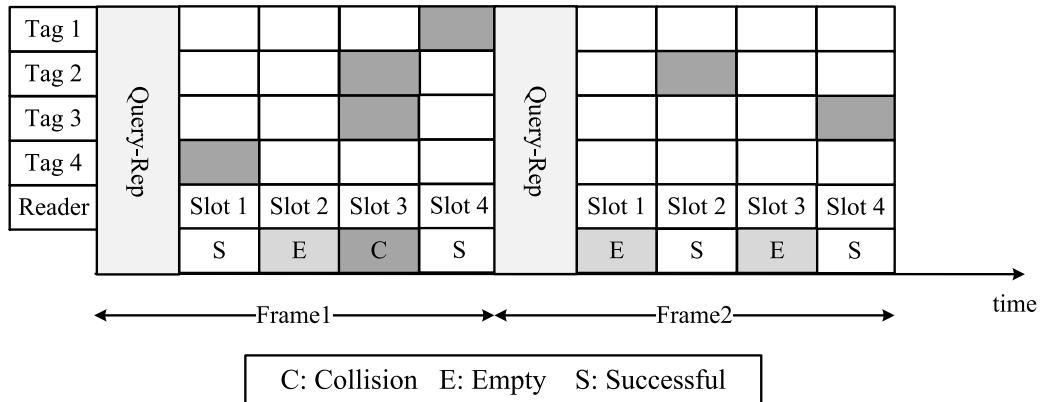


Figure 3.7: Example for Frame Slotted ALOHA.

According to figure 3.7, tag 4 transmits in the first slot alone. Thus, it is a successful slot. In the second slot, there is no tag reply. So, it is an empty slot. In the third slot, tags 2 and 3 reply together, which results in a collided slot. According to the FSA rules, tags 3 and 4 are not allowed to resubmit their IDs again during the same frame. Thus, in slot 4, only tag 1 is allowed to reply to have another successful slot. In the next frame, the same procedure is repeated until all tags are identified.

Dynamic Frame Slotted ALOHA (DFSA): The final type of ALOHA anti-collision protocols is Dynamic Framed Slotted ALOHA (DFSA) [52]. Using this algorithm, the number of slots per frame is variable as shown in figure 3.8. According to the previously published RFID work, DFSA [53] is the most widely used anti-collision protocol for RFID systems owing to its simplicity and robustness. In DFSA, the reading process is divided into successive frames, in which each frame includes a specific number of slots. During the reading process, each active tag randomly assigns itself to one of the available slots in

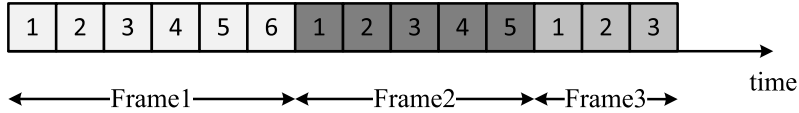


Figure 3.8: Slots of Dynamic Frame Slotted ALOHA.

the frame. Therefore, each slot can take one of the following three variable states: 1) Successful Slot: The reader receives a single tag reply during this slot, then the tag is identified and muted by the reader until the end of the reading process. 2) Collided Slot: The reader receives multiple tags replies, resulting in a collision. The collided tags normally remain in their active state and retry their transmission in the next frame. 3) Empty Slot: No tag responds are received by the reader and the slot remains unused.

Increasing the reading speed can directly be translated into the maximization of the number of successful slots in reference to the number of idle or collided slots. Based on the random access theory [54], for a given number of n tags, the expected number of empty E , successful S , and collided C slots in each frame with a length of L slots can be expressed by:

$$E = L \left(1 - \frac{1}{L}\right)^n, S = n \left(1 - \frac{1}{L}\right)^{n-1}, C = L - E - S \quad (3.1)$$

The conventional definition of the expected reading efficiency η_{conv} is given by the ratio between the expected number of successful slots S in a frame and the frame length L [55] to be:

$$\eta_{conv} = \frac{S}{L}. \quad (3.2)$$

Based on (3.1) and (3.2), the conventional definition of the reading efficiency is

$$\eta_{conv} = \frac{n}{L} \left(1 - \frac{1}{L}\right)^{n-1}. \quad (3.3)$$

Figure 3.9 shows the FSA reading efficiency η_{conv} for a constant frame length $L = 64$ with different numbers of tags. The main goal of optimizing the DFSA algorithm is finding the optimal frame length L , which maximizes the reading efficiency η_{conv} . Based on (3.3), the reading efficiency η_{conv} is maximized when:

$$L_{opt} = n. \quad (3.4)$$

In practical applications, the number of tags n in the interrogation region is unknown. Furthermore, the number of tags may even vary e.g., when the tags are mounted on moving goods. Therefore, such applications employ DFSA [56]. First, DFSA has to estimate the number of tags in the interrogation area, then it calculates the optimal frame size L for the next reading frame. Figure 3.10

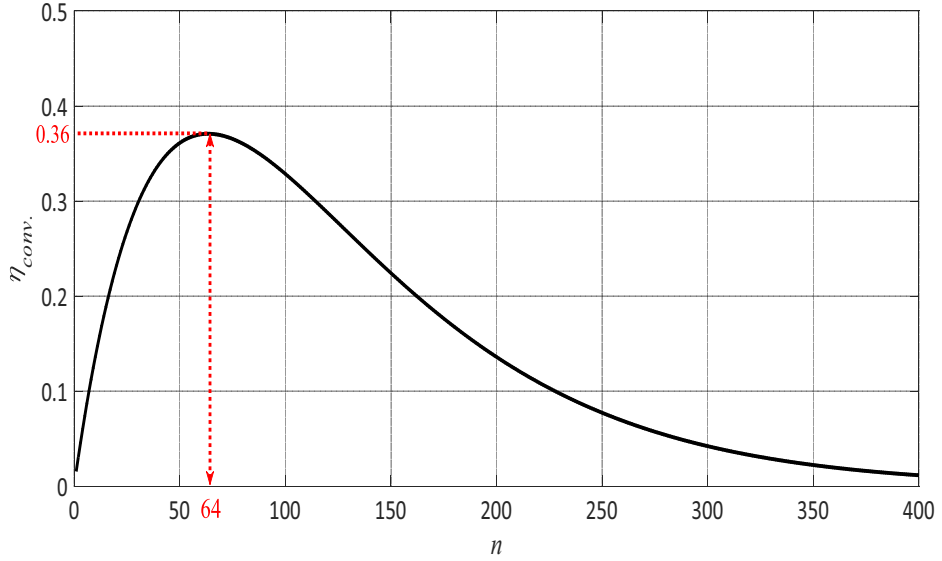


Figure 3.9: Conventional FSA reading efficiency η_{conv} as a function of the number of tags n , maximum reached for $L = n = 64$ tags of $\eta_{max} = (1/e) \simeq 0.36$.

presents a summary of DFSA. As shown in the chart, the reader starts with an initial frame length. Then, it broadcasts this frame length to the tags in the reading area. Afterwards, the reader performs a normal FSA. At the end of the frame, the reader checks if there are any successful or collided slots. If there is any, the reader estimates the remaining number of tags in the reading area, then optimizes the next frame length and starts another normal FSA. If not, the reading cycle is terminated.

3.3 DFSA with EPCglobal C1G2

In this section, an introduction about DFSA with EPCglobal C1 G2 [11] is presented. The reading process consists of multiple inventory rounds. Each inventory round typically has a different frame length. Figure 3.11 shows an example for the frame length adaptation in EPCglobal C1 G2. According to figure 3.11, the initial frame length is $2^{Q_{ini}}$, where $Q_{ini} = 4$. Then each slot is checked. If there is no tag reply, the frame length is decreased. If it is a collided slot, the frame length is increased. Finally, if the slot is a successful slot, the frame length remains the same.

Figure 3.12 shows an example for a timing diagram of different inventory rounds between a single RFID reader and different tag reply situations. The reader starts with a “Query” command. In this command, the reader broadcast the current frame length for all the tags in the reading area. Each tag has to

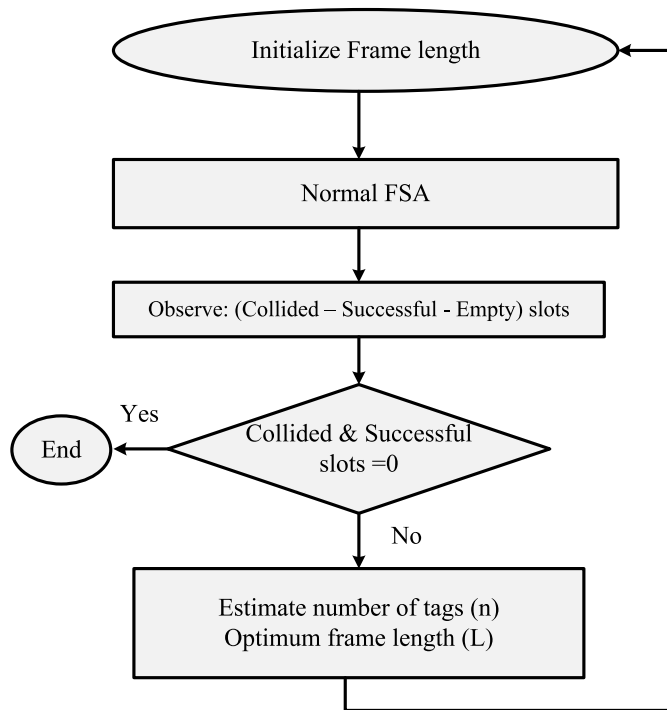


Figure 3.10: Flow chart of Dynamic Framed Slotted ALOHA (DFSA).

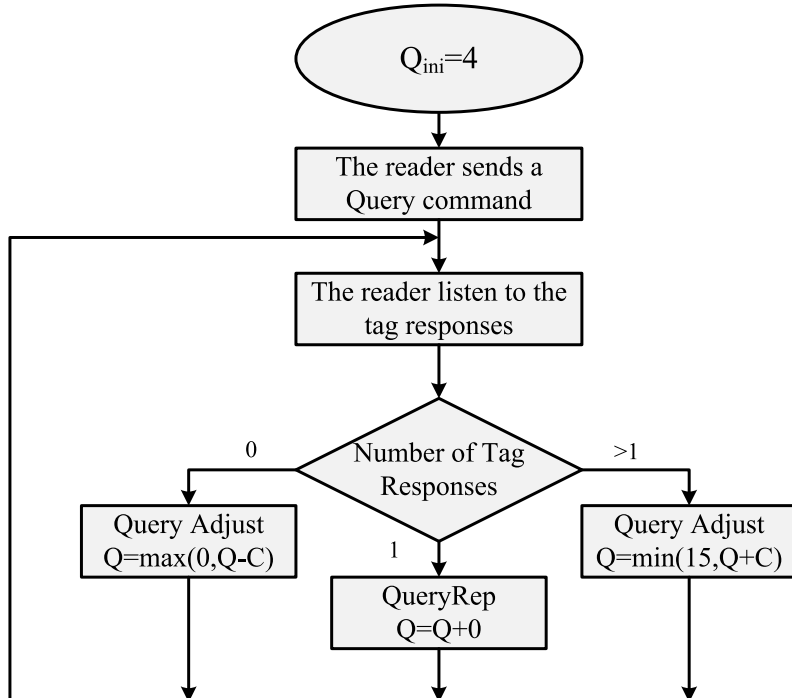


Figure 3.11: Conventional variable frame length procedure EPCglobal C1 G2.
[11]

choose a random slot between 0 and $2^Q - 1$.

Figure 3.12a shows the case of a single tag reply. In this case, the tag replies with its Random Number 16 (RN16), which is a 16 bits random number. When the reader receives a RN16 packet, it acknowledges the corresponding tag with an Acknowledge “ACK” command including its RN16. As soon as the tag receives a valid “ACK” command with its RN16, it replies with its unique Electronic Product Code (EPC). Finally, the reader sends a “Handle” command to the tag to mute it until the end of the reading process. In figure 3.12b, the reader starts broadcasting a “Query” command for tags in the reading area asking the existing tags to choose a random slot, and reply with their RN16s. In the presented example, three tags select the following slot. Therefore, the reader receives simultaneously three different RN16s. In this case, the conventional RFID reader is not able to decode any of these RN16s. Thus, the collided tags wait for the next frame to be identified. Afterwards, the reader broadcasts a “Query-rep” command to inform all the remaining tags that the next slot will start. Figure 3.12c shows the behavior of an empty slot in EPCglobal C1 G2. The reader starts the slot with a “Query” command, and waits for a tag reply within a defined time out period [11]. If there is no tag reply during this time period, the reader terminates the slot and starts a new one by sending a new “Query-rep” command.

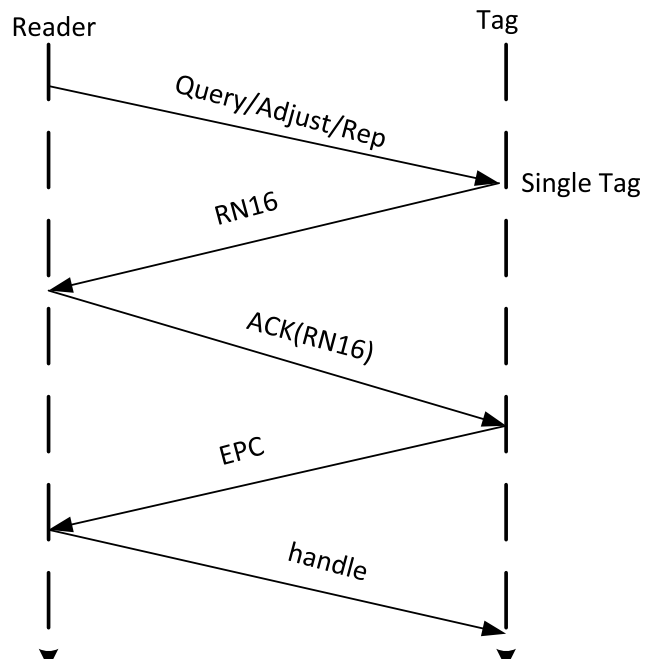
3.4 Cross Layer Anti-Collision Protocol

Recently, RFID receivers, that are able to convert a part of the collided slots into successful slots have been developed. Moreover, new RFID readers can even identify the type of the slots and terminate the empty and collided slots earlier. In this section, a brief discussion about these two parameters is presented. Afterwards, a motivation to reconfigure the MAC layer to make use of the PHY-layer parameters is presented.

3.4.1 Collision Recovery in UHF RFID

Collision recovery in RFID systems is the capability of the reader to convert a part of the collided slots into successful slots. According to EPCglobal C1 G2, the reader can only acknowledge a single tag per slot. According to [57], the collision recovery capability of the RFID system depends on different factors, namely; the capabilities of the receiver, e.g., number of antennas, the distance between the collided tags, and the type of the channel.

Recently, some research groups (e.g., [58]) have concentrated on collision recovery using the spatial diversity of the received signal. They proposed the following reading efficiency equation:



(a) Single tag reply.

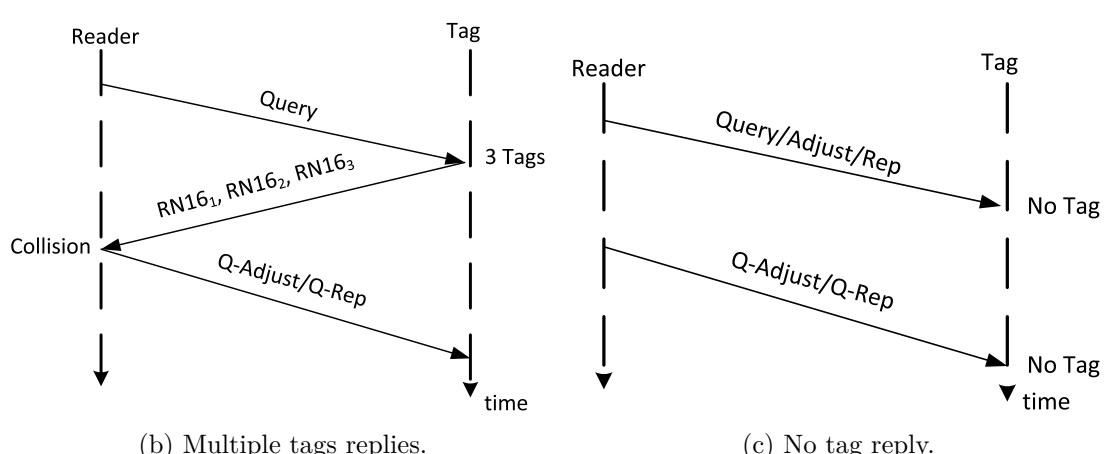


Figure 3.12: Example of an inventory between reader and different tags replies situations.

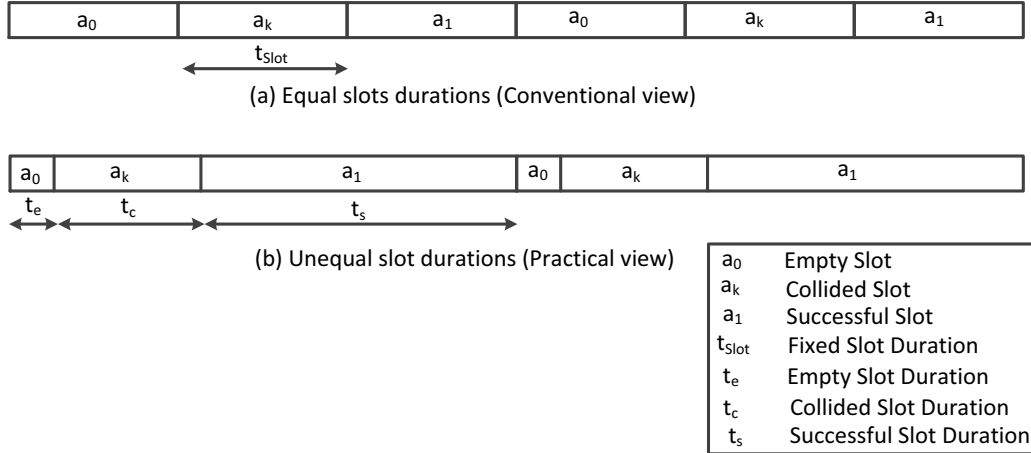


Figure 3.13: Equal and unequal views of slots in Frame Slotted ALOHA with frame length $L = 6$.

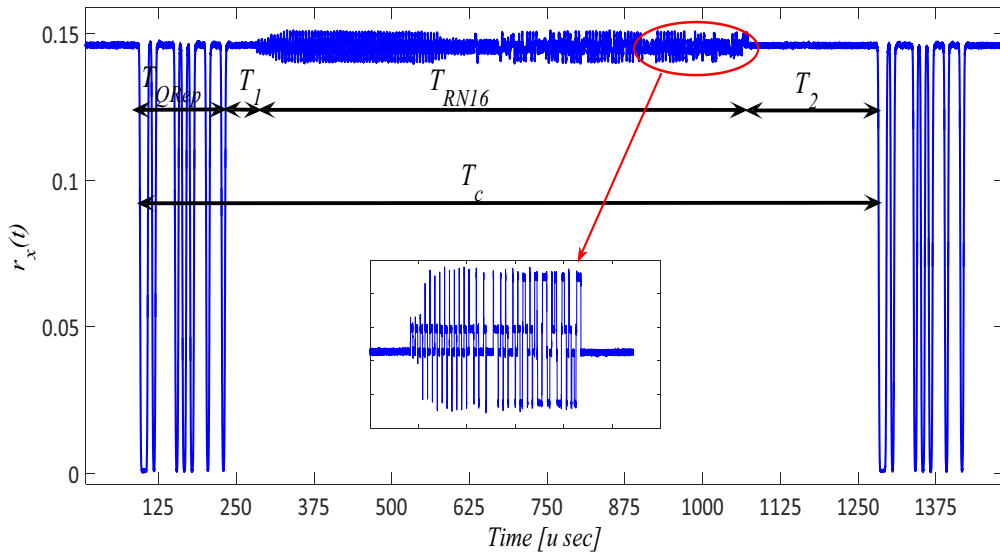
$$\eta = P(1) + \alpha \cdot \sum_{i=2}^n P(i), \quad (3.5)$$

where $\sum_{i=2}^n P(i)$ is the probability of collision, and α is the average collision resolving probability. In this efficiency equation, the RFID reader can convert a part of the collided slots into successful slots with a probability α . The authors assumed unlimited and equal collision resolving probability coefficients. For example, the probability to resolve two collided tags is identical to the probability to resolve ten collided tags, which is an unpractical assumption, because the more collided tags per slot are, the lower the collision recovery capability is. Another research groups [59–62] consider the limited capability of a RFID reader to resolve collisions. They propose a limited reading efficiency expressed by

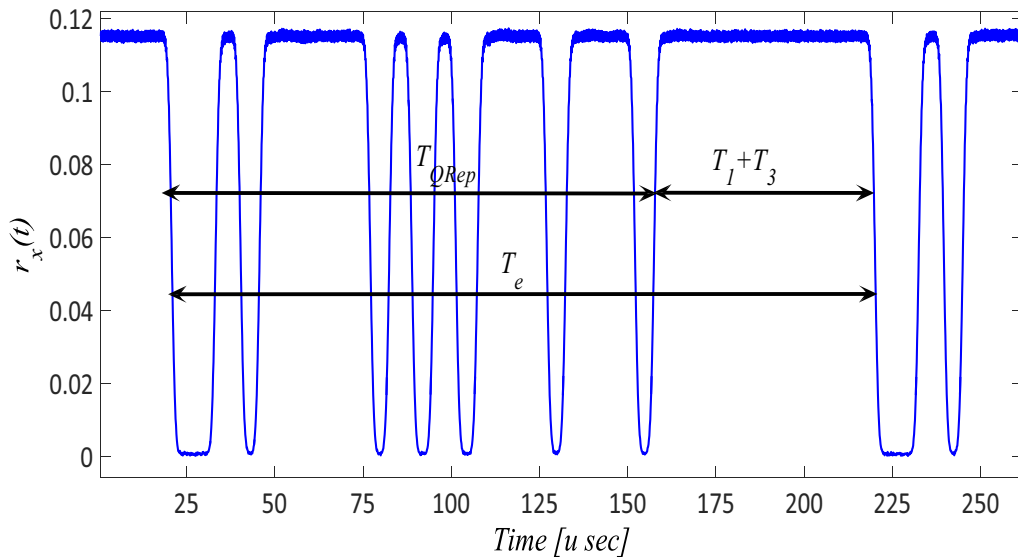
$$\eta = \sum_{i=1}^M P(i), \quad (3.6)$$

where $P(i) = \binom{n}{i} \left(\frac{1}{L}\right)^i \left(1 - \frac{1}{L}\right)^{n-i}$, and M represents the number of collided tags that the reader is capable to recover. The authors assume that the probability to recover one tag from i collided tags equals to 100%, independently of the actual i .

According to (3.5) and (3.6), the reading efficiency strongly depends on the capability of the PHY layer to resolve the collision. Thus, in this thesis, the effect of the collision recovery capability on the MAC layer optimization is addressed in more detail.



(a) Collided slot timing.



(b) Empty slot timing.

Figure 3.14: Slots durations measurements, where $r_x(t)$ is the received signal level, $f_s = 8 \text{ MHz}$, tag Backscatter Link Frequency $BLF = 160 \text{ kbps}$.

3.4.2 Slots Durations in EPCglobal C1 G2

Conventional RFID systems cannot identify the type of the slots in FSA [56]. Therefore, such systems consider that the slot duration of FSA is constant, neglecting the type of the slot. However, modern RFID readers can quickly identify the type of a slot, i.e., idle, successful, or collided. Hence, the durations of the different slot types are not identical, which normally reduces the overall reading time. Figure 3.13 shows two frames, each one with a frame length of $L = 6$ slots. The first frame in figure 3.13 (a) presents the conventional view of the frame with equal slots durations t_{Slot} for all slot types. The second frame in figure 3.13 (b) presents the behavior of the real RFID slots behavior. Here, the slot duration depends on the slot type.

Figure 3.14 shows an example of real measurements for slots durations using the Universal Software Radio Peripheral SDR receiver (USRP B210) [63]. In these measurements, the tag data rate is 160 kbps and a sampling frequency of $f_s = 8$ MHz is used, because the total RFID bandwidth in the European system is 4 MHz. For the given parameters and as shown in figure 3.14, the collided slot duration is $\simeq 1200 \mu\text{s}$, and the empty slot duration is $\simeq 200 \mu\text{s}$. Figure 3.14a shows a real collided slot between two tags. The number of Amplitude Shift Keying (ASK) levels in the RN16 is $A_L = 2^{N_c}$, where N_c is the number of collided tags. As shown in figure 3.14a, the number of ASK levels $A_L = 4$. In such a slot, the reader terminates the slot after recognizing that the slot is a collided slot. Figure 3.14b shows that the reader terminates the slot directly when it recognizes that there is no tag reply in this slot.

According to the above discussion, the reading efficiency equation is affected by the different slots durations. In this thesis, the different slot duration lengths are addressed with more details in the MAC layer optimization.

Summarizing, the main lack in the previous RFID research is that the MAC layer is optimized independently on the PHY layer. However, the PHY-layer properties affect the optimization parameters of the MAC layer, e.g., the number of tags estimation and the optimum frame length. This thesis concentrates on optimizing the DFSA anti-collision protocol. In the proposed algorithms, the PHY layer parameters are considered, which are the collision recovery capability of the RFID reader and the differences in slot durations.

Chapter 4

Estimation of the Tag Population

In this chapter, the most common estimation algorithms following the EPCglobal C1 G2 standard [11] are presented. Afterwards, a new number of tags estimation method called “Collision Recovery Aware Tag Estimation” is introduced. The proposed method takes into consideration the collision recovery probability of the PHY layer.

This chapter is organized as follows. Section 1 shows the conventional number of tags estimation algorithms with performance analysis comparisons between them. Section 2 presents the new collision recovery aware number of tags estimation method. Moreover, a closed form solution for the proposed algorithm is presented. The proposed solution presents a direct relation between the estimated number of tags and the frame length, as well as the number of successful and collided slots and the PHY layer collision recovery probability.

4.1 State-of-the-Art Estimation Algorithms

The performance of the FSA algorithm strongly depends on the accuracy of the number of tags estimation and the frame size. The number of tags estimation function calculates the number of tags based on feedback from the previous frame, which includes the number of slots filled with empty, successful, and collided slots. This information is then used by the estimation function to calculate the estimated remaining number of tags in the reading area, and hence the optimal frame size L is calculated, with the maximum possible accuracy, for a given round. According to the literature [53], the most common estimation algorithms are classified into two groups, direct Q-slot family and indirect Q-frame family.

Algorithm 4.1 Main procedure of direct Q-slot family

```

 $Q_{ini} = 4$ 
slot number = 0
loop
   $Q = \text{Round}(Q_f)$ 
  if slot number ==  $2^Q - 1$  then
    NewFrameSize( $Q$ )
    slot number = 0
  else
    slot number = slot number + 1
     $C = \text{Random}[0.1, 0.5]$ 
     $Q_f = Q$ 
  end if
  slot result = the result of recognition in this slot.
  if slot result == 'success' then
     $Q_f = Q_f + 0$ 
  else if slot result == 'empty' then
     $Q_f = Q_f - C$ 
  else if slot result == 'collision' then
     $Q_f = Q_f + C$ 
  end if
  end if
end loop

```

4.1.1 Direct Q-Algorithm Family

In Q-Algorithm [64–66], a parameter Q denotes the exponent of frame size used in FSA. A reader using FSA sends messages to tags in order to inform the next frame size. In general, reader sends the only exponent of frame size which is denoted by 2^Q , since an integer value is not appropriate as a message format due to the overheads. Once a frame size is determined, tags choose their slot to send their ID to a reader, using a random number generator. Q-Algorithm is designed to evaluate tags' replies and determine the next frame size. As shown in Algorithm 4.1 [65], when the Q-Algorithm starts, it takes tags' replies slot by slot. Then, it classifies slots into three categories; success, collision and empty slot. The next frame size is updated using those three factors. Specifically, when the result of tags' replies in a slot is empty, it subtracts a constant C from Q_f , because it is estimated that the used frame size is larger than ideal one. When a collision slot occurs, a constant C is added to Q_f , because it means the used frame size is smaller than the number of tags. According to the EPCglobal C1 G2 standards [11], the range of C is from 0.1 to 0.5. At the beginning of each slot, it rounds the Q_f value. Then, new frame size Q

is informed to tags. Direct Q-Algorithm has numerable advantages which are distinguished from another collision arbitration scheme using number of tags estimation algorithms as follows.

- Since direct Q-Algorithm does not depend on tag number estimation method, degradation of throughput by the estimation error does not occur.
- For the same reason, even if the number of tags increases, the computation cost by tag number estimation does not increase.
- Direct Q-Algorithm finds the optimal frame very quickly and does not reduce the throughput, because it evaluates the frame size in slot-by-slot manner instead of frame-by-frame as other schemes.

In spite of these advantages, direct Q-Algorithm is not appropriate to be directly applied to dense RFID networks [67], since the C parameter proposed in Q-Algorithm is not well optimized.

4.1.2 Indirect Q-frame Family

In this family, the proposed algorithms first calculate the estimated number of tags in the reading area \hat{n} . Then, it adjusts the optimum frame length L that maximizes the reading efficiency. The estimation process is based on information from the previous frame.

Lower Bound This method is proposed in [56], taking a trivial assumption for the lower bound of the number of tags in the reading area \hat{n} . It is not related to any theoretical lower bound. Additionally, it claims that each collided slot involves two collided tags. Therefore, it is presented by

$$\hat{n}_i = S_i + 2 \cdot C_i, \quad (4.1)$$

where i presents the frame index, S_i , and C_i successively present the number of successful and collided slots in frame i . The main advantage of this algorithm is the simplicity of its implementation. However, it gives inaccurate results, when the number of tags in the reading area is much higher than the frame length.

Schoute Algorithm The Schoute algorithm [52] is based on the hypothesis that the frame length is equivalent to the number of unidentified tags $L = \hat{n}$ since this is a direct way to optimize the system's throughput. Schoute's method also supposes that the number of unidentified tags \hat{n} could be infinite. Let P_c

be the probability that a slot is a collision slot and P_s be the probability that a slot is a successful slot. Then, the estimated collision rate C_{rate} is expressed as

$$C_{rate} = \frac{P_c}{1 - P_s}. \quad (4.2)$$

For dense RFID networks, \hat{n} is a large number, the rate C_{rate} can be thus calculated as

$$C_{rate} = \lim_{n \rightarrow \infty} \frac{P_c}{1 - P_s} \cong 0.418. \quad (4.3)$$

More details are discussed in [68].

Thus, the average number of tags involved in a collision slot C_{tag} is then computed as

$$C_{tag} = \frac{1}{C_{rate}} \cong 2.39. \quad (4.4)$$

Therefore, Schouste's method estimates the number of estimated tags \hat{n} to be

$$\hat{n}_i = S_i + 2.39 \cdot C_i, \quad (4.5)$$

where i presents the frame index, S_i , and C_i successively present the number of successful and collided slots in frame i . However, the supposed conditions in this method are too strict that some deviations would be generated if the real situation differs much from the strict conditions.

C-Ratio The authors of the C-Ratio estimation method [69] use the binomial distribution for the number of tags. The collision ratio is defined as the ratio between the number of collided slots C_i and the frame length L_i , where i is the frame index. Therefore, the C-Ratio can be expressed by

$$C_{ratio} \triangleq \frac{C_i}{L_i} = 1 - \left(1 - \frac{1}{L_i}\right)^{n_i} - \left(1 + \frac{n_i}{L_i - 1}\right). \quad (4.6)$$

The optimum value of \hat{n}_i is obtained by searching for all possible values of n , that makes the right hand side of (4.6) gives the closest value of C-Ratio under the condition that $n_i \geq 2 \cdot C_i$.

In [70], the authors used the same concept as the C-Ratio. However, they presumed independent binomial distributions of the tags in each slot. Thus, the modified C-Ratio is expressed by

$$\frac{C_i}{L_i} = \sum_{j=2}^{n_i} \binom{n_i}{j} \left(\frac{1}{L_i}\right)^j \left(1 - \frac{1}{L_i}\right)^{n_i-1}. \quad (4.7)$$

To simplify the searching process, this estimator suggests applying an upper bound to estimate the number of tags.

Error Minimization Estimation Vogt [54] proposes an estimation algorithm based on the Minimum Squared Error (MSE) estimation. It minimizes the distance between the observed empty E , successful S , collided C slots and their expected values E_{exp} , S_{exp} , C_{exp} for a given frame length L . It is presented by

$$\varepsilon_{conv}(L, S, C, E) = \min_n \{ |E_{exp} - E| + |S_{exp} - S| + |C_{exp} - C| \}, \quad (4.8)$$

where

$$E_{exp} = L_i \left(1 - \frac{1}{L_i}\right)^n, \quad S_{exp} = n \left(1 - \frac{1}{L_i}\right)^{n-1}, \quad C_{exp} = L_i - E_{exp} - S_{exp}. \quad (4.9)$$

However, this method requires numerical searching to find the optimum value of the number of tags \hat{n} , which is not an optimum solution for dense RFID applications

Maximum Likelihood (ML) Tag Estimation The main concept of ML number of tags estimation is to compute the conditional probability of observed events assuming that this conditional probability is function of the number of tags n . Subsequently, the \hat{n} is the estimated number of tags which maximizes this conditional probability. In [71], a ML number of tags estimation by finding the optimum \hat{n} that gives exact E empty slots, S successful slots, and C collided slots, if there are L total slots is proposed. In addition, a multi-nomial distribution with L repeated independent trials is used. Each trial has one of three possibilities: P_e empty, P_s successful, or P_c collision, where P_e , P_s , and P_c follow binomial distribution [56] and can be presented by

$$P_e = \left(1 - \frac{1}{L}\right)^n, \quad P_s = \frac{n}{L} \left(1 - \frac{1}{L}\right)^{n-1}, \quad P_c = 1 - P_e - P_s. \quad (4.10)$$

The probability that in L trials, empty outcome occurs E times, successful outcome occurs S times, and collision outcome occurs C times is

$$P(\hat{n}|L, S, C, E) = \frac{L!}{E!S!C!} P_e^E P_s^S P_c^C \quad (4.11)$$

This probability is the general term of the multi-nomial expansion of $(P_e + P_s + P_c)^L$. Therefore, for a read cycle with frame length L , a posterior probability for the number of tags n , E empty slots, S successful slots, and C collided slots are observed, is calculated as shown in (4.11).

4.1.3 Performance Comparison of Existing Estimation Protocols

According to literature [72–74], the most common comparison estimation performance metric is the relative estimation error ϵ versus the normalized number

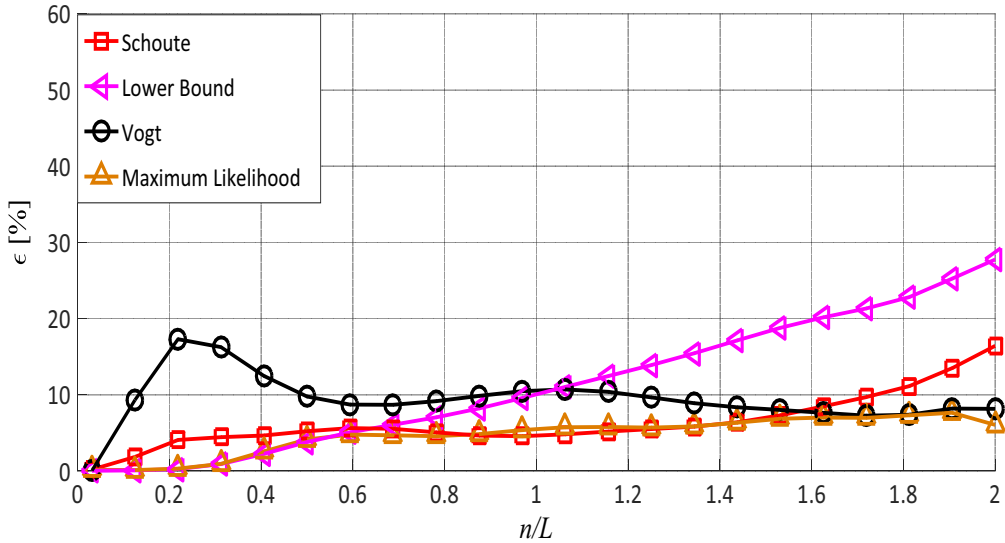


Figure 4.1: Relative estimation error ϵ as a function of the normalized number of tags n/L for the common state-of-the-art estimation algorithms.

of tags n/L . It presents the absolute difference between the actual number of tags and the estimated one divided by the actual number of tags in the reading area. Accordingly, it is defined to be

$$\epsilon = \left| \frac{\hat{n} - n}{n} \right| \times 100 \%. \quad (4.12)$$

Figure 4.1 shows the comparison of the most common number of tags estimation algorithms used in passive UHF RFID systems. The comparison metric is the average relative estimation error ϵ , which is calculated using Monte-Carlo simulations for FSA with 1000 iterations for each (n/L) value. According to figure 4.1, the simplest estimation algorithm presented is the lower bound algorithm [56]. However, it gives an inaccurate results compared to the other algorithms. Schoute algorithm [68] gives good results only when FSA frame length is equal to the number of tags $L = n$. The ML estimation method [71] is the most relative accurate estimation algorithm along the different values of L and n . It gives the minimum relative estimation error even in dense RFID networks, which is the main focus of the proposed work. However, according to [74], the complexity of the ML algorithm is much higher than the other estimation algorithm, because it searches for the value n that maximizes the estimation probability.

Figure 4.2 displays another comparison metric, which is the mean identification time required to identify the number of n tags. The comparison is between the average identification time using FSA algorithm with the most common existing number of tags estimation protocols. Perfect estimation presents the

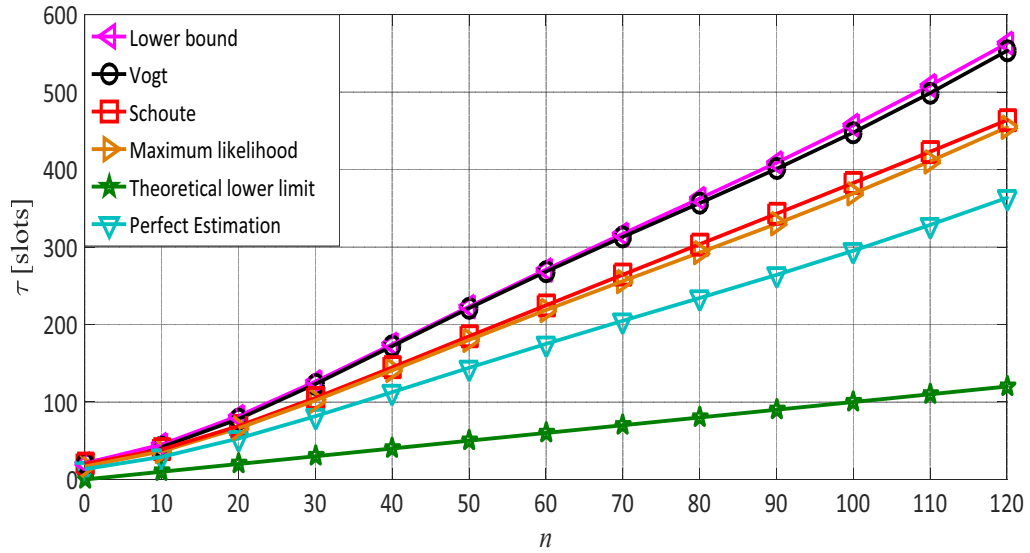


Figure 4.2: Mean identification time τ in slots using FSA for simulated common state-of-the-art estimation algorithms as a function of the number of tags in the reading area n .

mean identification time for FSA using known number of tags. The theoretical lower limit presents the theoretical minimum number of slots using FSA to identify n number of tags, which is n slots. Each result in figure 4.2 is calculated using Monte-Carlo simulations for FSA with 1000 iterations for each n . According to figure 4.2, the ML estimation algorithm [71] gives the lowest mean identification time compared to the other estimation algorithms. However, the numerical searching complexity of the ML estimator [71] limits the number of tags [53]. This leads us to search for a method, that gives accepted accuracy and suitable for dense RFID networks. Moreover, methods in [53, 71, 72] do not take into consideration the collision recovery capabilities effect of the modern RFID PHY layer.

4.2 Novel Collision Recovery Aware Tag Estimation

The aforementioned literature proposed various estimation methods. The ML estimation method gives the most precise results compared to other methods, however, it possesses two main disadvantages: 1) It uses numerical searching, which needs many calculations and iterations to find the optimum estimated value. 2) The PHY layer effect is neglected, which is an inaccurate assumption as discussed in the previous chapter. Modern systems are capable of converting

part of collided slots into successful slots e.g., [60, 61]. In such systems, the number of collided and successful slots delivered to the MAC layer are inaccurate in regards to the real number of tags at the reading area. Therefore, it is important to take into consideration the collision recovery capability. The authors in [58] use the estimation approach of [54], hence, considering the collision recovery probability. However, this method leads to multi-dimensional searching, which needs many iterations and complex calculations.

In this section, a new closed-form solution for the estimated number of tags \hat{n} is proposed. It considers the collision recovery probability of the PHY layer. An example for calculating the collision recovery probability using a simple RFID receiver is presented. This solution gives a direct and linear relation between the estimated number of tags \hat{n} and the frame length L .

4.2.1 System Model under Collision Recovery Probability

In this section, a new number of tags estimation method is presented. The proposed method is based on the classical ML estimation presented in [71]. According to the aforementioned method, the optimum value of \hat{n} which maximizes the conditional probability of the observing vector $v = \langle C, S, E \rangle$ is used, given that n tags transmit at a frame length L

$$P(\hat{n}|L, S, C, E) = \frac{L!}{E!S!C!} P_e^E P_s^S P_c^C, \quad (4.13)$$

where C, S, E are the number of collided, successful, and empty slots per a frame length L , and P_e, P_s, P_c are respectively the probabilities of empty, successful and collided transmissions per slot. Owing to the fact that modern RFID readers have a collision recovery capability, thereby, the PHY layer is able to convert part of collided slots into successful slots based on the following relation

$$E = E_b, S = S_b + \alpha \cdot C_b, C = C_b - \alpha \cdot C_b, \quad (4.14)$$

where C_b, S_b, E_b are successively the expected number of collided, successful, and empty slots before the collision recovery of the system, and C, S , and E are respectively the expected number of collided, successful, and empty slots after collision recovery of the system. α is a variable that indicates the collision recovery capability of the PHY layer. The calculation of the collision recovery probability is discussed in detail in the following sections. Figure 4.3 clarifies the flow diagram of the proposed system. In this system, the PHY layer gives the MAC layer information about its collision recovery capability.

On the MAC layer, only the values of C, S, E are known after the PHY-layer collision recovery. In this stage, there is no information about these values

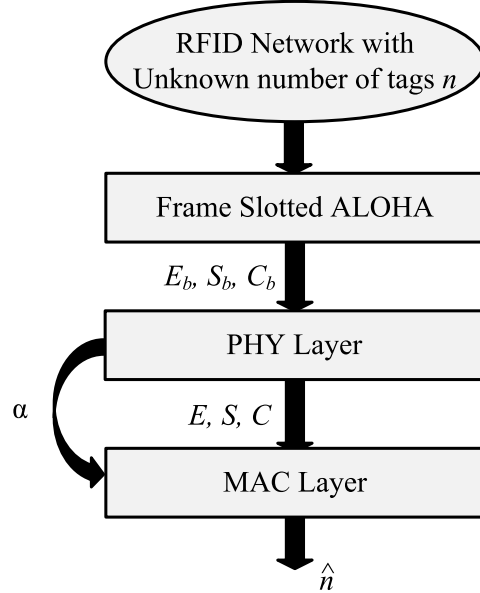


Figure 4.3: PHY layer collision recovery capability.

before the collision recovery. Thus, the conventional estimation systems, including the classical ML number of tags estimation in (4.13), use the values of C , S , E after collision recovery in their calculations. However, these values are not accurate indicators for the actual number of tags in the reading area. In the proposed solution, the value of the current average collision recovery probability α is estimated, as it is shown in detail in the following section. Finally, the expected corresponding values of C_b , S_b , E_b are calculated as

$$E_b = E, C_b = \left\lfloor \frac{C}{1 - \alpha} \right\rfloor, S_b = S - \left\lceil \frac{\alpha}{1 - \alpha} \right\rceil C, \quad (4.15)$$

Under the condition

$$L = E_b + S_b + C_b. \quad (4.16)$$

Thus, $C_{b(max)} = L - E_b$ and $S_{b(min)} = 0$. Therefore, the proposed collision recovery aware ML conditional probability can be formalized as

$$P(\hat{n}|L, S, C, E, \alpha) = \frac{L!}{E_b! S_b! C_b!} P_e^{E_b} P_s^{S_b} P_c^{C_b}. \quad (4.17)$$

According to [75], for those situations in which n is large and $\frac{1}{L}$ is very small, the Poisson distribution [76] can be used to approximate the binomial distribution. Figure 4.4 shows the success probability using Binomial distribution and its Poisson approximation versus the number of tags with different frame lengths. According to figure 4.4, the larger the number of tags n and the longer the frame

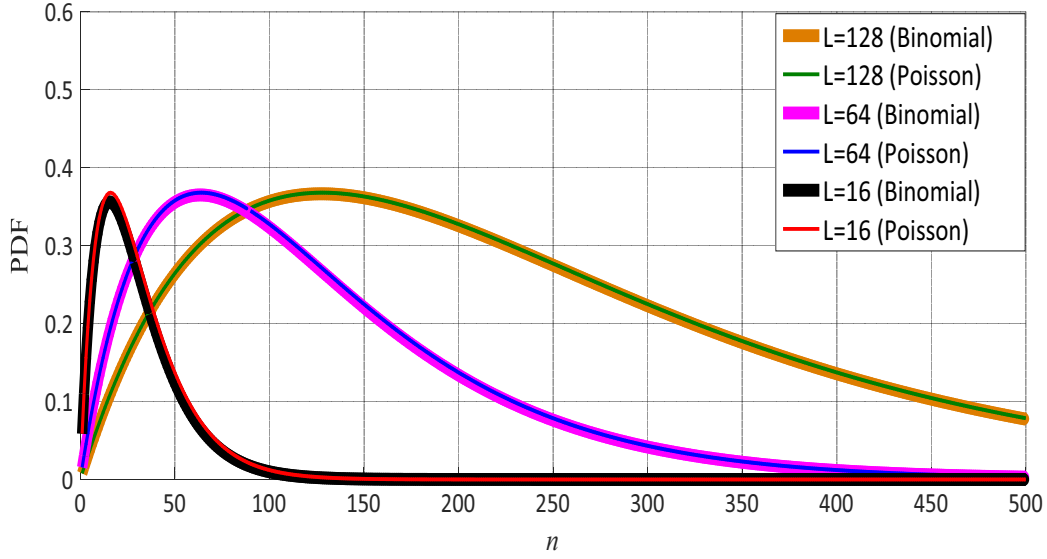


Figure 4.4: Probability Density Function (PDF) as a function of the number of tags n for the Binomial distribution and its Poisson approximation for the probability of success using different frame lengths.

length L , the better the approximation. Based on figure 4.4, this approximation is valid under conditions $n \geq 10$ and $L \geq 16$ with high precision.

In dense RFID networks, the Poisson distribution with mean $\gamma = \frac{\hat{n}}{L}$ is applicable [53]. Thus, the probability functions can be presented as

$$P_e = e^{-\gamma}, P_s = \gamma \cdot e^{-\gamma}, P_c = 1 - e^{-\gamma} - \gamma \cdot e^{-\gamma}. \quad (4.18)$$

After substituting by (4.18) in (4.17), the proposed conditional probability is

$$P(\hat{n}|L, S, C, E, \alpha) = \left(\frac{L!}{E_b! S_b! C_b!} \right) \gamma^{S_b} \cdot e^{-\gamma \cdot L} \cdot (e^{-\gamma} - 1 - \gamma)^{C_b}. \quad (4.19)$$

The term of $\frac{L!}{E_b! S_b! C_b!}$ is not a function of the number of tags. It is only an offset and can be normalized. Thus, the proposed normalized conditional probability is

$$P(\hat{n}|L, S, C, E, \alpha) \simeq \gamma^{S_b} \cdot e^{-\gamma \cdot L} \cdot (e^{-\gamma} - 1 - \gamma)^{C_b}. \quad (4.20)$$

Equation (4.20) gives a conditional probability for the estimated number of tags for a given number of successful, collided, empty slots and collision recovery probability. The computation of (4.20) can be done by numerical searching to obtain the optimum value of \hat{n} which maximizes (4.20). Hence, the calculation of (4.20) needs a multi-dimensional lookup table, which is time consuming, especially in case of dense network containing large number of tags n [53].

4.2.2 Derivation of the Proposed Closed Form Solution

This section proposes a closed form solution for the collision recovery aware estimation. This is achieved by differentiating (4.20) with respect to γ and equating the results to zero. After differentiating, the equation can be simplified to be

$$e^{-\gamma} \left(1 + \frac{\gamma(\gamma \cdot L - S_b)}{(\gamma \cdot L - S_b - \gamma \cdot C_b)} \right) - 1 = 0. \quad (4.21)$$

The analysis of (4.21) indicates that the relevant values for γ are in the region close to one [77]. Hence, we can develop a Taylor series for $e^{-\gamma}$ around one which leads to be

$$e^{-\gamma} \simeq 1 - \gamma + \frac{1}{2}\gamma^2 - \frac{1}{6}\gamma^3. \quad (4.22)$$

After substituting in (4.21) and some additional simplifications, the final equation is a fourth order polynomial

$$\underbrace{\frac{1}{120}(L - C_b)\gamma^4}_{(a)} + \underbrace{\frac{1}{24}\left(L - C_b - \frac{S_b}{5}\right)\gamma^3}_{(b)} + \underbrace{\frac{1}{6}\left(L - C_b - \frac{S_b}{4}\right)\gamma^2}_{(c)} + \underbrace{\frac{1}{2}\left(L - C_b - \frac{S_b}{3}\right)\gamma}_{(d)} - \underbrace{\left(C_b + \frac{S_b}{2}\right)}_{(e)} = 0. \quad (4.23)$$

Equation (4.23) has four roots [78]

$$\begin{aligned} \gamma_{1,2} &= -\frac{b}{4a} - S \pm 0.5 \sqrt{\underbrace{-4S^2 - 2P + \frac{q}{S}}_X} \\ \gamma_{3,4} &= -\frac{b}{4a} + S \pm 0.5 \sqrt{\underbrace{-4S^2 - 2P - \frac{q}{S}}_Y}, \end{aligned} \quad (4.24)$$

where $P = \frac{8ac-3b^2}{8a^2}$, $q = \frac{b^3-4abc+8a^2d}{8a^3}$,

with $S = 0.5 \sqrt{-\frac{2}{3}P + \frac{1}{3a}\left(Q + \frac{\Delta_0}{Q}\right)}$, $Q = \sqrt[3]{\frac{\Delta_1 + \sqrt{\Delta_1^2 - 4\Delta_0^3}}{2}}$,

and $\Delta_0 = c^2 - 3bd + 12ae$, $\Delta_1 = 2c^3 - 9bcd + 27ad^2 - 72ace$

According to equation (4.24), the signs of the polynomial coefficients are constant and have the following signs: $a > 0$, $b > 0$, $c > 0$, $d > 0$, and $e < 0$. Using Descartes' rules of sign [78], the number of real positive solutions for a polynomial can be counted. Assuming that the polynomial in (4.23) is $P(\gamma)$, and let ν be the number of variations in the sign of the coefficients a, b, c, d, e , so

$\nu = 1$. Let n_p be the number of real positive solutions. According to Descartes' rules of sign

- $n_p \leq \nu$ which means that $n_p = 0$ or 1 .
- $\nu - n_p$ must be an even integer. Therefore, $n_p = 1$.

Hence, there is only one valid real positive solution for the equation. Hereby, the valid solution is identified. There are two possible solutions

1. One positive real solution and the remaining three solutions are negative. In this case, all solutions are real and we just need to identify the root with the largest values among the four solutions. According to (4.24), the value of the square roots \sqrt{X} and \sqrt{Y} are positive reals, because we do not have complex solutions. This means, $\gamma_1 > \gamma_2$ and also $\gamma_3 > \gamma_4$. So, the solution is either γ_1 or γ_3 . Moreover, the value of S should be also a positive real, and q has always negative real value. So $\gamma_3 > \gamma_1$ which means in this case that our solution is γ_3 .

2. Two complex solutions, one real positive solution, and one negative solution. In this case, we have either $\gamma_{1,2}$ or $\gamma_{3,4}$ real solutions. S should be a positive real number, and the complex value comes only from the square roots \sqrt{X} and \sqrt{Y} . Moreover, q has always negative real value. Therefore, in (4.24) the value of $X < Y$. So $\gamma_{1,2}$ must be the complex roots, and as mentioned before that $\gamma_3 > \gamma_4$, so γ_4 is the negative root and γ_3 is the positive real root.

Based on the above discussion, the proposed closed form solution for the collision recovery aware tag estimation is

$$\hat{n} = \left(-\frac{b}{4a} + S + 0.5\sqrt{-4S^2 - 2P - \frac{q}{S}} \right) \cdot L. \quad (4.25)$$

Equation (4.25) gives a direct and linear relation between the estimated number of tags \hat{n} and the current frame length L , and gives an alternative solution to the numerical searching with (4.20). Thus, using (4.25), neither look-up tables nor searching is needed. This reduces the complexity and the processing time of the estimation algorithm.

4.2.3 Collision Recovery Probability Calculation

The collision recovery capability is the ability of the reader to actively convert collided slots into successful slots. This capability does not only exist in modern RFID readers, but also in the simple readers, e.g. when the tags are well separated. Thus, the received signal power of the nearest tag is much stronger than the received signal power from the far tag. Therefore, this ability is a function of two main parameters: First, the characterization of the RFID reader, (e.g. receiver type, number of antennas, etc.). Second, the value of

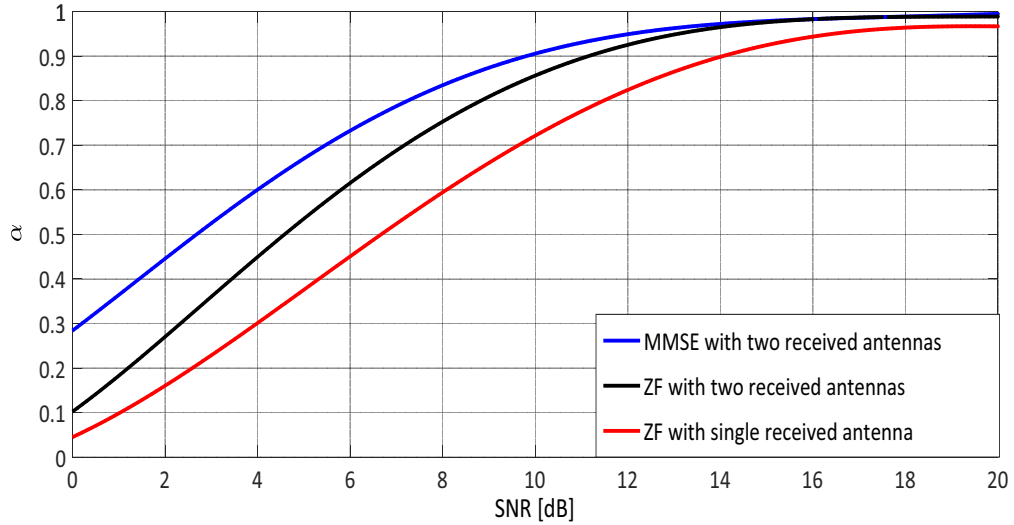


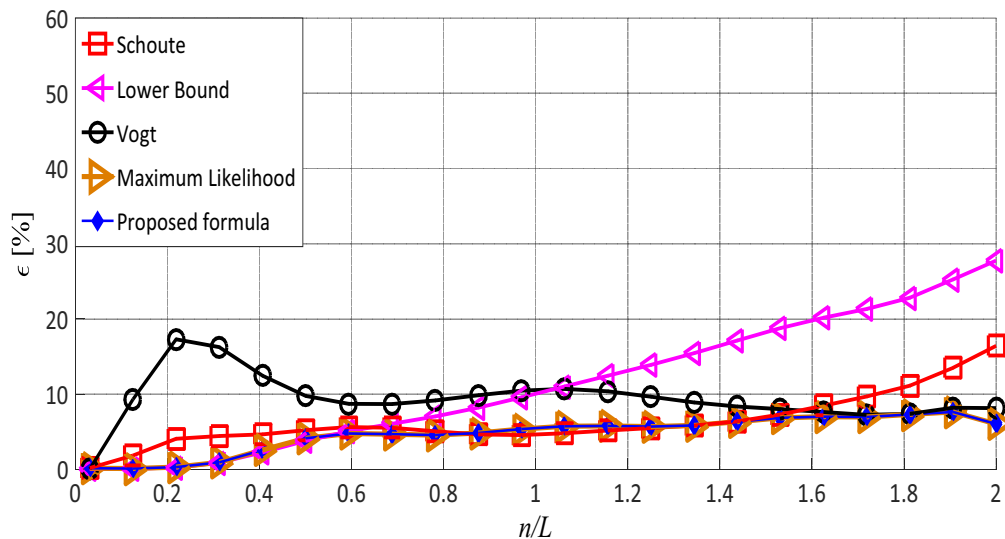
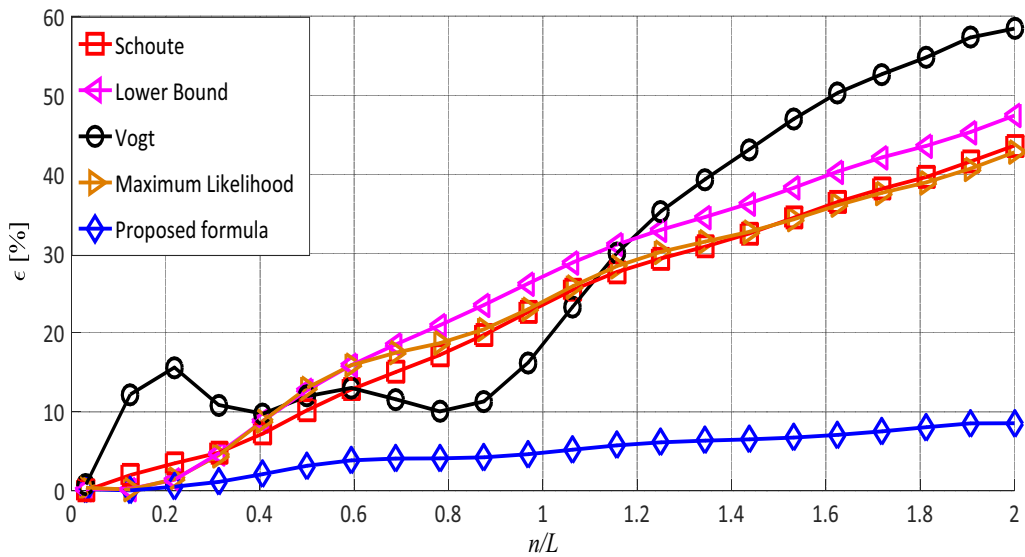
Figure 4.5: Collision recovery probability α as a function of the SNR.

the current Signal-to-Noise Ratio (SNR). Therefore, the higher the collision recovery probability value, the more collided slots can be recovered.

Figure 4.5 shows the values of the capture probabilities versus the average SNR per frame for three receivers proposed in [79]. These three receivers are: 1) the Minimum Mean-Square Error (MMSE) receiver, 2) the Zero Forcing (ZF) receiver with two receiver antennas, and 3) the ZF receiver with a single receiver antenna. The authors of [79] present Bit Error Rate (BER) curves for the different receiver types as a function of the SNR. Thus, the BER can be mapped to a Packet Error Rate (PER) by means of simulations using the same methodology presented in [77]. Afterwards, the collision recovery probability is calculated as $\alpha = (1 - PER)$. In this thesis, the average capture probability is calculated from the corresponding average SNR at the current frame. According to figure 4.5, the higher SNR value is, the higher the collision recovery capability of the reader is. The MMSE receiver gives better performance than the ZF receiver, and the performance increases when the number of received antennas is increased. According to measurements, the practical SNR range for the successful slots is between 4 dB and 12 dB [77].

4.2.4 Performance Analysis

In this section, the performance comparison between the proposed collision recovery aware number of tags estimation and the most common state-of-the-art estimation algorithms are presented. Again, the relative estimation error is used as a comparison metric, which is calculated using Monte-Carlo simulations for FSA with 1000 iterations for each (n/L) value.

(a) System has no collision recovery capability ($\alpha = 0$).(b) System has collision recovery capability ($\alpha = 0.7$).Figure 4.6: Relative estimation error ϵ as a function of the normalized number of tags n/L .

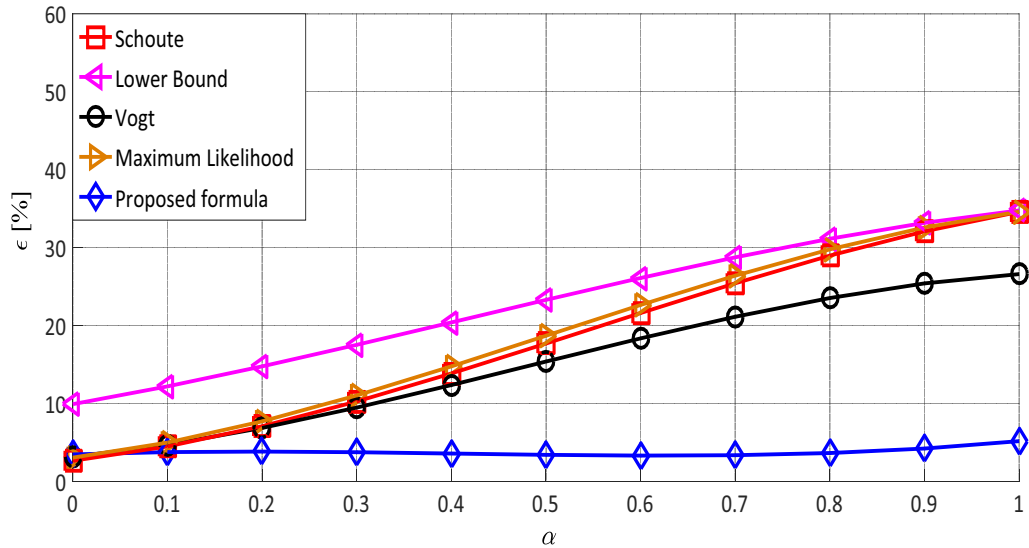
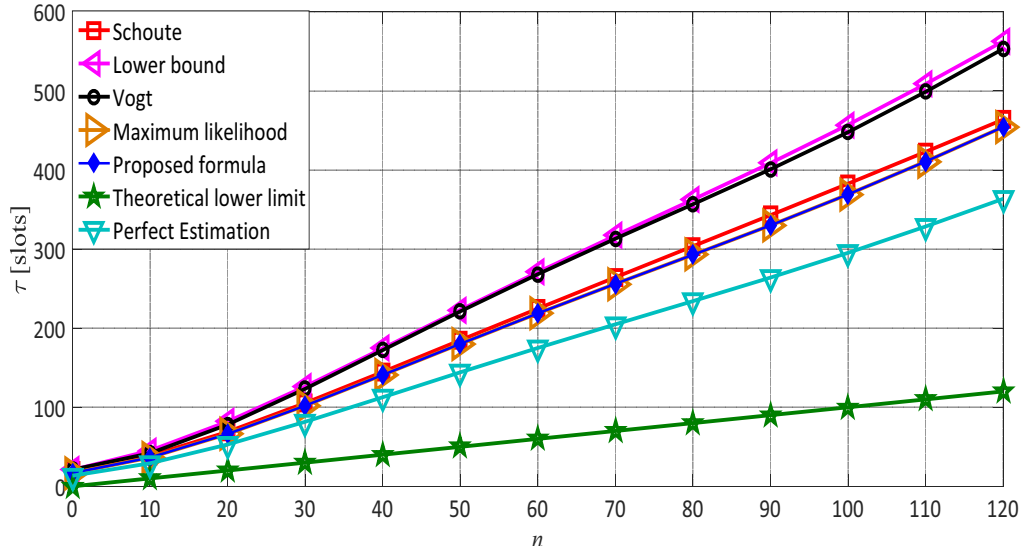
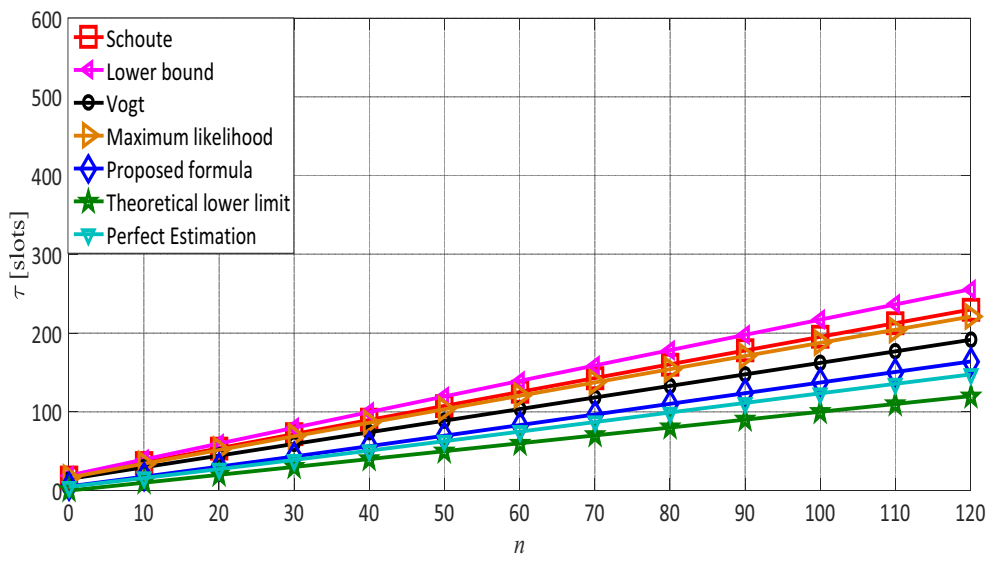


Figure 4.7: Relative estimation error ϵ s a function of the collision recovery probability α using FSA with $L = n$.

Figure 4.6a shows the percentage of the relative estimation error for the proposed system compared to the literature. These simulations assume a system that has no collision recovery capability ($\alpha = 0$). According to figure 4.6a, when the number of tags compared to the frame length increases, the relative estimation error increases as well. This is due to the increase of the number of collided slots per frame. As presented in the previous section, the ML estimation [71] gives better results compared to the existing state-of-the-art. According to figure 4.6a, the proposed system gives identical relative estimation error compared to the classical ML estimation algorithm [71]. Moreover, the proposed system gives a closed form solution of the estimated number of tags instead of the numerical solution proposed in [71]. This advantage decreases the complexity of the estimation algorithm compared to the conventional ML [71].

Figure 4.6b demonstrates the influence of the collision recovery capability on the proposed estimation protocol compared to other estimation protocols. In these simulations, the MMSE RFID reader, which is proposed in [80], is used. These simulations use an average SNR=6 dB. According to figure 4.5, the corresponding collision recovery probability is $\alpha = 0.7$. As shown in figure 4.6b, the proposed solution has more accurate estimation performance compared to the existing methods in the state-of-the-art [56, 68, 71].

Figure 4.7 shows the relative estimation error versus the full range of the collision recovery probability $0 \leq \alpha \leq 1$. Simulation results in 4.7 are calculated using Monte-Carlo simulations for FSA with 1000 iterations for each value of α . In these simulations, the number of tags in the reading area is equal to

(a) System has no collision recovery capability ($\alpha = 0$).(b) System has collision recovery capability ($\alpha = 0.7$).Figure 4.8: Mean identification time τ in slots using FSA as a function of the number of tags in the reading area n .

the frame length, i.e. $n = L$, which is the optimum case for the conventional FSA. Based on figure 4.7, when the value of the collision recovery probability increases, the relative estimation error of all estimation algorithms increases. An exception is the proposed estimation protocol that has almost constant performance, independent of the value of the collision recovery probability. The proposed method takes into account the collision recovery probability, which is produced by the PHY-layer. According to figure 4.7, the relative estimation error of the proposed algorithm is 4 %, which verifies the results of figure 4.6a at $\frac{n}{L} = 1$ and the simulation results of figure 4.6b at $\frac{n}{L} = 1$.

In dense RFID applications, the average identification delay, e.g., the number of slots, is the most important performance metric. Thus, figure 4.8a displays the average identification delay for a number of tags, which is calculated using Monte-Carlo simulations for FSA with 1000 iterations for each n value. In these simulations, FSA is applied with an initial frame length of $L_{ini} = 16$, which is the conventional initial frame length used in the EPCglobal C1 G2 standard [11]. Figure 4.8a shows the identification time for systems with no collision recovery capability ($\alpha = 0$). According to figure 4.8a, the proposed system assigns identical results compared to the conventional ML estimation [71] and better results than the other systems given in the existing state-of-the-art. Figure 4.8b shows the average identification delay for systems exhibiting a collision recovery probability $\alpha = 0.7$. According to figure 4.8b, the average identification delay has decreased for all systems due to the collision recovery capability of the PHY-layer. The proposed system gives better results compared to the existing state-of-the-art due to the performance of estimation only.

According to EPCglobal C1 G2, the RFID reader cannot acknowledge more than a single tag per slot. Therefore, the theoretical lower limit to identify n tags is n slots. According to figure 4.8b, there is still room of improvement between the proposed algorithm and the FSA theoretical lower limit with $\simeq 30\%$. Therefore, in the next chapter, new proposals regarding the FSA frame length taking into consideration the PHY-layer properties are presented.

Chapter 5

Frame Length Optimization

In FSA, there are two main factors controlling the reading efficiency, and hence the reading time in RFID systems. These two factors are precision of the number of tags estimation, which is discussed in chapter 4, and the optimal FSA frame length calculation, which is discussed in this chapter. Previous studies have focused on the frame length calculations using the conventional Dynamic Framed Slotted ALOHA algorithms [54]. In such systems, only the single tag reply is considered as a successful slot, and if multiple tags respond simultaneously, a collision occurs. Then all tags' replies in collided slots are discarded. In such systems, the optimum frame length is equal to the number of tags in the reading area $L = n$ [81]. However, as mentioned before, modern system can recover collisions and convert a part of the collided slots into successful ones [82]. In such systems, it is more beneficial to increase the number of collided slots compared to the number of empty slots by decreasing the optimum frame length. This is because these systems gain more from the collided slots compared to the empty slots by converting the collided slots to successful slots. In addition, most of the previous studies assumed constant slot durations regardless the type of the slot [52, 54, 56, 81]. However, the durations of the slots in RFID systems depend on the slot type, i.e., empty, successful, or collided. In such systems, the empty slot duration is shorter than the collided slot durations and shorter than the successful slot duration. Therefore, in such systems, it is better to increase the frame length, because the losses from the empty slots is less than the losses from the collided ones. To solve the above contradiction, this chapter discusses the optimum DFSA frame length taking into consideration the collision recovery capability and the different slot durations. These optimizations are discussed in different scenarios depending on the RFID system.

This chapter is organized as follows. Section 1 discusses the effect of the different slot durations, where a new closed form solution for the optimum frame length is proposed. In Section 2, the effect of the collision recovery probability

with constant coefficients in addition to the time differences in slot durations is considered. Then, a new closed form solution for the optimum frame length, which maximizes the system performance, is presented. Section 3 illustrates the influence of using multiple collision recovery coefficients assuming constant slot durations, thus eliciting a new reading efficiency called multiple collision recovery coefficients reading efficiency. Then, a novel closed form solution for the optimum frame length is also derived for this system. Section 4 shows a new closed form solution for the optimum frame length for a system; taking into consideration the time difference in slot durations, in addition to the multiple collision recovery coefficients. Finally, Section 5 presents performance comparisons between the proposed frame lengths and the existing state-of-the-art FSA algorithms.

5.1 Time Aware System

Recently, some research groups have focused on optimizing the frame length in case of non-equal slot durations. In [83, 84], the authors proposed a numerical solution for the optimal frame length. This method depends on searching for the optimal frame length, which maximizes the reading efficiency. Moreover, it also depends on the tag-to-reader data rate, which makes the searching process more complicated. In [85], the mean number of resolved tags in unit time is optimized. This is done by considering the different slot durations. However, this approach is based on a complex multidimensional table look-up, which may be time consuming. [86] suggested to search for the optimum frame length that minimizes the mean time needed to resolve a number of tags. However, the authors reached a recursive Bellman-equation, which is difficult to be applied in systems with real-time restrictions.

In this section, we propose a novel closed form solution for the optimum frame length in FSA for RFID systems. The proposed solution gives a direct and linear relation between the frame length L , and the number of tags n in the reading area. Furthermore, it includes a factor representing the different slot durations.

5.1.1 Closed Form Solution for Time Aware System

For calculating the proposed optimal time-aware frame size L_{TA} , which considers the different slot durations, it is important to define the time-aware reading efficiency η_{TA} . The time-aware reading efficiency is defined as the ratio between the total successful time and the total frame time to be

$$\eta_{TA} = \frac{t_s \cdot S}{t_e \cdot E + t_s \cdot S + t_c \cdot C}, \quad (5.1)$$

where $t_s \cdot S$, $t_e \cdot E$, and $t_c \cdot C$ are respectively the expected total successful, idle, and collided times. Furthermore, S , E , and C are the expected numbers of successful, empty and collided slots. t_s , t_e , t_c are respectively the successful, idle, and collided slot durations.

The next step is to derive the new optimum frame length L_{TA} under the time-aware environment. According to EPCglobal C1 G2, L is always integer. Thus, L_{TA} can be optimized by finding the value of L which maximizes the time-aware reading efficiency. This is achieved by differentiating the reading efficiency in (5.1) with respect to the frame length L and equating the result to zero, where L can only have integer values

$$\frac{\partial \eta_{TA}}{\partial L} = 0. \quad (5.2)$$

According to (3.1), E , S , and C are function of L . Taking into consideration that t_e , t_s , t_c are constants for a given system specification, the equation is

$$\frac{(t_e E + t_s S + t_c C)t_s \frac{\partial}{\partial L}(S) - t_s S \frac{\partial}{\partial L}(t_e E + t_s S + t_c C)}{(t_e E + t_s S + t_c C)^2} = 0. \quad (5.3)$$

After multiplying both sides by the denominator and dividing by t_s (non-zero constant), the equation can be simplified to be

$$(t_e E + t_c C) \frac{\partial}{\partial L}(S) + t_s S \frac{\partial}{\partial L}(S) = S \frac{\partial}{\partial L}(t_e E + t_c C) + t_s S \frac{\partial}{\partial L} S. \quad (5.4)$$

After subtracting the term which is multiplied by t_s , the equation finally becomes

$$\{t_e E + t_c C\} \frac{\partial}{\partial L}(S) = S \frac{\partial}{\partial L} \{t_e E + t_c C\}. \quad (5.5)$$

Then, substituting by the values of E , S , and C from (3.1) leads to

$$\begin{aligned} & \left\{ t_e L \underbrace{\left(1 - \frac{1}{L}\right)^n}_{E} + t_c \underbrace{\left(L - \left(1 - \frac{1}{L}\right)^{n-1} (L - n - 1)\right)}_C \right\} \\ & \times \underbrace{\frac{\partial}{\partial L} n \left(1 - \frac{1}{L}\right)^{n-1}}_S \\ & = n \underbrace{\left(1 - \frac{1}{L}\right)^{n-1}}_S \\ & \times \frac{\partial}{\partial L} \left\{ t_e L \underbrace{\left(1 - \frac{1}{L}\right)^n}_{E} + t_c \underbrace{\left(L - \left(1 - \frac{1}{L}\right)^{n-1} (L - n - 1)\right)}_C \right\}. \end{aligned} \quad (5.6)$$

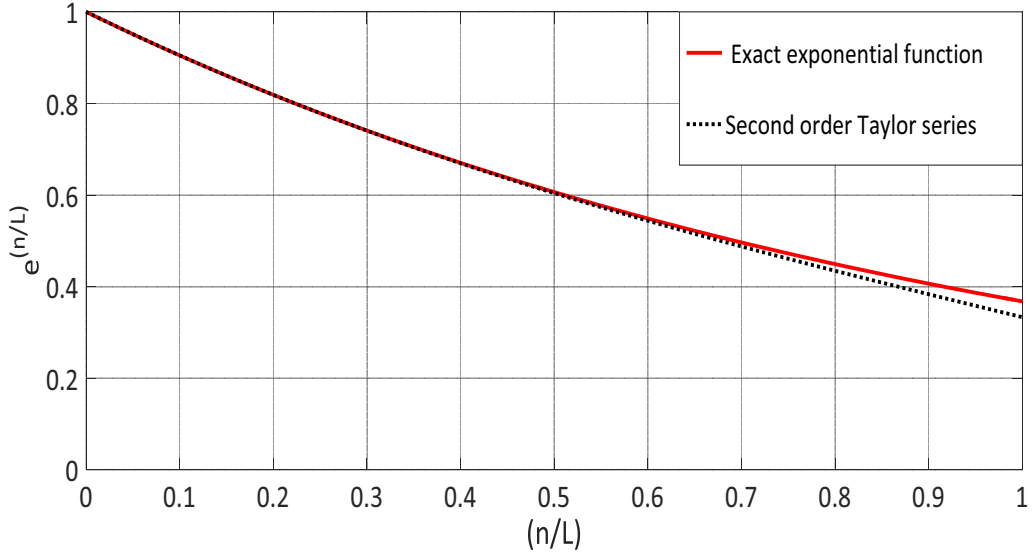


Figure 5.1: The exponential function $e^{-\frac{n}{L}}$ compared to the second order Taylor series approximation

By simplifying the result, the final exact equation for the proposed time-aware frame length is given by the following implicit equation

$$\left(1 - \frac{n}{L_{TA}}\right) = (1 - C_t) \left(1 - \frac{1}{L_{TA}}\right)^n, \quad (5.7)$$

where n is the number of tags, and C_t is the slot durations constant defined as $C_t = \frac{t_e}{t_c}$ with $0 < C_t \leq 1$, as $t_e \leq t_c$ in practical applications. Equation (5.7) shows the exact relation between the proposed time-aware frame length L_{TA} and the number of tags n .

Unfortunately, (5.7) is an implicit equation. Thus, an approximation is used to convert it to explicit equation. The equation can be expressed as

$$\left(1 - \frac{1}{\beta}\right) = (1 - C_t) \left(1 - \frac{1}{\beta n}\right)^n, \quad (5.8)$$

where $\beta = \frac{L_{TA}}{n}$. As we are focusing on systems with many tags, the following approximation can be used

$$\lim_{n \rightarrow \infty} \left(1 - \frac{1}{\beta n}\right)^n = e^{-\frac{1}{\beta}}, \quad (5.9)$$

which simplifies (5.7) to be

$$\left(1 - \frac{1}{\beta}\right) = (1 - C_t) e^{-\frac{1}{\beta}} \quad (5.10)$$

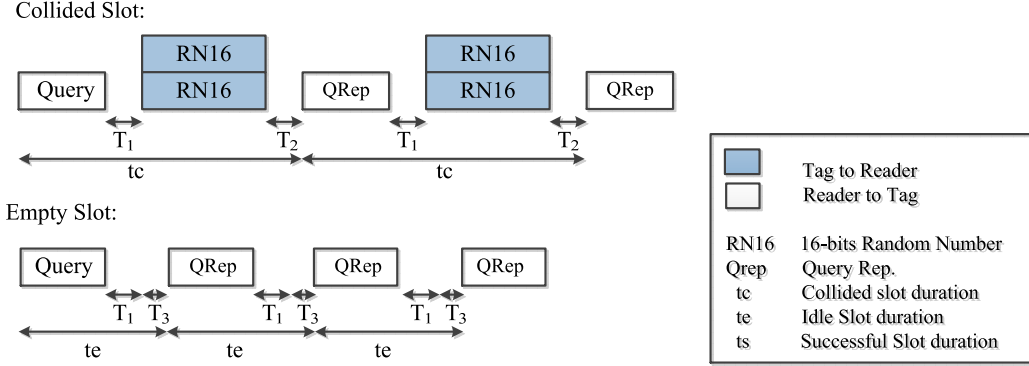


Figure 5.2: FSA inventory rounds for collided and empty slots according to the EPCglobal C1 G2 standard

The analysis of (5.7) indicates that the relevant values for $\beta = \frac{L_{TA}}{n}$ are in the region close to 1. Hence, a Taylor series for $e^{-\frac{1}{\beta}}$ around one is developed which leads to be

$$e^{-\frac{1}{\beta}} \simeq 1 - \frac{1}{\beta} + \frac{1}{2\beta^2} \quad (5.11)$$

According to figure 5.1, this approximation is very accurate in the range of $\frac{n}{L} \leq 1$. After substituting by (5.10) and with additional simplifications, it leads to be

$$\beta^2 C_t - \beta C_t + 0.5(C_t - 1) = 0 \quad (5.12)$$

By solving (5.12), and rejecting the negative solution we finally obtain

$$L_{TA} = \frac{n}{2} \left(1 + \sqrt{\frac{2}{C_t} - 1} \right). \quad (5.13)$$

The proposed equation gives a linear relation in reference to the number of tags n , and includes the slot durations constant C_t , which can be easily varied as a function of the transmission rate and the working standard.

5.1.2 Slot Durations Constant Calculation for the EPCglobal C1 G2

In this section, the calculation method of the slot duration constant C_t from the PHY layer parameters is discussed. Figure 5.2 shows the timing constraints of FSA inventory rounds for collided and empty slots according to the EPCglobal C1 G2 standard [11]. Each slot contains different sequences of reader-to-tag commands and corresponding tags' replies. The slot durations constant is

$$C_t = \frac{t_e}{t_c}. \quad (5.14)$$

Table 5.1: Available slots duration constants C_t of the EPCglobal C1 G2 standard

Divide Ratio: DR	Modulation: M	Pilot Length: n_p	C_t
8	1	0	0.47
		12	0.41
	2	4	0.35
		16	0.28
	4	4	0.23
		16	0.18
	8	4	0.14
		16	0.1
	1	0	0.7
		12	0.65
	2	4	0.57
		16	0.5
64/3	4	4	0.43
		16	0.35
	8	4	0.3
		16	0.22

As shown from figure 5.2, the empty slot duration t_e is given by

$$t_e = T_{QRep} + T_1 + T_3. \quad (5.15)$$

Here, T_{QRep} is the query repeat command time

$$T_{QRep} = T_{FS} + T_{command}, \quad (5.16)$$

with, $T_{FS} = 3.5 \cdot T_{ari}$, $T_{command} = 6 \cdot T_{ari}$, and $T_{ari} = \frac{DR}{2.75} T_{pri}$. By substituting in (5.16) we get

$$T_{QRep} = 3.5 \cdot DR \cdot T_{pri}, \quad (5.17)$$

where T_{ari} is reader symbol duration, $T_{pri} = \frac{1}{BLF}$, BLF is the tag backscatter link frequency and DR is the so-called divide ratio constant that can take two values $DR = 8$ or $\frac{64}{3}$. Finally, M equals to 1, 2, 4, or 8, which represents the modulation types FM0, Miller 2, 4, or 8, respectively. T_1 is the time from the reader transmission to the tag response, which can be expressed by

$$T_1 = \max \{DR \cdot T_{pri}, 10 \cdot T_{pri}\} \quad (5.18)$$

Next, T_3 is the time that the reader waits after T_1 before issuing another command. As it has no constraints, it can be assumed to be zero. After substituting by (5.17 and 5.18) in (5.15), t_e can be expressed by

$$t_e = T_{pri} \cdot (3.5 \cdot DR + \max\{DR, 10\}). \quad (5.19)$$

Next, the collided slot duration t_c is given by

$$t_c = T_{QRep} + T_1 + T_2 + T_{RN16}, \quad (5.20)$$

where T_2 is the reader response time starting from the end of the tag response, $T_2 = 6 \cdot T_{pri}$, and T_{RN16} is the duration of 16 bits temporary data, 6 bits preamble, n_p pilot tones, i.e. $T_{RN16} = (22 + n_p) \cdot T_{pri}$. Therefore, t_c can be expressed by

$$t_c = T_{pri} \cdot (3.5 \cdot DR + \max\{DR, 10\} + 6 + 22 \cdot M + n_p \cdot M). \quad (5.21)$$

From (5.19) and (5.21), the final expression of C_t is

$$C_t = \frac{3.5 \cdot DR + \max\{DR, 10\}}{3.5 \cdot DR + \max\{DR, 10\} + 6 + 22 \cdot M + n_p \cdot M}. \quad (5.22)$$

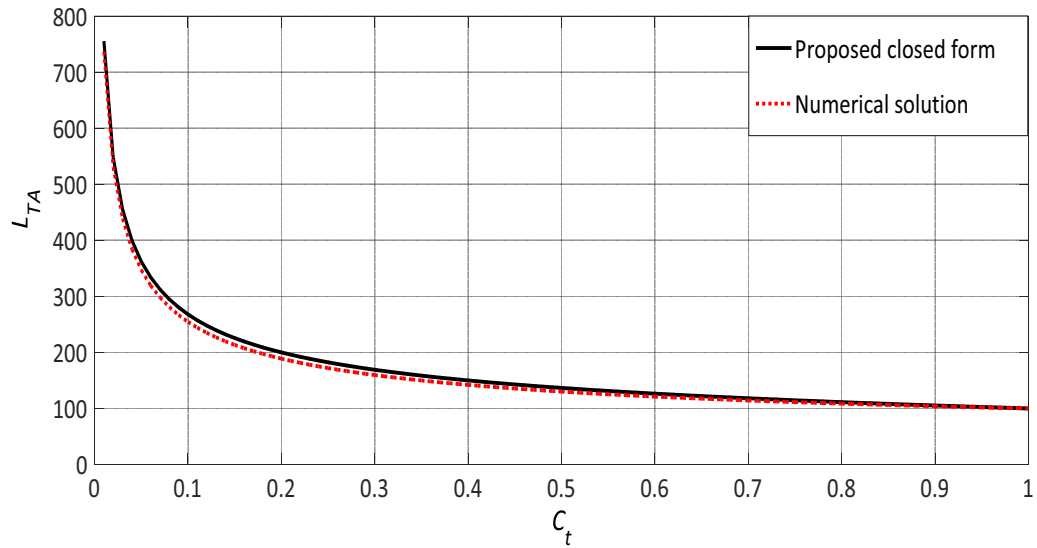
Table 5.1 shows the values of the slot durations constant of the EPCglobal C1 G2 standard. According to table 5.1, the slot durations constant C_t varies from 0.1 to 0.7, and this affects the optimum frame length directly.

5.1.3 Closed Form Solution vs. Numerical Solution

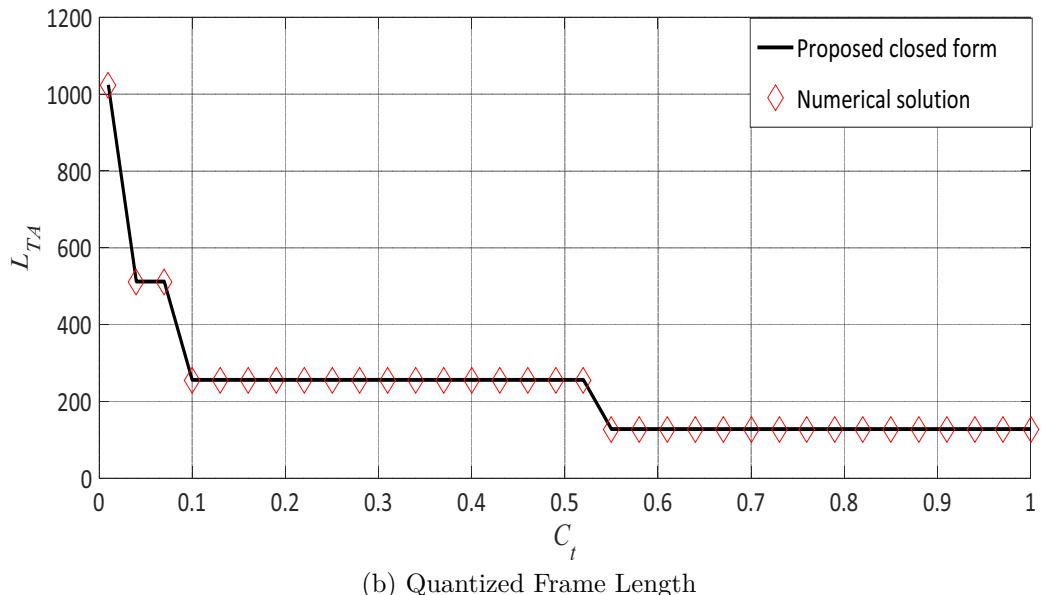
Figure 5.3a displays the behavior of the proposed frame length formula in (5.13) compared to the numerical solution in [86] for the complete range of the slot durations constant C_t for $0 < C_t \leq 1$. In the simulation, a fixed number of $n = 100$ tags is used. According to figure 5.3, the proposed equation approaches the numerical solution proposed in [86] in the full range of C_t with very small bias coming from the Taylor series approximation in (5.11). According to the EPCglobal C1 G2 standard [11], the frame length can take only quantized values (power of 2). Thus, in figure 5.3b only the next quantized frame length is selected, which decreases the effect of the Taylor approximation. According to 5.3b, the proposed frame length fully matches the numerical solution in the full range of C_t .

5.1.4 Mean Reading Time Reduction

In conventional FSA systems, the slot durations are considered as constant slots. Thus, the total identification time is calculated by counting the average total number of slots needed to identify the complete number of tags in the



(a) Non-quantized Frame length



(b) Quantized Frame Length

Figure 5.3: Time aware optimum frame length L_{TA} using (5.13) compared to the numerical solution as a function of the slot durations constant C_t ($n = 100$ tags). The conventional case with identical slot durations corresponds to $C_t = 1$.

reading area. Then, according to literature, the mean reduction in number of slots is calculated according to the following equation

$$\zeta \% = \left(\frac{\text{Slots}_{\text{conv.}} - \text{Slots}_{\text{proposed}}}{\text{Slots}_{\text{conv.}}} \right) \times 100 \quad (5.23)$$

In time aware systems, the slot durations are variable. Therefore, the total identification time can only be calculated as time in seconds. Afterwards, the percentage of mean reading time reduction is calculated as

$$\zeta_t \% = \left(\frac{T_{\text{conv.}} - T_{\text{proposed}}}{T_{\text{conv.}}} \right) \times 100 \quad (5.24)$$

Figure 5.4 shows simulation results for the reading time reduction of the proposed optimal time-aware frame length L_{TA} with reference to the classical optimal frame length $L = n$ as a function of the slot durations constant C_t . These simulations assume a perfect knowledge of the number of tags n . According to the figure, $C_t = 0$ means that the idle slot durations time $t_e = 0$. In this case, the optimum frame length L is theoretically infinite. According to the EPCglobal C1 G2 standard [11], the frame length takes only quantized values (power of 2). According to figure 5.3b, the number of tags in the reading area $n = 100$ tags. Thus, the quantized optimum frame length is $L = 1024$ slots. In this case, the proposed time-aware frame length can reduce the average reading time up to 12% compared to the conventional optimization criterion. When $C_t = 1$, the slot durations have identical length i.e., $t_e = t_c$, as in the conventional FSA, therefore, the reading efficiency in this case is obtained when $L = n$.

In practice, the number of tags in the interrogation region is unknown. Hence, the anti-collision algorithms in real RFID systems consist of two stages. One estimates the number of tags in the interrogation area \hat{n} whereas the other calculates the optimal frame length L_{opt} based on \hat{n} for maximizing the reading efficiency. Figure 5.5 illustrates the mean reduction of the reading time using the proposed time-aware frame length for the proposed ML number of tags estimation and the most well-known tag estimation algorithms using the value of the slot durations constant $C_t = 0.2$. The main purpose of these simulations is to show the practical effect on the reading time by working with the proposed frame length using different tag estimation algorithms. Each curve presents the mean reduction of the reading time between the proposed frame length and the conventional frame length $L = n$ using the same estimation algorithm. Results in figure 5.5 is calculated using Monte-Carlo simulations for FSA with 1000 iterations for each n value.

In case of the Lower bound [54] and Schoultz [52] number of tags estimation algorithms, the reading time is reduced by 13% to 16%. In case of more

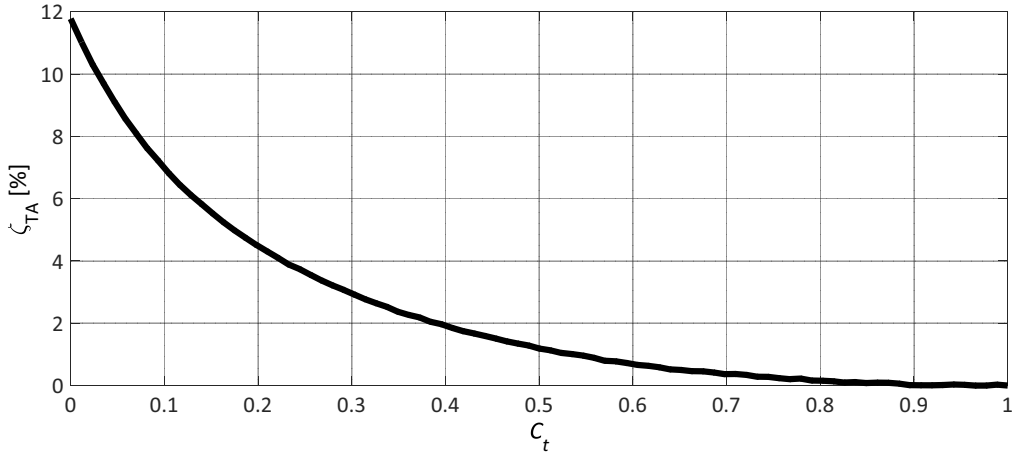


Figure 5.4: Percentages of the mean reading time reduction ζ_{TA} using the proposed TAFSA for an ideally known number of tags as a function of the slot duration constant C_t

accurate estimation algorithm such as Vogt [81] and the proposed ML in chapter 4, the mean reduction of reading time is between 9 % and 12 %. According to figure 5.5, the better the estimation algorithms, the less reading time reduction, because it decreases the number of iterations in FSA process. However, using a non-accurate number of tags estimation algorithms, FSA needs more iterations, with more FSA frame length adaptations. That gives more importance for the proposed formula compared to the classical frame length adaptations.

5.2 Time and Collision Recovery System

As mentioned in chapter 4, modern RFID readers can convert a part of collided slots into successful slots, which is called the collision recovery capability α . According to the state-of-the-art [58, 86, 87], the previous research is divided into three diverse groups. The first group considered only the average collision recovery probability for the frame length optimizations, such as [58]. The authors propose a closed form equation for the optimum frame length maximizing the reading throughput per frame. The second group observes only the different slot durations, such as [86, 87] as shown in the first proposal in the previous section. However, no closed form solution for the optimum frame length is derived. They calculate the optimum frame length numerically. The third group contemplates the different slot durations and the collision recovery probability, such as [84, 88, 89]. Both [84, 88] give numerical solutions for the optimum frame length versus the collision recovery probability and the number of tags. The main problems of their numerical solutions are the multiple degrees of freedom. The solutions require a complex multidimensional look-up table, which has to

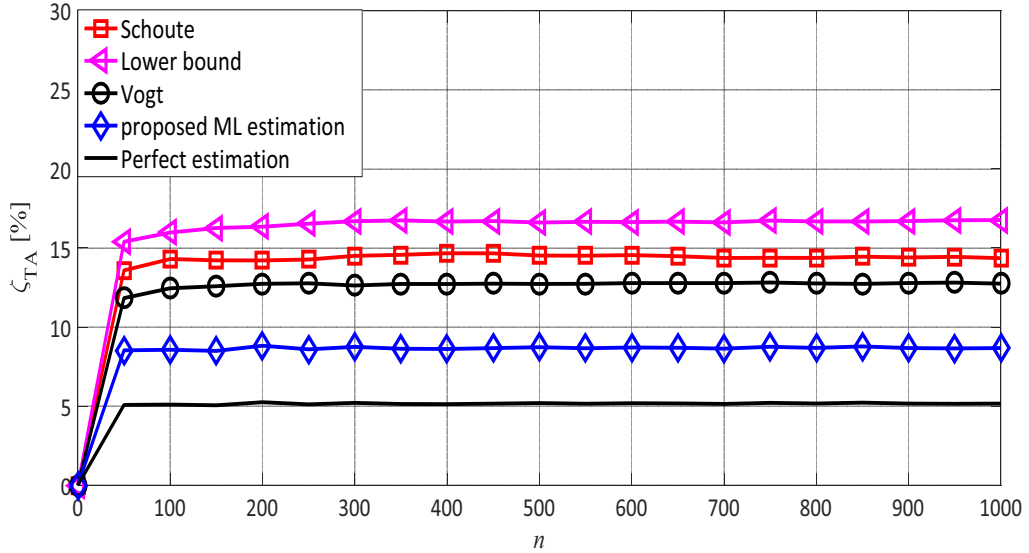


Figure 5.5: Percentages of the mean reading time reduction ζ_{TA} as a function of the number of tags n using the proposed TAFSA compared to the conventional frame length $L = n$ for different estimation algorithms, $C_t = 0.2$.

consider all possible degrees of freedom. The authors in [89] use curve fitting to find a closed form solution for the optimum frame length at a specific collision recovery probability and timing. However, this solution cannot be generalized for all values of slot's timing and collision recovery probabilities.

In this section, a closed form solution for the optimum frame length is derived by optimizing the reading throughput per frame, which does not require any look-up table [84, 88]. In addition, the average collision recovery probability and the different slot durations are considered. Moreover, the calculation method of the collision recovery probability based on the PHY layer is clarified.

5.2.1 Closed Form Solution for Time and Collision Recovery System

In this subsection, the proposed optimal time and collision recovery aware frame size L_{TCA} is derived, which considers the different slot durations and the collision recovery probability. Thus, a new reading efficiency called Time and Collision Recovery Aware reading efficiency η_{TCA} is introduced. The main properties of this efficiency are the consideration of the different slot durations and the average collision recovery probability.

In this efficiency, we added the average collision recovery probability α to the time aware efficiency in (5.1). Therefore, the time and collision recovery probability aware efficiency can then be written as

$$\eta_{TCA} = \frac{t_s \cdot S_c}{t_e \cdot E_c + t_s \cdot S_c + t_c \cdot C_c}. \quad (5.25)$$

where E_c , S_c and C_c are respectively the expected number of empty, successful, and collided slots after adding the effect of the collision recovery probability α . Their relation is given by

$$E_c = E, S_c = S + \alpha \cdot C, C_c = (1 - \alpha) \cdot C. \quad (5.26)$$

The target is to find the optimum frame length L_{TCA} which maximizes the proposed reading efficiency in (5.25). This is again achieved by differentiating the reading efficiency η_{TCA} of (5.25) with respect to the frame length L and equate the result to zero.

Clearly, the frame length L is an integer value. Therefore, differentiating the equation is not fully correct. However, the resulting error is negligible as it is shown later. According to (5.26), E_c , S_c , and C_c are functions of L . However, t_e , t_s , t_c are constants for a given system configuration. Thus, the equation can be simplified to be

$$\frac{(t_e E_c + t_s S_c + t_c C_c) t_s \frac{d}{dL}(S_c) - t_s S_c \frac{d}{dL}(t_e E_c + t_s S_c + t_c C_c)}{(t_e E_c + t_s S_c + t_c C_c)^2} = 0 \quad (5.27)$$

After multiplying both sides by the denominator and dividing by t_s (non-zero constant), and subtracting the term, which is multiplied by t_s , the equation results in

$$(t_e E_c + t_c C_c) \frac{d}{dL}(S_c) = S_c \frac{d}{dL}(t_e E_c + t_c C_c). \quad (5.28)$$

Then, the substitution by the values of E_c , S_c , and C_c from (5.26) leads to the final exact equation for the proposed time and collision recovery probability aware frame length

$$\begin{aligned} & (1 - \alpha) \cdot (1 - \frac{n}{L_{TCA}}) + \alpha \cdot C_t \cdot \left(1 - \frac{1}{L_{TCA}}\right) \\ & + (C_t - 1) \cdot (1 - \alpha) \cdot \left(1 - \frac{1}{L_{TCA}}\right)^n = 0, \end{aligned} \quad (5.29)$$

where n is the number of tags, and C_t is the slot durations constant defined by $C_t = \frac{t_e}{t_c}$. Equation (5.29) shows the exact relation between the proposed collision recovery, the time-aware optimum frame length L_{TCA} and the number of tags n . This equation takes into consideration the collision recovery probability and the different slot durations. However, this solution depends on a recursive equation. For reaching an explicit equation, (5.29) can be expressed by

$$\begin{aligned} & (1 - \alpha) \cdot (1 - \frac{1}{\beta}) + \alpha \cdot C_t \cdot \left(1 - \frac{1}{\beta n}\right) \\ & + (C_t - 1) \cdot (1 - \alpha) \cdot \left(1 - \frac{1}{\beta n}\right)^n = 0, \end{aligned} \quad (5.30)$$

where $\beta = \frac{L_{TCA}}{n}$. As we are focusing on systems with many tags n , again the following approximation can be used

$$\lim_{n \rightarrow \infty} \left(1 - \frac{1}{\beta n}\right)^n = e^{-\frac{1}{\beta}}, \quad (5.31)$$

which simplifies (5.30) to

$$(1 - \alpha) \cdot \left(1 - \frac{1}{\beta}\right) + \alpha \cdot C_t \cdot \left(1 - \frac{1}{\beta n}\right) + (1 - \alpha) \cdot (C_t - 1) e^{-\frac{1}{\beta}} = 0. \quad (5.32)$$

The analysis of (5.29) indicates that the relevant values for $\beta = \frac{L_{TCA}}{n}$ are again in the region close to one [84]. Hence, we can develop a Taylor series for $e^{-\frac{1}{\beta}}$ around one which leads to be

$$e^{-\frac{1}{\beta}} \simeq 1 - \frac{1}{\beta} + \frac{1}{2\beta^2}. \quad (5.33)$$

After substituting in (5.32) and some additional simplifications, we get

$$\beta^2 C_t - \beta C_t (1 + \frac{\alpha}{n}) - 0.5 (1 - \alpha) \cdot (1 - C_t) = 0. \quad (5.34)$$

As $\frac{\alpha}{n} \ll 1$, (5.34) can be expressed by

$$\beta^2 C_t - \beta C_t - 0.5 (1 - \alpha) \cdot (1 - C_t) = 0. \quad (5.35)$$

By solving (5.35) and rejecting the negative solution we finally reach the final solution

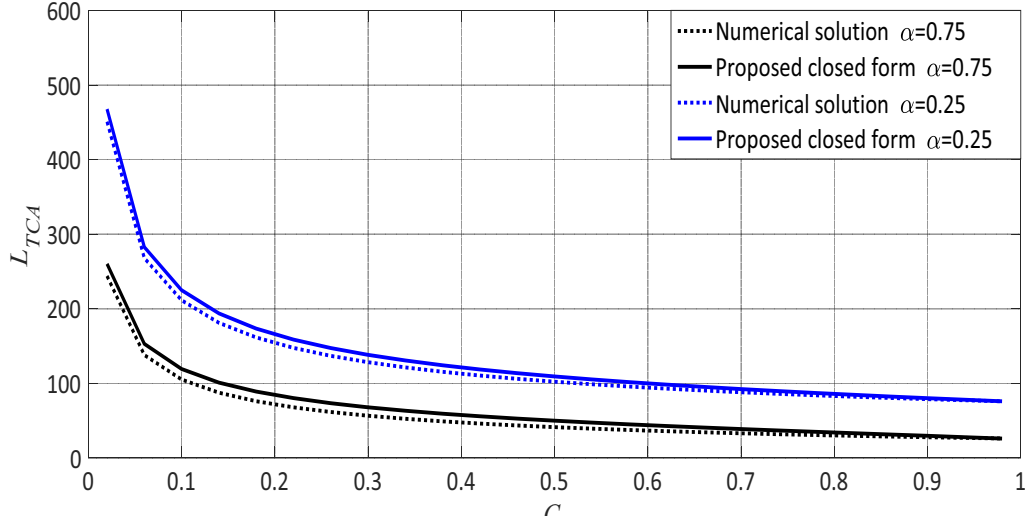
$$L_{TCA} = \frac{n}{2} \left((1 - \alpha) + \sqrt{(1 - \alpha)^2 + \frac{2}{C_t} (1 - \alpha) \cdot (1 - C_t)} \right). \quad (5.36)$$

According to state-of-the-art, [88] is the only work which used the same performance metric η_{TCA} to get the optimum frame length. However, in this work the authors did not propose any closed form solution and they have to rely on multi-dimensional look-up tables.

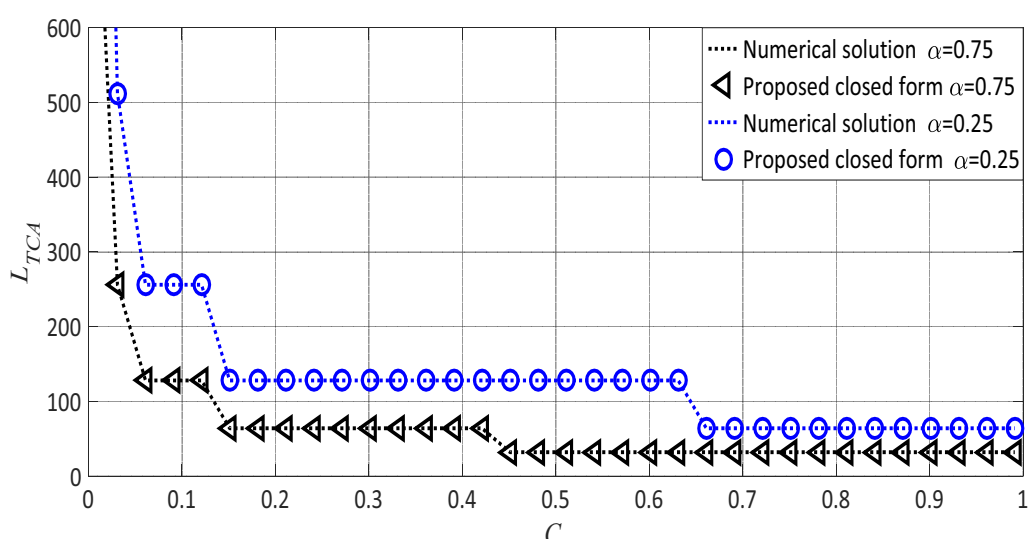
As mentioned before, the value of α strongly depends on the receiver type and the SNR. The value of collision recovery α could be one of the values of figure 4.5, depending on the receiver type and the value of SNR.

5.2.2 Closed Form Solution vs. Numerical Solution

Now, the proposed closed form equation in (5.36) is compared with the numerical results in [88]. Figure 5.6a shows both algorithms for the full range of the slot durations constant C_t . Assuming a fixed number of $n = 100$ tags, figure



(a) Non-quantized Frame Length.



(b) Quantized Frame Length.

Figure 5.6: Optimum frame length L_{TC_A} using (5.36) compared to the numerical solution as a function of the slot durations constant C_t ($n = 100$ tags) for the capture probabilities $\alpha = 0.25, 0.5, 0.75$.

5.6a indicates that the proposed closed form approaches the numerical solution for different α in the full range of C_t . Due to the Taylor series approximations in (5.33), there are slight differences between the proposed closed form and the numerical solution. However, as previously mentioned, the EPCglobal C1 G2 standard [11] frame length is allowed to take only quantized values (power of 2). Thus, the next quantized frame length is selected and this eliminates the approximation error. Figure 5.6b shows that the proposed frame length fully matches the numerical solution in the full range of C_t .

5.2.3 Mean Reduction of Reading Time

As mentioned previously, the most common performance metric of comparison is the mean reduction in reading time compared to the conventional frame length $L = n$. Figure 5.7 illustrates simulation results for the reading time reduction of the proposed optimal TCA frame length L_{TCA} with reference to the classical optimal frame length $L = n$ for $C_t = 0.2$ and different values of the collision recovery probability α . These simulations assume a perfect knowledge of the number of tags n . According to figure 5.7, the mean reading time reduction increases when the value of α increases, which gives more advantage to the proposed solution compared to the conventional one. Results in figure 5.7 is calculated using Monte-Carlo simulations for FSA with 1000 iterations for each n value.

Figure 5.8 shows the mean reduction of the reading time using the proposed TCA frame length compared to the conventional frame length $L = n$ taking into consideration the effect of the number of tags estimation algorithms. The simulations use $C_t = 0.2$ and average collision recovery capability $\alpha = 0.7$. Results in figure 5.8 is calculated using Monte-Carlo simulations for FSA with 1000 iterations for each n value. According to figure 5.8, the proposed solution results in 18 % average saving in reading time compared to the conventional FSA using the proposed ML estimation algorithm. As discussed in the previous section, the minimum mean reading time reduction is obtained upon having perfect knowledge of the number of tags in the reading area, because it results in the minimum number of iterations for FSA process.

5.3 Multiple Collision Recovery System

To simplify the analysis, previous sections considered systems with equal collision recovery probability coefficients regardless the number of collided tags per slot. For example, the probability to resolve two collided tags is equal to the probability to resolve three or four collided tags per slot. However, in practice, the probability of recovering one tag from two collided tags is more than the probability to identify a single tag from three collided tags. Therefore, in this

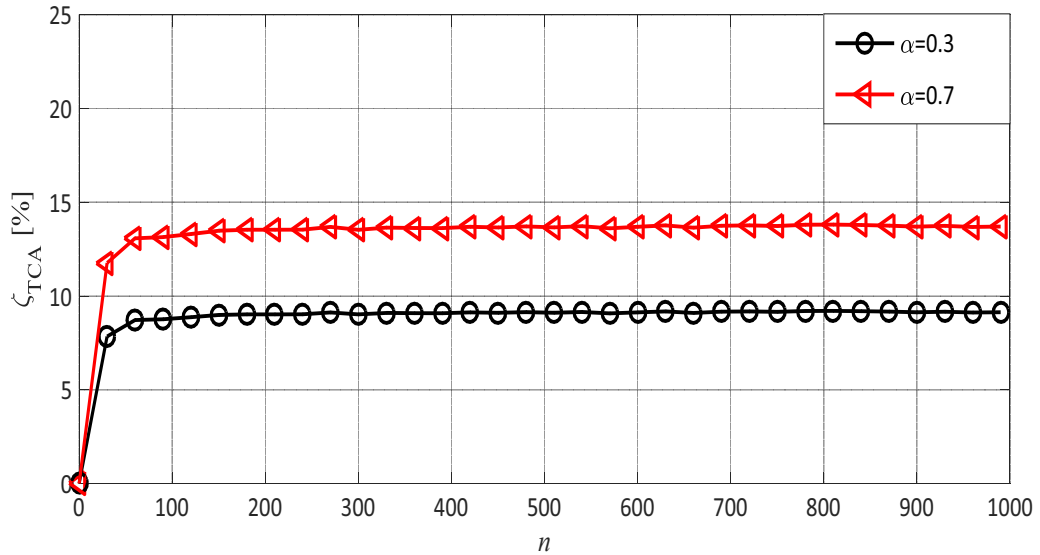


Figure 5.7: Percentages of the mean reading time reduction ζ_{TCA} using the proposed TCA as a function of the number of tags n compared to the conventional frame length $L = n$ for perfect number of tags estimation using $C_t = 0.2$ and different values of α .

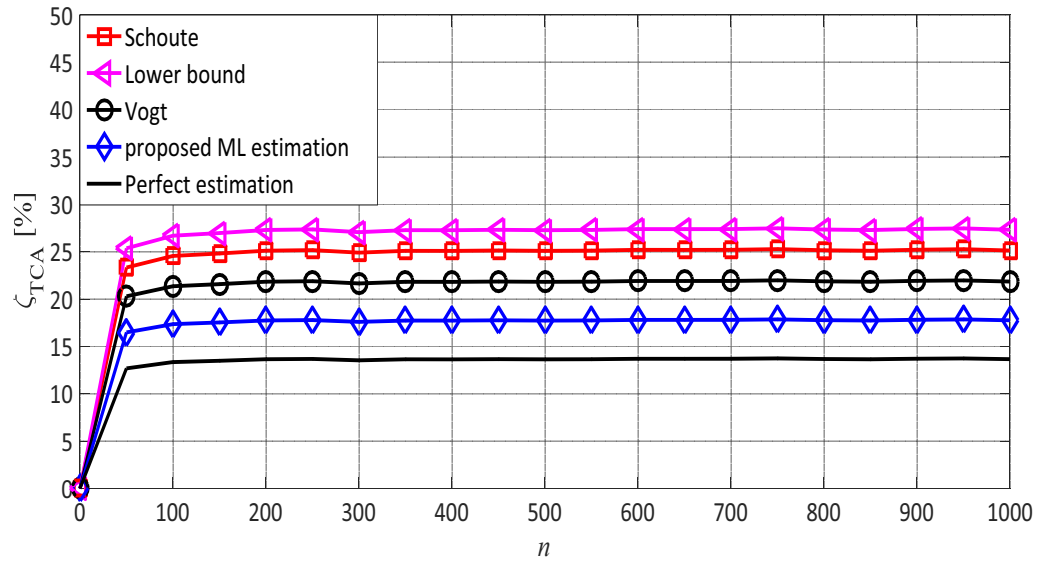


Figure 5.8: Percentages of the mean reading time reduction ζ_{TCA} using the proposed TCA as a function of the number of tags n compared to the conventional frame length $L = n$ for different anti-collision algorithms using $C_t = 0.2$ and $\alpha = 0.7$.

section, the collision recovery probability is considered as a variable coefficient α_i , where i is the number of collided tags per slot.

In this section, a new reading efficiency metric called multiple collision recovery coefficients reading efficiency η_{MCRC} is proposed. It includes a unique collision resolving coefficient for each number of collided tags. Hence, a novel closed form solution for the optimum FSA frame length is proposed, which maximizes the proposed efficiency metric. Then, these coefficients is calculated based on a simple RFID reader model to show how the proposed system could be applied on real-life applications.

5.3.1 Closed Form Solution for Multiple Collision Recovery Aware System

This section introduces a new FSA efficiency metric called Multiple Collision Recovery Coefficients Reading Efficiency η_{MCRC} . Afterwards, a closed form solution for the new optimum frame length L_{MCRC} under multiple collision recovery coefficients environment is presented.

The main contribution of this efficiency is that it contains a specific collision recovery coefficient α_i for each probability of collision $P_{col.}(i)$. These new coefficients indicate the ability of the reader to recover one tag from i collided tags. The proposed reading efficiency η_{MCRC} is expressed by

$$\eta_{MCRC} = P(1) + \sum_{i=2}^n \alpha_i P_{col.}(i). \quad (5.37)$$

Figure 5.9 presents the distribution of the average collision probability in a frame of length $0.5 \cdot n \leq L \leq 2 \cdot n$ uniformly. The simulations results are done using Monte-Carlo simulations of the FSA algorithm under condition of frame length $0.5 \cdot n \leq L \leq 2 \cdot n$ uniformly, which is the practical range of the frame length in RFID systems according to [84].

As shown in figure 5.9, the probability that the collided slot comes from two, three, or four collided tags is equal to $P_{col.}(2) + P_{col.}(3) + P_{col.}(4) \simeq 96\%$, and for the remaining tag collisions $\sum_{i=5}^n P_{col.}(i) \simeq 4\%$. Moreover, the values of the collision recovery coefficients α_i , $i > 4$ are practically very small. Therefore, the proposed η_{MCRC} for the practical RFID environment can be expressed as

$$\eta_{MCRC} = P(1) + \alpha_2 P_{col.}(2) + \alpha_3 P_{col.}(3) + \alpha_4 P_{col.}(4), \quad (5.38)$$

where α_2 , α_3 , and α_4 are respectively the second, third, and fourth collision recovery coefficients.

The next step is to derive a closed form solution for the new optimum frame length L_{MCRC} under multiple collision recovery coefficients environment. L_{MCRC} can be optimized by finding the value of L which maximizes η_{MCRC} . According to [90], if $L \gg 1$, and $n \gg i$, we can assume a Poisson distribution

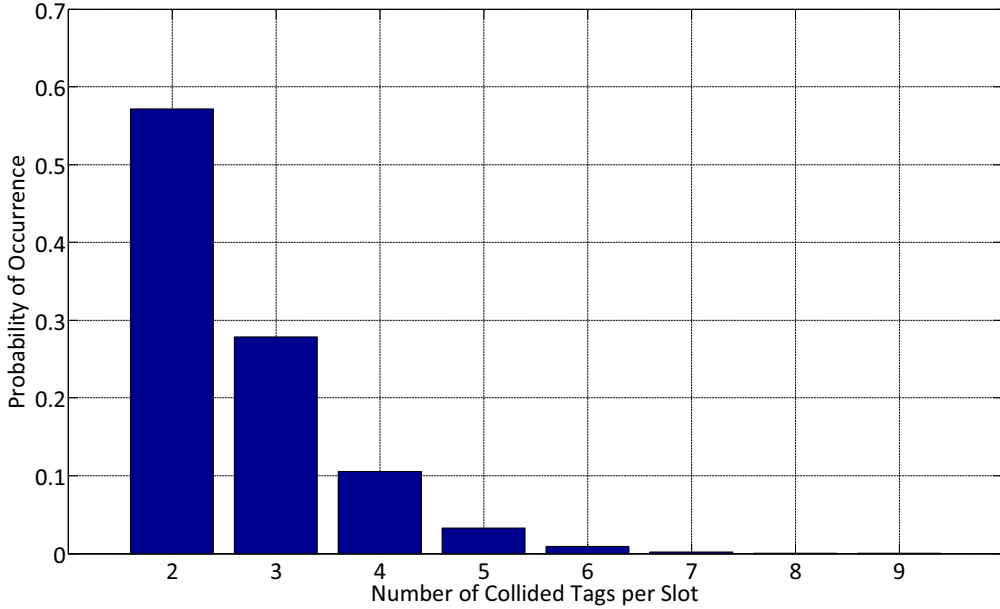


Figure 5.9: Distribution of collision probability for a collided slot in FSA, under condition of $\frac{n}{2} \leq L \leq 2n$.

$$P(i) \simeq \frac{1}{i!} \cdot \beta^{-i} \cdot e^{-\frac{1}{\beta}}, \quad (5.39)$$

where $\beta = \frac{L}{n}$. After substituting with (5.39) in (5.38) we get

$$\eta_{MCRC} = e^{-\frac{1}{\beta}} \cdot \left(\beta^{-1} + \frac{\alpha_2}{2} \beta^{-2} + \frac{\alpha_3}{6} \beta^{-3} + \frac{\alpha_4}{24} \beta^{-4} \right). \quad (5.40)$$

Now we have to find the value of β which maximizes η_{MCRC} . This is achieved by differentiating the reading efficiency in (5.40) with respect to β and equate the result to zero. After differentiating, the equation can be simplified to be

$$-e^{-\frac{1}{\beta}} \cdot \left(\beta^{-2} + \beta^{-3}(\alpha_2 - 1) + \frac{\beta^{-4}}{2}(\alpha_3 - \alpha_2) + \frac{\beta^{-5}}{6}(\alpha_4 - \alpha_3) - \frac{\beta^{-6} \cdot \alpha_4}{24} \right) = 0. \quad (5.41)$$

Multiplying the equation by $-e^{\frac{1}{\beta}} \cdot \beta^6$, it finally results in

$$\underbrace{\frac{1}{a} \beta^4}_{a} + \underbrace{(\alpha_2 - 1)\beta^3}_{b} + \underbrace{\frac{(\alpha_3 - \alpha_2)}{2} \beta^2}_{c} + \underbrace{\frac{(\alpha_4 - \alpha_3)}{6} \beta}_{d} - \underbrace{\frac{\alpha_4}{24}}_{e} = 0. \quad (5.42)$$

Equation (5.42) has four roots [91]

$$\begin{aligned}\beta_{1,2} &= -\frac{b}{4a} - S \pm 0.5 \sqrt{\underbrace{-4S^2 - 2P + \frac{q}{S}}_X} \\ \beta_{3,4} &= -\frac{b}{4a} + S \pm 0.5 \sqrt{\underbrace{-4S^2 - 2P - \frac{q}{S}}_Y},\end{aligned}\quad (5.43)$$

where $P = \frac{8ac-3b^2}{8a^2}$, $q = \frac{b^3-4abc+8a^2d}{8a^3}$

$$\text{and, } S = 0.5 \sqrt{-\frac{2}{3}P + \frac{1}{3a} \left(Q + \frac{\Delta_0}{Q} \right)}, \quad Q = \sqrt[3]{\frac{\Delta_1 + \sqrt{\Delta_1^2 - 4\Delta_0^3}}{2}}.$$

$$\text{with, } \Delta_0 = c^2 - 3bd + 12ae, \quad \Delta_1 = 2c^3 - 9bcd + 27ad^2 - 72ace$$

Based on practical ranges for the collision recovery coefficients, α_i , $0 \leq \alpha_i \leq 1$, and $\alpha_2 \geq \alpha_3 \geq \alpha_4$. Therefore, we can prove that the signs of the polynomial coefficients are constant and not changing in all ranges of α_i and are presented as $\{a > 0, b < 0, c < 0, d < 0, \text{ and } e < 0\}$.

According to Descartes' rules of sign [78], there is only one valid real positive solution for the equation. After analyzing (5.42) using Descartes' rules of sign [78], the proposed closed form optimum frame length L_{MCRC} under the multiple collision recovery coefficients environment is

$$L_{MCRC} = \left(-\frac{b}{4a} + S + 0.5 \sqrt{-4S^2 - 2P - \frac{q}{S}} \right) \cdot n. \quad (5.44)$$

According to (5.44), the proposed equation gives a linear relation with reference to the number of tags n , and includes the effect of different collision recovery coefficients. When the RFID reader has no collision resolving capability, i.e. $\alpha_2 = \alpha_3 = \alpha_4 = 0$, the proposed formula gives $L_{MCRC} = n$, which is identical to the frame length in the conventional case. When the RFID reader has a full and equal collision resolving capability for the two, three, and four collided tags per slot, i.e. $\alpha_2 = \alpha_3 = \alpha_4 = 1$, the proposed formula gives $L_{MCRC} = 0.452 \cdot n$, which matches the results in [59].

5.3.2 Collision Recovery Coefficients Calculations

Now the calculation of the collision recovery coefficients α_2 , α_3 and α_4 is clarified, which are the main optimization variables in our proposal. The values of these coefficients are strongly dependent on the receiver type. Calculations of the collision recovery coefficients are done based on an RFID reader model that utilizes the capture effect. The reader resolves the collision based on the strongest tag reply. Therefore, the collision can be resolved with a certain probability, if the strongest tag reply is stronger than the summation of the other collided tags at the same slot.

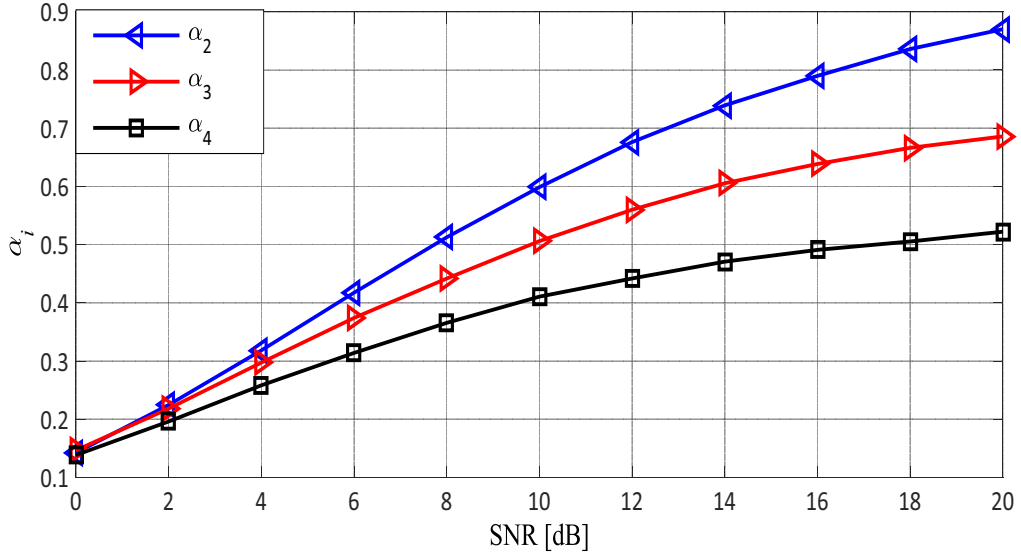


Figure 5.10: Simulation results for the average collision recovery coefficients α_i as a function of the SNR using the strongest tag reply receiver. α_2 , α_3 , and α_4 are respectively the collision recovery probability for two, three, and four collided tags per slot.

The main advantage of this reader is that it does not need any channel state information (CSI) to recover the strongest tag. According to EPCglobal C1 G2 standard [11], collisions in RFID systems occur only within the 16 bits packet called *RN16*. If any single bit error occurs in this packet, the total packet must be considered lost. Therefore, the meaning of the collision recovery probability coefficients α_i is the probability that the RFID reader can identify a complete *RN16* packet from i collided tags. Therefore, the collision recovery coefficient can be expressed by $\alpha_i = (1 - PER_i)$, where PER_i is the Packet Error Rate for i collided tags. In this work, we measure the SNR for each slot, then we calculate the average SNR per frame as $E\left\{\frac{|h|^2 \cdot x^2}{\sigma^2}\right\}$, where σ is the standard deviation of the Additive White Gaussian Noise (AWGN) per slot, and at last, a normalized signal power is used, i.e. $E\{x^2\} = 1$. Moreover, the equivalent channel coefficients h follow Rayleigh fading, which is a common assumption for dense RFID applications [79], because there is no dominant Line-of-Site communication link between the tags and the reader [79]. The channel coefficients are independent on zero mean circularly symmetric complex Gaussian random variables with normalized energy $E\{|h|^2\} = 1$, and all tags are statistically identical, which means all of them experience the same average path loss. Therefore, the average SNR per frame is $E\left\{\frac{1}{\sigma^2}\right\}$.

Figure 5.10 shows the values of the collision recovery coefficients versus the average SNR per frame using the strongest tag reply receiver. In these

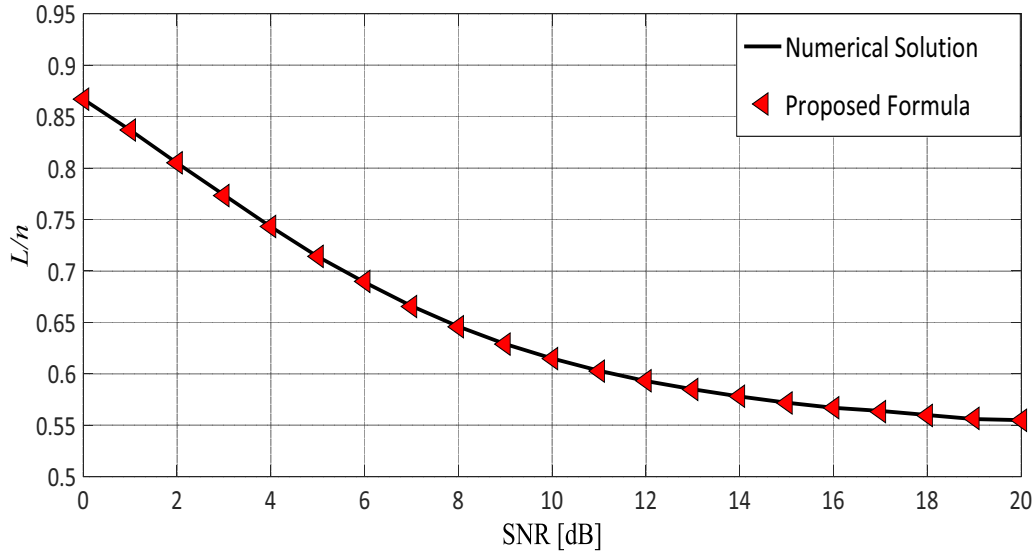


Figure 5.11: Normalized frame length (L/n) comparison using the proposed formula in (5.44) and the numerical solution as a function of the SNR.

simulations, a sampling frequency of $f_s = 8$ MHz is used, and the tags used FM0 as an encoding scheme. Finally, to clarify the worst-case effect of the collision recovery coefficients, we used the highest symbol rate BLF = 640 kHz.

5.3.3 Closed Form Solution vs. Numerical Solution

For each RFID reader, each SNR leads to corresponding values for the collision recovery coefficients α_2 , α_3 and α_4 . Figure 5.11 shows a comparison between the proposed formula (5.44) and the numerical solution which maximizes the reading efficiency in (5.40) versus the SNR. Both simulations used the same receiver model, which is the strongest tag reply receiver, which is presented in the previous section. According to figure 5.11, the proposed formula gives identical results compared to the numerical solution at the complete SNR range.

5.3.4 Mean Reading Time Reduction

The total average number of slots needed to identify a complete bunch of tags is calculated using the strongest tag reply receiver in [57]. FSA with initial frame length $L_{ini.} = 16$ is used as anti-collision algorithm. Figure 5.12 illustrates a comparison between the percentages of saving time using the proposed MCRC and the conventional frame length $L = n$ assuming perfect number of tags estimation. The simulation uses $C_t = 0.2$ and different SNR values. According to figure 5.12, when the value of the SNR increases, the collision recovery

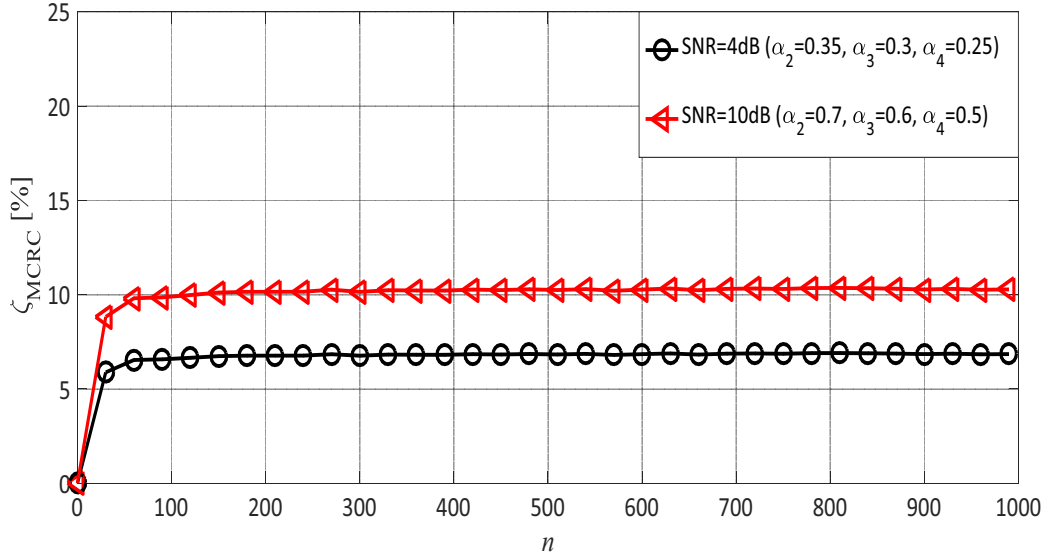


Figure 5.12: Percentages of the mean reading time reduction ζ_{MCRC} using the proposed MCRC as a function of the number of tags n compared to the conventional frame length $L = n$ for perfect number of tags estimation using $C_t = 0.2$ and different SNR values.

probability increases as well. Hence, the mean reading time reduction also increases.

Figure 5.13 shows the percentages of saving time with the proposed MCRC compared to the conventional frame length $L = n$ using different anti-collision algorithms with $C_t = 0.2$ and $SNR = 10$ dB. Results in figure 5.13 is calculated using Monte-Carlo simulations for FSA with 1000 iterations for each n value.

In this section, the FSA reading efficiency is proposed for equal slot durations system with multiple collision recovery coefficients. However, there are differences in the slot durations depending on the slot type. Therefore, in the following section, the FSA reading efficiency considers the differences in slot durations as well as the differences in the collision recovery coefficients.

5.4 Time and Multiple Collision Recovery System

In this section, a new FSA reading efficiency metric called time aware multiple collision recovery coefficients reading efficiency η_{TAMCRC} is presented. The main contribution of this new efficiency is, that it contains a unique collision recovery coefficient α_i for each probability of collision $P(i)$. These new coefficients indicate the ability of the reader to recover one tag from i collided tags,

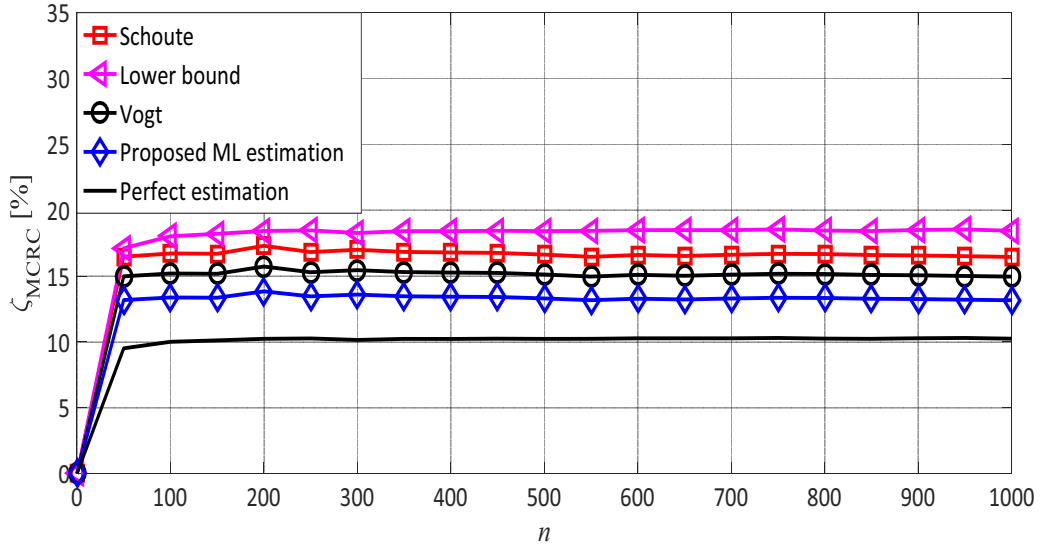


Figure 5.13: Percentages of the mean reading time reduction ζ_{MCRC} using the proposed MCRC frame length as a function of the number of tags n compared to the conventional frame length $L = n$ using different anti-collision algorithms with $C_t = 0.2$ and $SNR = 10$ dB with strongest tag reply receiver, which leads to $(\alpha_2 = 0.6, \alpha_3 = 0.5, \alpha_4 = 0.4)$.

where it varies based on the number of collided tags. Moreover, it takes into consideration the different slot durations.

5.4.1 Closed Form Solution for Time Multiple Collision Recovery Aware System

As shown in the previous section, the probability that a collision is resulted from two or three collided tags is $\simeq 85\%$. Moreover, the values of the remaining collision recovery coefficient α_i when $i \geq 4$, i.e., 4 or more collided tags are small. Therefore, only up to three collided tags are considered. The next step is normalizing the slot duration t_k of successful and collided tags to unity. Furthermore, it is assumed that empty slots are shorter than successful slots (i.e. $t_0 \leq t_k$), which is the case for practical readers. Then, the proposed reading efficiency η_{TAMCRC} can be expressed by

$$\eta_{TAMCRC} = \frac{P(1) + \alpha_2 P_{col.}(2) + \alpha_3 P_{col.}(3)}{1 + P(0) \cdot (C_t - 1)}, \quad (5.45)$$

where $C_t = \frac{t_0}{t_k}$ represents the slots durations constant, and α_2, α_3 are respectively the second, third collision recovery coefficients.

The next step is to derive a closed form for the new optimum frame length

L_{TAMCRC} which maximizes η_{TAMCRC} . After substituting by (5.39) in (5.45) we obtain

$$\eta_{TAMCRC} = \frac{e^{-\frac{1}{\beta}} \cdot (\beta^{-1} + \frac{\alpha_2}{2}\beta^{-2} + \frac{\alpha_3}{6}\beta^{-3})}{1 + e^{-\frac{1}{\beta}} \cdot (C_t - 1)}, \quad (5.46)$$

where, $\beta = \frac{L}{n}$.

Now we have to find the value of β which maximizes η_{TAMCRC} . This is achieved by differentiating the reading efficiency in (5.46) with respect to β and equate the result to zero

$$\frac{\partial \eta_{TAMCRC}}{\partial \beta} = 0. \quad (5.47)$$

After differentiating and simplifications, the final equation is a fourth order polynomial

$$a \cdot \beta^4 + b \cdot \beta^3 + c \cdot \beta^2 + d \cdot \beta + e = 0, \quad (5.48)$$

where, $a = \underbrace{-C_t}_{(<0)}$

$$b = \underbrace{C_t \cdot (1 - \alpha_2) - 1}_{(<0)}$$

$$c = \underbrace{2 - C_t - \alpha_2}_{(>0)} + \underbrace{\frac{C_t}{2}(\alpha_2 - \alpha_3)}_{(>0)}$$

$$d = \underbrace{\frac{1}{2}(\alpha_2 - \alpha_3) + \frac{1}{2}\alpha_2 \cdot (1 - C_t) + \frac{1}{6}C_t \cdot \alpha_3}_{(>0)}$$

$$e = \underbrace{\frac{1}{6}\alpha_3 \cdot (2 - C_t)}_{(>0)}$$

As $0 \leq \alpha_i \leq 1$, $0 < C_t \leq 1$, and $\alpha_2 \geq \alpha_3$, (5.48) has four roots [91]

$$\begin{aligned} \beta_{1,2} &= -\frac{b}{4a} - S \pm 0.5 \sqrt{\underbrace{-4S^2 - 2P + \frac{q}{S}}_X} \\ \beta_{3,4} &= -\frac{b}{4a} + S \pm 0.5 \sqrt{\underbrace{-4S^2 - 2P - \frac{q}{S}}_Y}, \end{aligned} \quad (5.49)$$

with $P = \frac{8ac - 3b^2}{8a^2}$, $q = \frac{b^3 - 4abc + 8a^2d}{8a^3}$

$$\text{and } S = 0.5 \sqrt{-\frac{2}{3}P + \frac{1}{3a} \left(Q + \frac{\Delta_0}{Q} \right)}, \quad Q = \sqrt[3]{\frac{\Delta_1 + \sqrt{\Delta_1^2 - 4\Delta_0^3}}{2}}$$

$$\text{with } \Delta_0 = c^2 - 3bd + 12ae, \quad \Delta_1 = 2c^3 - 9bcd + 27ad^2 - 72ace$$

According to the practical ranges of the collision recovery coefficients α_i and C_t , it can be proved that the signs of the polynomial coefficients are constant and do not change in all ranges of α_i and C_t . Thus, their signs are

$$a < 0, b < 0, c > 0, d > 0, \text{ and } e > 0$$

According to Descartes' rules of sign [78], there is only one valid real positive solution for the equation. After analyzing (5.42) using Descartes' rules of sign [78], the proposed closed form optimum frame length L_{TAMCRC} under time and multiple collision recovery coefficients environment leads to be

$$L_{TAMCRC} = \left(-\frac{b}{4a} - S + 0.5 \sqrt{-4S^2 - 2P + \frac{q}{S}} \right) \cdot n. \quad (5.50)$$

The proposed equation gives a linear relation with reference to the number of tags n . It considers the effect of different collision recovery coefficients and the slot durations constant. The values of these coefficients are set based on the RFID reader type as shown in [92]. The value of C_t can be calculated based on the transmission rate as shown in [77]. Based on (5.50), if the RFID reader has no collision resolving capability ($\alpha_2 = \alpha_3 = 0$) and equal slots durations are used ($C_t = 1$), we get $L_{TAMCR} = n$. This is identical to the optimum frame length in the conventional case.

5.4.2 Closed Form Solution vs. Numerical Solution

In this section, the accuracy of the proposed closed form compared to the numerical solution is discussed. Figure 5.14a illustrates a frame length comparison between the proposed formula in (5.50) and the numerical solution, which maximizes the reading efficiency in (5.45). The comparison presents the relation between the frame length and the full range of the slot durations constant $C_t = [0 \rightarrow 1]$ and different values of collision recovery coefficients α_i . Both simulations used the same receiver model, which is the strongest tag reply receiver. According to figure 5.14, the proposed formula approaches the numerical solution within the full range of the complete range of C_t . As mentioned before, the EPCglobal C1 G2 standard [11] only allows taking quantized frame lengths (power of 2). Figure 5.14b shows that the proposed frame length fully matches the numerical solution in the full range of C_t .

5.4.3 Mean Reading Time Reduction

Figure 5.15 presents the saved time using the proposed TMCRC compared to the conventional frame length $L = n$ assuming perfect number of tags estima-

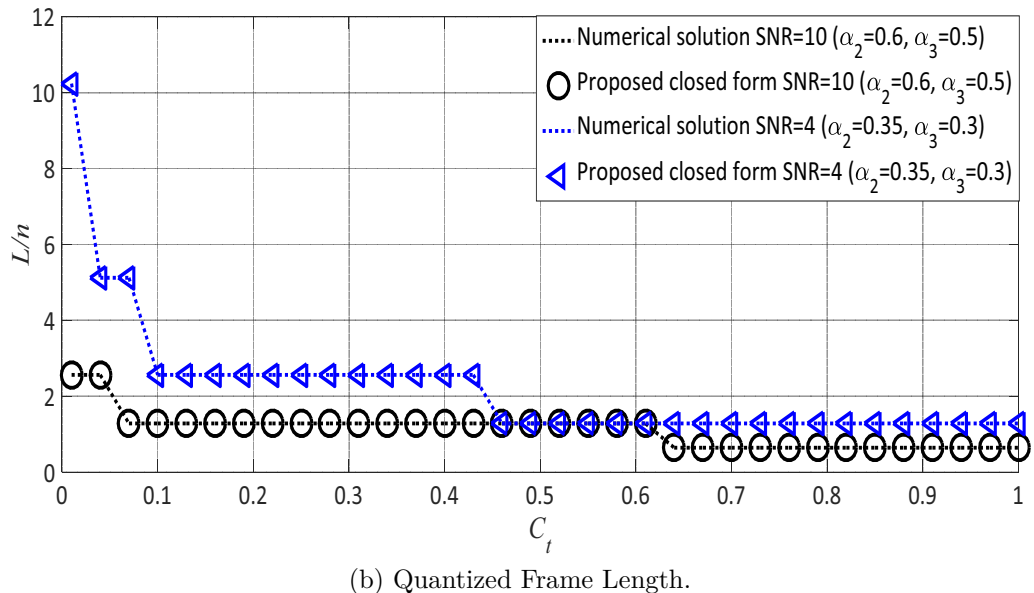
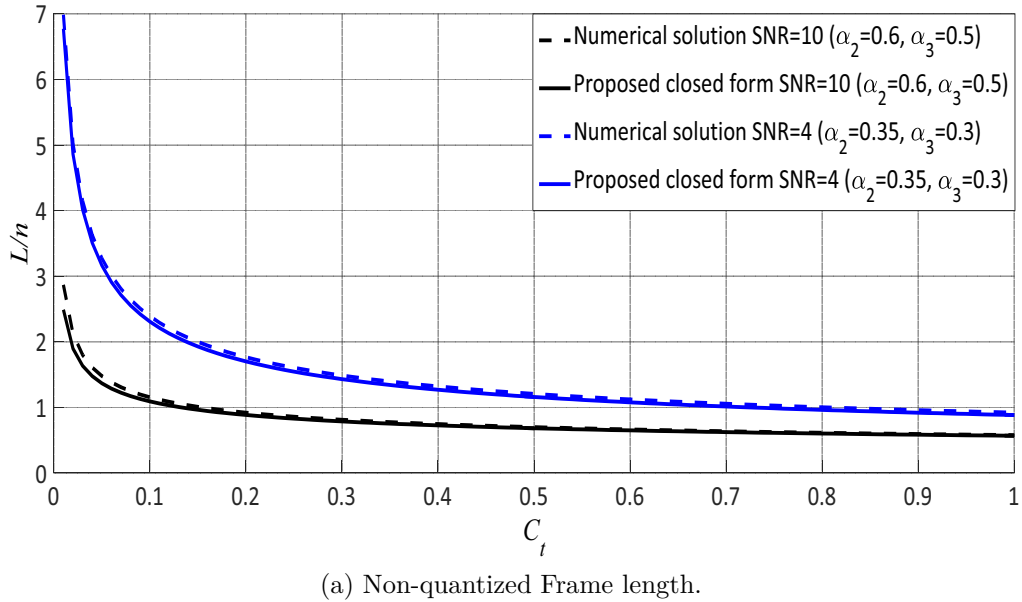


Figure 5.14: Normalized optimum frame length $L_{T_{AMC}RC}$ using (5.50) compared to the numerical solution as a function of the slot durations constant C_t ($n = 100$ tags).

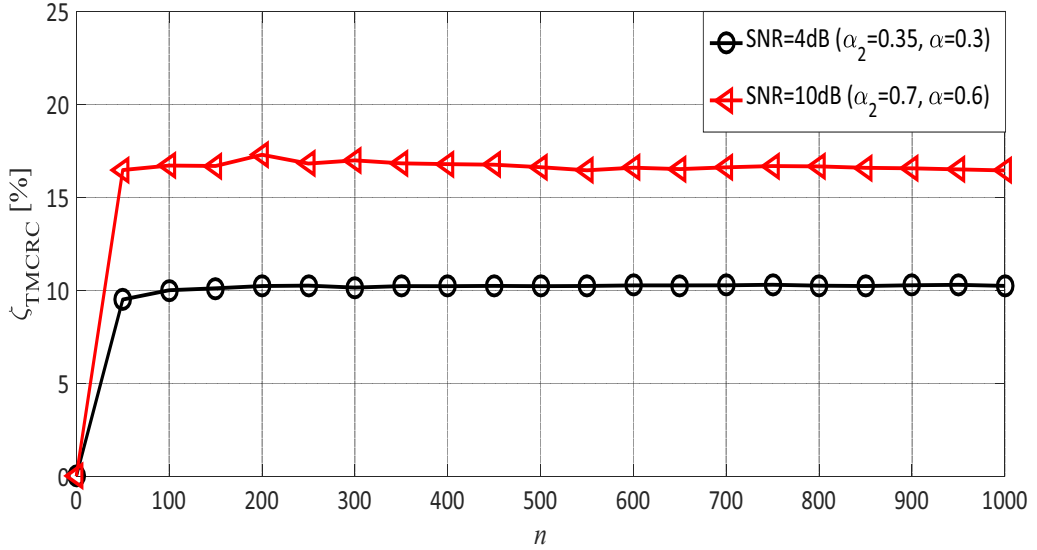


Figure 5.15: Percentages of the mean reading time reduction ζ_{TMCRC} using the proposed TMCRC as a function of the number of tags n compared to the conventional frame length $L = n$ for perfect number of tags estimation using $C_t = 0.2$.

tion. The simulation results are based on the slot durations constant $C_t = 0.2$. It is considered as a practical value used in the EPCglobal C1 G2 standards [11]. The simulation results are done using different values of SNR, as each SNR leads to corresponding values for the collision recovery coefficients α_2 , α_3 and α_4 . According to figure 5.15, when the value of the SNR increases, the collision recovery probability increases. Hence, the mean reduction in reading time also increases.

Figure 5.16 shows the percentages of saving time using the proposed TMCRC compared to the conventional frame length $L = n$ using different anti-collision algorithms with $C_t = 0.2$ and strongest tag reply receiver with average $SNR = 8$ dB, which is corresponding to $\alpha_2 = 0.52$, $\alpha_3 = 0.45$ and $\alpha_4 = 0.35$. Results in figure 5.16 is calculated using Monte-Carlo simulations for FSA with 1000 iterations for each n value. According to figure 5.16, the mean reduction in reading time for different estimation algorithms is between 10% and 18%. FSA with perfect number of tags estimation algorithm leads to less number of iterations in the reading process. Thus, it results in the minimum mean reading time reduction value. On the other hand, FSA with simple estimation algorithm e.g. lower bound leads to more number of iteration and higher percentage of the saved time.

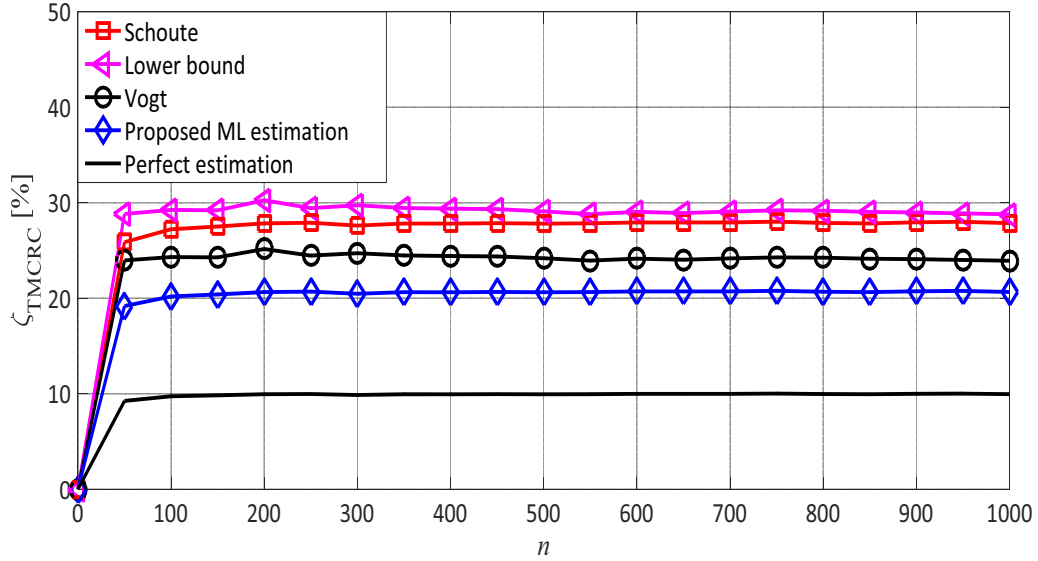


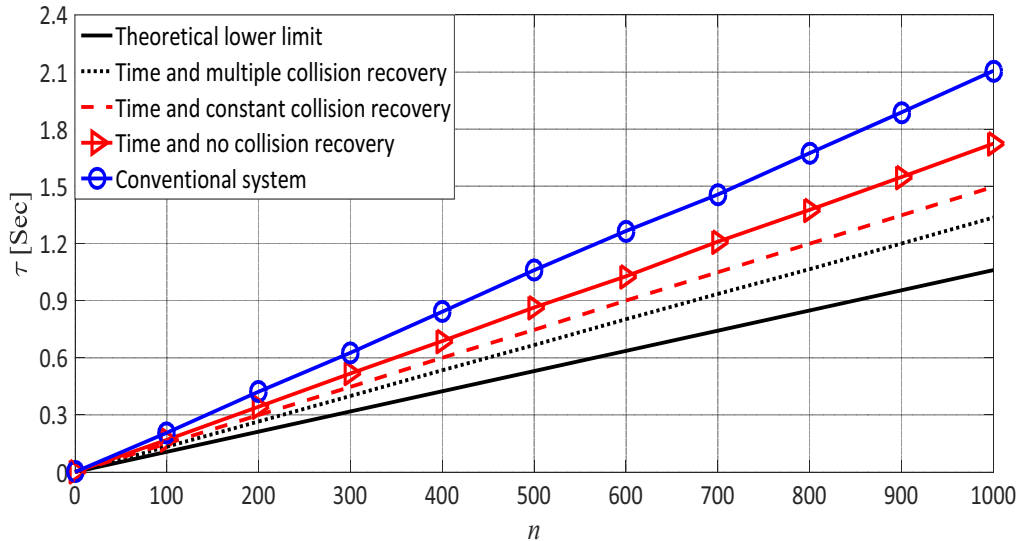
Figure 5.16: Percentages of the mean reading time reduction ζ_{TMCRC} using the proposed TMCRC as a function of the number of tags n compared to the conventional frame length $L = n$ using different anti-collision algorithms with $C_t = 0.2$ and $SNR = 10$ dB.

5.5 Comparison of the Proposed Algorithms

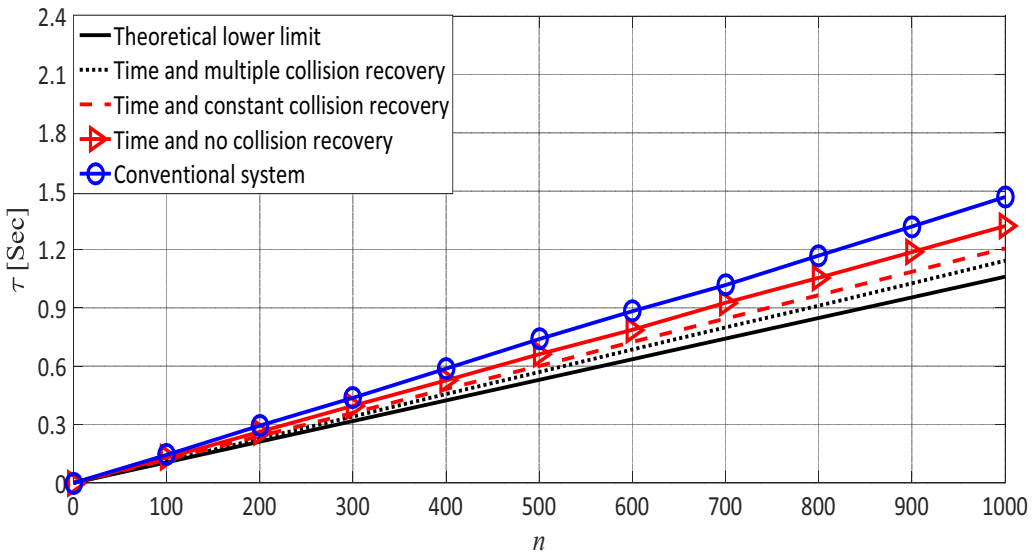
The most crucial performance metric in RFID systems is the average total reading time for an existing number of tags in the reading area. This section summarizes the performance of the DFSA using the proposed frame lengths. It compares between the average total reading time of the proposed frame lengths and the conventional one which takes $L_{opt} = n$. Furthermore, it illustrates how far are the proposed systems compared to the theoretical lower limit of the EPCglobal C1 G2 standard [11], which gives the minimum identification time for UHF RFID system. The theoretical lower limit is achieved when the system identifies a single tag per slot. Therefore, the minimum number of slots required to identify n tags is n successful slots.

Figure 5.17 shows the simulation results of the average reading time for DFSA using the following parameters. Slots durations constant $C_t = 0.2$, with $te = 60\ \mu s$, $tc = 300\ \mu s$, and $ts = 1060\ \mu s$, which are the practical values from real measurements using a Universal Software Defined Radio Peripheral (USRP B210) [63]. The strongest tag reply receiver is used with average $SNR = 10$ dB, which leads to the following collision recovery coefficients, $\alpha_2 = 0.6$, $\alpha_3 = 0.5$, $\alpha_4 = 0.4$. Results in figure 5.17 is calculated using Monte-Carlo simulations for FSA with 1000 iterations for each n value.

Figure 5.17a shows the average reading time for DFSA using lower bound number of tags estimation algorithm. The main objective of these simulations



(a) Using simple number of tags estimation algorithm (Lower Bound).



(b) Using the proposed collision recovery aware ML number of tags estimation algorithm.

Figure 5.17: Average reading time τ of the proposed systems, the conventional FSA and the theoretical limit as a function of the number of tags n .

Table 5.2: Performance analysis for the proposed frame length formulas, where $C_t = 0.2$, $\alpha_2 = 0.7$, $\alpha_3 = 0.6$

(a) Average reading time reduction using the proposed frame length formulas compared to the conventional DFSA $L = n$

	Simple estimation algorithm Lower Bound (LB)	Proposed estimation Maximum Likelihood (ML)
Time and no CR	16 %	8 %
Time and constant CR	26 %	18 %
Time and multiple CR	30 %	22 %

(b) Average remaining room of improvement for the proposed frame length formulas to reach the theoretical lower limit of EPCglobal C1 G2

	Simple estimation algorithm Lower Bound (LB)	Proposed estimation Maximum Likelihood (ML)
Time and no CR	35 %	20 %
Time and constant CR	25 %	15 %
Time and multiple CR	15 %	10 %

is to evaluate the performance of the proposed frame lengths formulas without the effect of the proposed ML number of tags estimation algorithm. As discussed in chapter 4, the lower bound number of tags estimation neglects the collision recovery capability of the PHY layer and gives the minimum number of the remaining tags in the reading area. According to figure 5.17a, the Time Aware frame length proposal gives 16 % saving in the average total reading time compared to the conventional FSA. The Time and Constant Collision Recovery Aware frame length proposal saves 10 % more than the Time Aware frame length, because of the new information about the collision recovery coefficient. In the time and constant collision recovery aware, the average collision recovery probability is $\alpha = \alpha_2 = 0.6$. In case of the time and multiple collision recovery frame length, the algorithm achieves 30 % average saving in the reading time compared to the conventional DFSA. This is due to considering the different values of the collision recovery coefficients $\alpha_2 = 0.6$, $\alpha_3 = 0.5$.

Figure 5.17b shows the average reading time with the proposed collision recovery aware ML number of tags estimation. The main target is to evaluate the performance of the proposed frame lengths formulas using the proposed ML number of tags estimation algorithm. According to figure 5.17b, the time aware frame length proposal gives 10 % saving in the average total reading time compared to the conventional FSA. The time and constant collision recovery aware frame length proposal results in 18 % average saving in the reading time compared to the conventional DFSA. In case of the time and multiple collision

recovery frame length, the proposed solution results in 22 % average saving in the reading time compared to the conventional DFSA.

According to figure 5.17, the percentage of saving in reading time with a simple number of tags estimation algorithm is more than the percentage of saving time using the proposed ML number of tags estimation. This is because the total identification time with simple number of tags estimation is more than that with the proposed ML number of tags estimation. Thus, the number of reading cycles and frame length adaptation with simple number of tags estimation is more than the number of reading cycles with the proposed number of tags estimation. However, the average reading time for DFSA using the proposed frame length formulas with the proposed ML estimation is less than the average reading time with simple number of tags estimation. Table 5.2 shows a summary of the performance analysis for the proposed frame length formulas with simple number of tags estimation and with ML number of tags estimation.

According to the above results, there is still a gap of 10 % between the proposed systems and the theoretical limit of the EPCglobal C1 G2 standard [11]. The main reason of this is, that the allowed optimization was only in the reader side. To follow the EPCglobal C1 G2 standard [11], the tags could not be modified. Consequently, in the next chapter, backwards compatible improvement of the EPCglobal C1 G2 standard are proposed. The proposed system is compatible with the EPCglobal C1 G2 standard, i.e., the proposed tags could be jointly operated with conventional tags and identified by conventional readers without affecting the performance. Additionally, conventional tags can also be operated together with the proposed tags and can be identified by the proposed reader.

Chapter 6

Improvements of the EPCglobal C1 G2

The EPCglobal C1 G2 is the most employed UHF RFID standard. It allows only for a single tag acknowledgment per slot, even if the PHY layer is able to identify multiple collided tags. Recent studies have focus on this problem e.g., [90]. They use the post-preamble proposed in [92] with a Multi Input Multi Output (MIMO) receiver to resolve collisions. The authors assume that all the recovered tags can be acknowledged in parallel. However, this technique is not compatible with the EPCglobal C1 G2 standards [11], due to the post-preamble. Therefore, their proposal requires a new RFID standard. Furthermore, acknowledging more than one tag in parallel would cause a new problem called “ACK Collision” due to the simultaneous reception of multiple Acknowledgment “ACK” commands at the tag side. Moreover, this parallel acknowledgment causes Electronic Product Code (EPC) collisions at the reader side. The EPC packet is much longer than the *RN16* packet, so it needs an advanced collision recovery algorithm, which decreases the system performance.

To overcome these pitfalls, this chapter proposes a system that is capable of acknowledging multiple tags within a single slot, resulting in a significant increase in performance. The main advantage of this proposal is the compatibility with the existing EPCglobal C1 G2 tags and readers. Hence, the proposed tags can be identified by conventional readers without affecting the performance. Furthermore, the existing tags can be read simultaneously with the proposed tags by the proposed reader.

This chapter is organized as follows. Section 1 presents a brief discussion about the conventional reading process using the EPCglobal C1 G2 standard. Section 2 describes the proposed new system including the modifications of the tags and the reader. The performance of the proposed system is analyzed in section 3. Finally, section 4 provides the practical measurements and the simulation results.

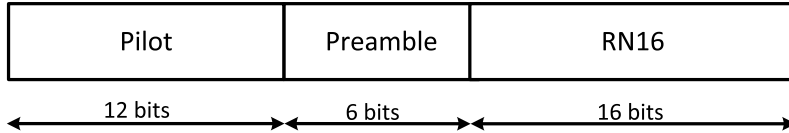


Figure 6.1: Conventional tag response

6.1 EPCglobal C1 G2 Reading Process

This section describes, the conventional reading algorithm of the EPCglobal C1 G2 standard. The reader initially powers the tags in the reading area with a Continuous Wave (CW). At this time, the powered tags are in the ready state waiting for the frame length information from the reader. Then, the reader broadcasts the frame length and notifies all tags with the beginning of a new frame with a “Query” command. As soon as the tags receive this command, each tag selects a slot from the frame by setting its slot counter, and enters the “Arbitrate” state. When the tag’s slot counter is equal to zero, the tag enters the “Reply” state and starts back-scattering its 16 bits Random Number (*RN16*) as a temporary ID in addition to a 18 bits pilot and preamble used for synchronization as shown in figure 6.1.

As discussed before, in FSA [49], there are three probabilities for each slot: First, empty slot, where no tag has selected this slot to transmit its information in it. The reader transmits a “Query-Rep” command asking the tags decrement their slot counters. Second, successful slot, where only one tag selects this slot to transmit its information in it. The reader transmits an “ACK” command including the received *RN16*. Then, the acknowledged tag enters the “Acknowledged” state and replies with its permanent Electronic Product Coder “EPC” code. Third, collided slot, where the reader receives simultaneously multiple replies from different tags. In this case, there are two possibilities:

1. Systems have no collision recovery capability: The reader fails to identify any *RN16*, so it queries the next slot by sending another “Query-Rep” command. As soon as the collided tags receive the “Query-Rep” command, they enter the “Arbitrate” state waiting for the next frame. The maximum reading efficiency in such systems is 36%, when the working frame length is equal to the remaining number of tags in the reading area.
2. Systems have collision recovery capability: They have the ability to identify one *RN16* from the collided ones. Then, the reader broadcasts an “ACK” command including the identified *RN16*. The tag, which has the same *RN16*, replies its “EPC” code, and mutes itself until the end of the reading process. However, the remaining tags forget their *RN16s* and enter the “Arbitrate” state waiting for the next frame. The main drawback

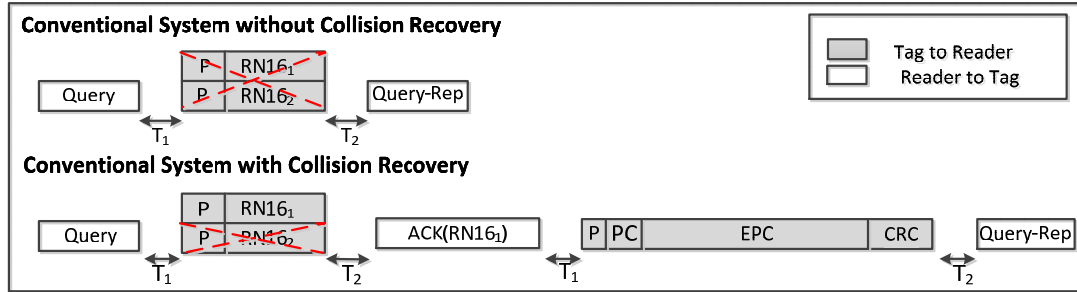


Figure 6.2: Example of two tags collided slot according to EPCglobal C1 G2 standard

of such systems is that the reader can only acknowledge one tag from the collided tags in a slot, even if it has the capability to identify all the responding *RN16s*. To overcome this drawback, backwards compatible extension are proposed in the following sections.

Figure 6.2 presents an example for a collided slot with two collided tags. It shows the differences between the conventional systems with and without collision recovery capability. According to figure 6.2, the reader, which has no collision recovery capability, couldn't identify any of the two collided *RN16s*. However, the reader, which has collision recovery capability, identified *RN16₁* and acknowledged the corresponding tag.

6.2 Proposed System Description

In this section, the description of the proposed tags and readers is presented. Afterwards, the performance of the proposed system is compared to conventional systems. The proposed system has the same hardware of conventional systems. The main difference between the proposed system and the conventional one is the signal format between the new reader and the new tags.

6.2.1 Proposed Tag

The proposed tags have the ability to act like conventional UHF EPCglobal C1 G2 tags, which is the default mode. However, they load extra properties, when they are in the ready state and receive a new command called “Switch” command from the proposed reader. The following part presents the main modifications in the signal format of the proposed tag:

According to the EPCglobal C1 G2 standard [11], conventional tags reply with two possible preambles with the *RN16* packet: The short version with 6 bits preamble and the long version with 18 bits (12 bits zeros as a pilot + 6

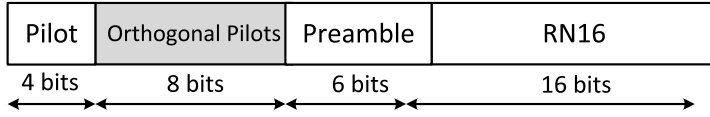


Figure 6.3: Tag response of the proposed tags including the new pilot sequences.

Table 6.1: Set of 8 orthogonal sequences.

Sequence	Orthogonal Pilots
P_1	1 -1 1 -1 1 -1 1 -1 1 -1 1 -1 1 -1 1 -1
P_{18}	1 -1 1 -1 1 -1 1 1 -1 1 -1 1 -1 1 -1 -1
P_{69}	1 -1 1 1 -1 1 -1 1 -1 1 -1 -1 1 -1 1 -1
P_{86}	1 -1 1 1 -1 1 -1 -1 1 -1 1 1 -1 1 -1 -1
P_{171}	1 1 -1 1 -1 -1 1 -1 1 1 -1 1 -1 -1 1 -1
P_{188}	1 1 -1 1 -1 -1 1 1 -1 -1 1 -1 1 1 -1 -1
P_{239}	1 1 -1 -1 1 1 -1 1 -1 -1 1 1 -1 -1 1 -1
P_{256}	1 1 -1 -1 1 1 -1 -1 1 1 -1 -1 1 1 -1 -1

bits of the short version). The proposed tag's signal format has only the long version, but with a new structure. Figure 6.3 presents the new structure of the *RN16* packet. As shown in figure 6.3, the new structure has the identical 6 bits of the long conventional long pilot. However, the 12 bits zeros of the conventional long pilot are divided to two parts. The first part with 4 bits zeros used for synchronization and the second part with 8 bits orthogonal pilots used for channel estimation. Table 6.1 shows an example of the orthogonal pilots, which are similar to the orthogonal post-preamble used in [92]. The 8 orthogonal pilot bits have to be orthogonal to the other pilot bits and also to the conventional pattern P_1 (8 zero bits). This property gives our proposal the advantage to have the conventional long version tag reply as a valid tag response in the new system. This is in contrast to the proposal by [92], where the conventional tags are not compatible with their system.

In case of a resolved collision of multiple *RN16s*, the proposed pseudo-

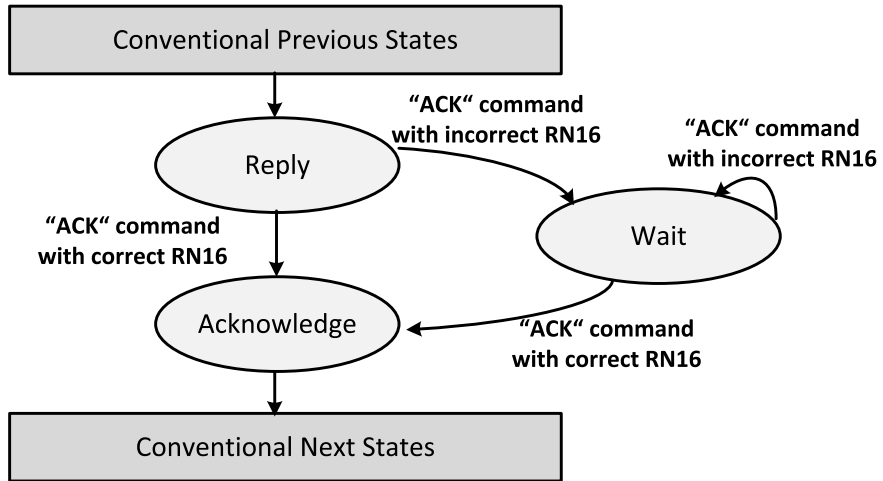


Figure 6.4: Modified part of the proposed tag's state diagram.

parallel reading process is applied. A tag receiving its valid *RN16* replies with its EPC and goes to the “Acknowledged” state. In contrast, a tag receiving an invalid *RN16* (e.g. valid for another tag) goes to a new state called “Wait” state. In the latter state the tag memorizes its *RN16* until one of the two possibilities occurs: a) receiving an “ACK” command containing its *RN16*. In this case the tag replies with its EPC and goes to the “Acknowledged” state, b) receiving the “ACK” command with wrong *RN16*. In this case, the tag remains in the “Wait” state waiting for a new command. Figure 6.4 presents a state diagram with the required modifications of the tag state diagram given in figure 6.19 of [11].

6.2.2 Proposed Reader

The proposed reader applies the normal FSA based on the conventional UHF EPCglobal C1 G2 standard, which means that it is able to operate normally with conventional tags. However, it starts the reading process with a new command called “Switch” command to switch the new tags from the conventional mode to the new mode. It should be transmitted before the “Query” command. The conventional tags consider the “Switch” command as an unknown command, but the proposed tags recognize that they are working in the new system. Table 6.2 provides an example for the “Switch” command code, which is a 16 bits command from the future use part of EPCglobal C1 G2 standard (*cf.* table 6.18 of [11]).

As discussed before, the EPCglobal C1G2 standard does not support multiple acknowledgments per slot. On the other hand, the proposed system should benefit from the collision resolving capabilities of the modern readers. Therefore, the proposed reader has the capability of converting the collided slot into

Table 6.2: Proposed format of “Switch” command, which is used for switching the proposed tags from the conventional mode to the new mode.

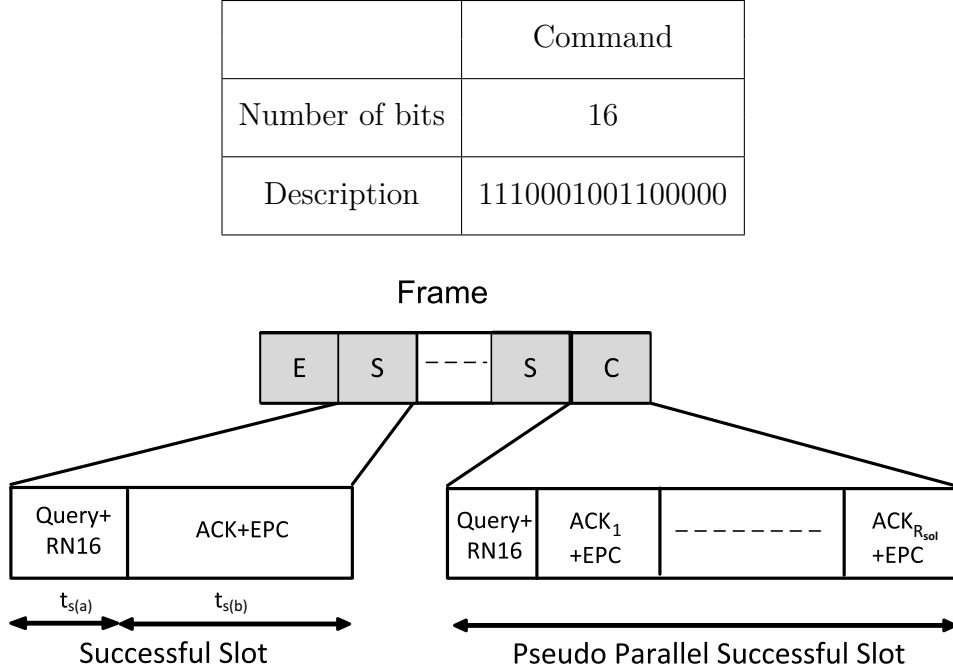


Figure 6.5: Example of the proposed pseudo-parallel successful slot with parallel “Query” command and $RN16$ followed by successive “ACK” commands and EP Cs.

a pseudo-parallel successful slot as shown in figure 6.5.

The reader starts each slot with a “Query-Rep” command asking for the $RN16$ of each tag. Then, each tag transmits its $RN16$ including one random orthogonal pilot from table 6.1. In case of a collided slot, the reader executes the following steps:

- The reader uses the orthogonal pilots to do channel estimation for the collided tags. Afterwards, it employs the channel information to recover the collided $RN16s$ using a MIMO receiver, e.g. the receiver proposed in [90].
- The reader counts the number of recovered $RN16s$ replies in the “Reply Counter”.
- The reader recognizes whether one of these replies is a conventional pilot or not by checking if one of the collided pilots is P_1 (the conventional one) in table 6.1. If yes, the reader considers it as a conventional tag.

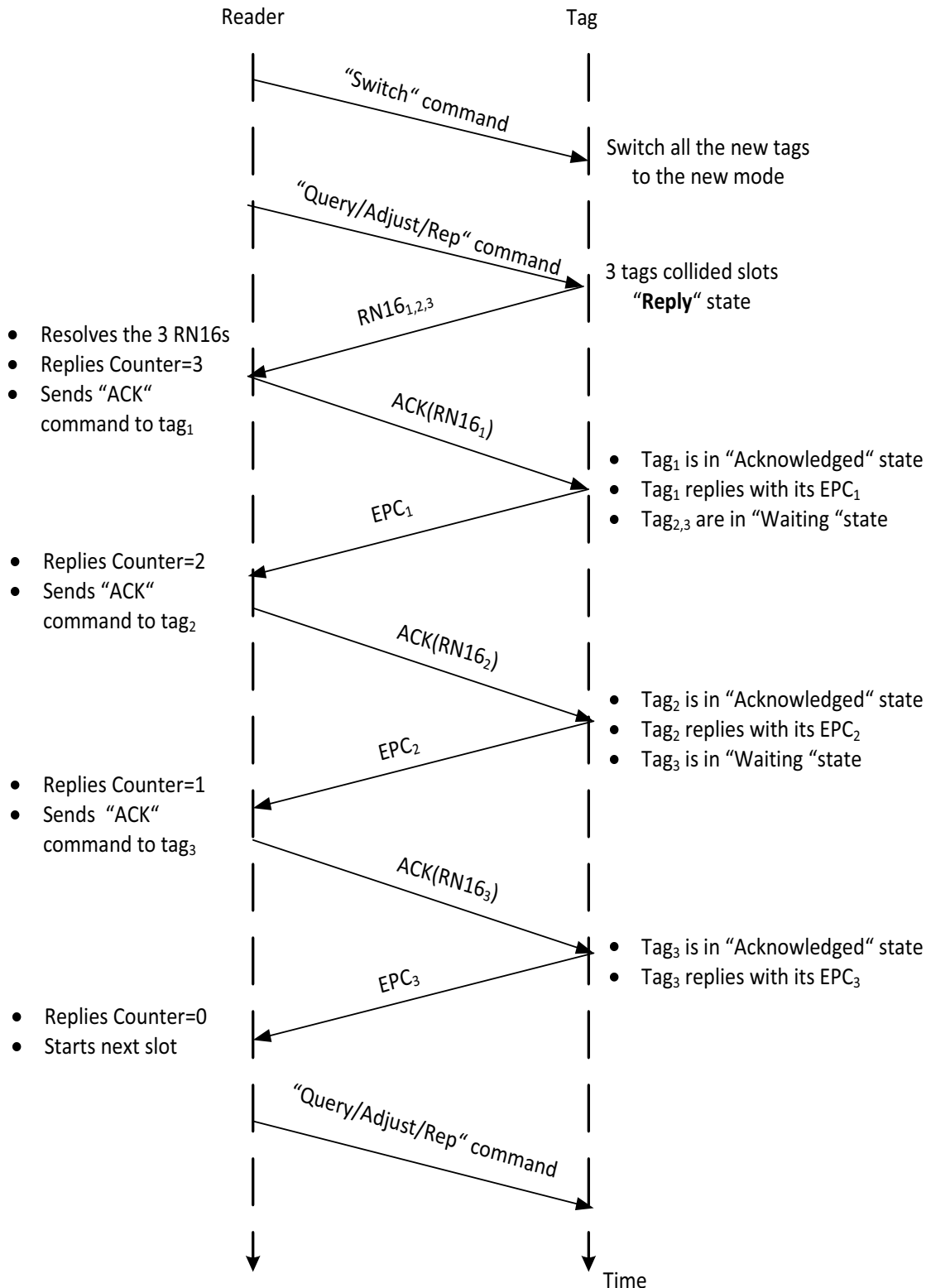


Figure 6.6: Example of an inventory round using the proposed reader and 3 collided tags.

Afterwards, the reader starts acknowledging the collided tags successively ordering them from the weakest to the strongest reply. The “Reply Counter” counts down with each received EPC from a tag. Then, it sends successive “ACK” commands until the “Reply Counter” reaches zero. Figure 6.6 shows an example for a complete inventory round between the proposed reader and three collided tags. According to figure 6.6, the reader started an inventory round with a “Switch” command. Thus, the three tags switched to the new mode. Then the reader sent a “Query” command to the tags asking them for their *RN16s*. The three tags replied with their *RN16s* at the first slot and produced collided slot. In this case, the reader was able to resolve the three collided *RN16s*. Afterwards, the reader applied the pseudo-parallel slot concept to acknowledge the three tags during the same slot.

6.3 Performance Analysis

In the conventional DFSA, the reading efficiency is the probability of a single tag reply $P(R = 1)$, where $P(R)$ is the probability that exactly R tags are active in one slot. It can be presented by [52]

$$P(R) = \binom{n}{R} \left(\frac{1}{L}\right)^R \left(1 - \frac{1}{L}\right)^{n-R}. \quad (6.1)$$

Thus, the reading efficiency of the conventional system is presented by

$$\eta_{conv} = \left(\frac{n}{L}\right) \left(1 - \frac{1}{L}\right)^{n-1}. \quad (6.2)$$

In the proposed system, the reader has the capability to resolve up to M collided tags. Therefore, the proposed reading efficiency can be presented by

$$\eta_{proposed} = \sum_{R=1}^M P(R) \cdot R_{sol}. \quad (6.3)$$

For the proposed case, $M = 8$ is the number of orthogonal codes which are presented in table 6.1. R_{sol} is the number of recovered tags.

The collision recovery capability of the proposed system depends on the pilots of the replied tags. For the proposed case, the unique scenarios ($1 + 1 + \dots + 1$) are only considered, i.e. if more than one tag uses the same pilot sequence, the reader will not be able to resolve this collision. Therefore, we have limited number of scenarios. Thus, (6.4) considers the effect of the unique scenarios:

$$\eta_{proposed} = \sum_{R=1}^M P(R) \cdot R_{sol} \cdot \sum_{l=1}^R P_{S_l}(R), \quad (6.4)$$

Table 6.3: Example for unique pilot collision scenarios for up to eight colliding tags per slot.

Number of received tags R	Probability of unique scenario P_{S_1}
1	$P_{S_1} = 1$
2 1+1	$P_{S_1} = 0.875$
3 1+1+1	$P_{S_1} = 0.656$
4 1+1+1+1	$P_{S_1} = 0.41$
5 1+1+1+1+1	$P_{S_1} = 0.205$
6 1+1+1+1+1+1	$P_{S_1} = 0.077$
7 1+1+1+1+1+1+1	$P_{S_1} = 0.019$
8 1+1+1+1+1+1+1+1	$P_{S_1} = 0.002$

where $P_{S_l}(R)$ represents the probability that scenario S_l happens. It can be calculated from the binomial distribution as explained in [90]. Table 6.3 shows all values of the unique scenarios $P_{S_l}(R)$.

For the proposed case, the system is not able to acknowledge the recovered tags in parallel. It uses the discussed pseudo-parallel method. According to figure 6.5, the conventional successful slot t_s is divided into two parts: The first part presents the “Query-Rep” command and the $RN16$ tag reply $t_{s(a)}$. The second part is the “ACK” command and the EPC tag reply $t_{s(b)}$. Thus, the successful slot time is:

$$t_s = t_{s(a)} + t_{s(b)}, \quad (6.5)$$

where $t_{s(a)}$ and $t_{s(b)}$ can be expressed by

$$t_{s(a)} = T_{qRep} + T_1 + T_2 + T_{RN16}. \quad (6.6)$$

$$t_{s(b)} = T_{ACK} + T_1 + T_2 + T_{EPC}. \quad (6.7)$$

Table 6.4 shows numerical values from the EPCglobal C1 G2 standard [11] as a function of the link pulse-repetition interval T_{pri} . According to these values, the time of the “Query-Rep” command and receiving the $RN16s$ presents 30% of

Table 6.4: System Parameters of EPCglobal C1 G2 standard.

Parameters	Values
T_{Q-Rep}	$78 T_{pri}$
T_1	$10 T_{pri}$
T_2	$20 T_{pri}$
T_{RN16}	$34 T_{pri}$
T_{ACK}	$236 T_{pri}$
T_{EPC}	$102 T_{pri}$

the conventional successful slot duration. The time of the “ACK” command and the EPC tag reply represents 70% of the conventional successful slot duration.

In the proposed system, the reader sends a “Query” command in parallel to all the tags and receives the $RN16s$ in parallel. Then, the reader sends successive “ACK” commands to the resolved tags. Therefore, the duration of the proposed pseudo-parallel slot is

$$t_{pseudo} = t_{s(a)} + R_{sol} \cdot t_{s(b)}, \quad (6.8)$$

where R_{sol} is the number of recovered tags. These tags are acknowledged successively. Therefore, the proposed efficiency should include a factor representing the effect of the pseudo-parallel spreading in time. This factor is called the pseudo-parallel factor φ . According to the numerical values in table 6.4, it can be expressed by

$$\varphi = \left(\frac{1}{0.3 + 0.7 \cdot R_{sol}} \right). \quad (6.9)$$

Based on the above discussion, the proposed reading efficiency formula considering the advantages of the new system is formulated as follows:

$$\eta_{proposed} = \sum_{R=1}^M P(R) \cdot \left(\sum_{l=1}^R P_{S_l}(R) \cdot R_{sol} \cdot \varphi \right), \quad (6.10)$$

6.4 Measurement and Simulation Results

The proposed tag’s signal modifications are implemented on the Wireless Identification Sensing Platform (WISP 5.0) [93], and the proposed reader modifications are implemented on the Universal Software Radio Peripheral (USRP B210) [63]. Figure 6.7a provides a measurement of the envelop signal for reader to tag (down link) communication. According to figure 6.7a, the reader starts with a normal “Select” command to set some conventional tag parameters.

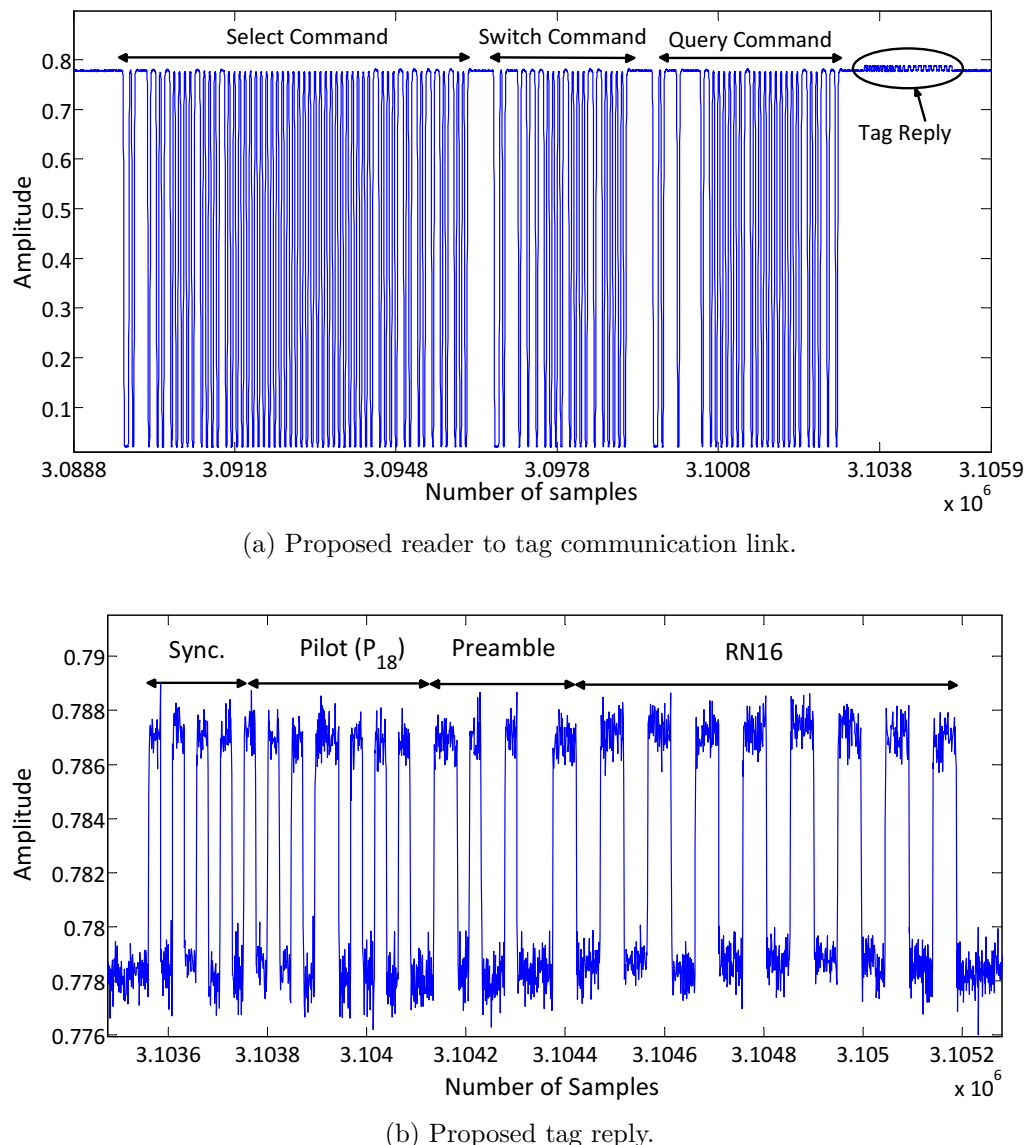


Figure 6.7: Communication link measurement.

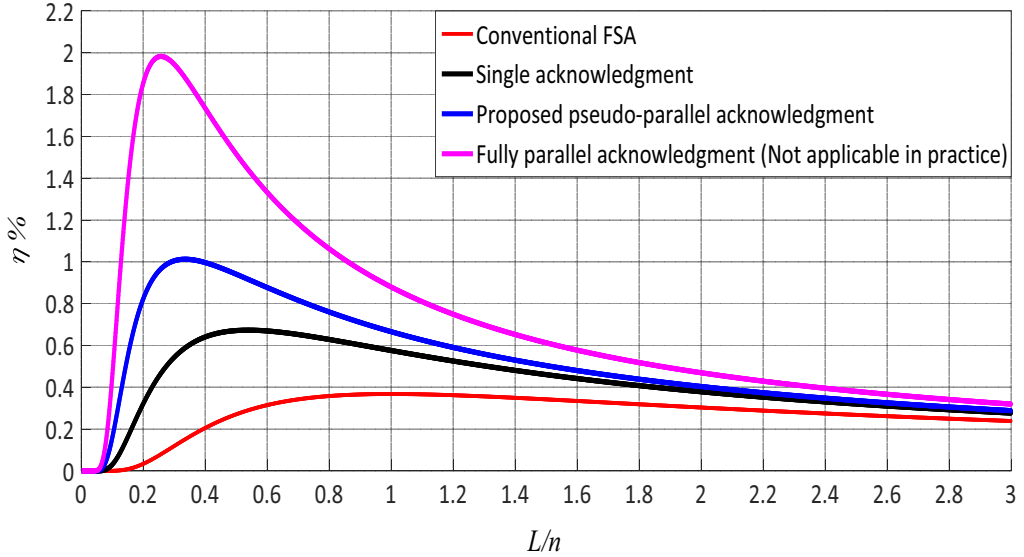


Figure 6.8: Average FSA reading efficiency η for the conventional FSA and different acknowledgment scenarios using 8-orthogonal pilots as a function of the normalized frame length L/n .

Then, it broadcasts the “Switch” command to make the existing tags switch to the new mode. The conventional tags don’t recognize this command, so they ignore it. Afterwards, the reader sends the “Query” command asking the tags to reply with their *RN16s*. Figure 6.7b presents the tag reply (up link) communication. As shown in figure 6.7b, the proposed tag reply starts with 4 bits zeros used for synchronization followed by 8 bits (one of the orthogonal pilots in table 6.1). In this example the tag replies with P_{18} . It is followed by the 6 bits preamble. Finally, the tag replies with its *RN16*. The system is tested in a mixed network between the conventional and the proposed tags. The *RN16* of the conventional and proposed tags were identified successfully.

The performance analysis is achieved through Monte Carlo simulations. Figure 6.8 shows a comparison between the reading efficiency of the conventional FSA and the different acknowledgment scenarios using the 8 orthogonal pilot sequences. The first scenario is the fully parallel acknowledgment scenario, which is proposed by [90]. This system assumes fully parallel acknowledgment for all recovered tags. It results in 200 % maximum reading efficiency. This means that, two tags, on average, are identified per classical slot. However, this method is not compatible with the EPCglobal C1 G2 standard and can not be applied in practice, because it produces a collision in the tag side. The second scenario uses only single acknowledgment system. It acknowledges only a single tag and neglect the other tags replies. It results in 67 % maximum reading efficiency. This system does not benefit from the strong collision recovery

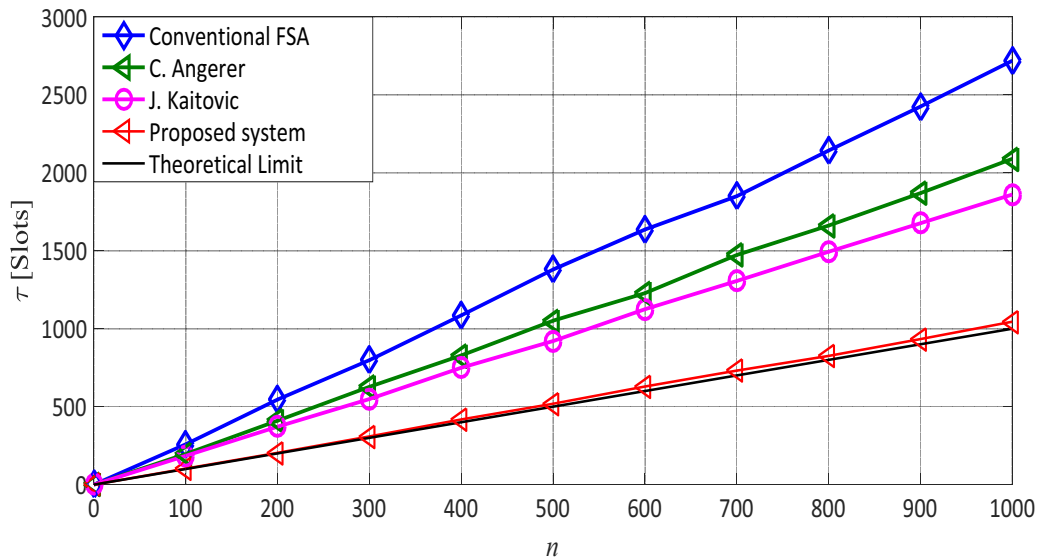


Figure 6.9: Comparison between the average reading time τ as a function of the number of tags in the reading area n for different systems.

capability of the reader. The third one is the proposed pseudo-parallel successful slot. This system compromises between the single tag acknowledgment and the fully parallel acknowledgment. It results in 100% maximum reading efficiency. This means that it approaches the theoretical lower reading time limit of the EPCglobal C1 G2 standard [11].

Figure 6.9 shows the average reading time of the proposed system compared to the conventional FSA and other recent EPCglobal C1 G2 compatible systems using collision recovery techniques. According to figure 6.9, the average reading time of the proposed system is decreased compared to the conventional FSA by 60%. In [79], the authors proposed a collision recovery system that is able to recover up to two collided tags. Accordingly, the average reading time of the proposed system is lower than the reading time of [79] and [94] by 50% and 35%, respectively. Finally, the proposed system approaches the theoretical limit of the EPCglobal C1 G2 standard [11].

Chapter 7

Conclusions and Future Work

Nowadays, there is a great interest in RFID due to the number of applications used in this field. RFID systems provide low cost and low power object identification and tracking mechanisms. It is the key requirement for different ultra-dense applications, e.g., logistics, access management and timing sports events. In such applications, a dense number of tags is expected, which requires fast identification.

The main goal of this thesis is to increase the system throughput and to identify tags faster in the reader range. The transmission of tags is scheduled on the MAC layer with an anti-collision protocol called DFSA. The identification time directly depends on the DFSA reading efficiency anti-collision protocol. The DFSA reading efficiency is controlled by two main parameters, the accuracy of number of tags estimation algorithm and the frame length optimization. The PHY layer of the modern RFID receivers has been improved. Modern RFID receivers have a collision recovery capability, which means that some of collided slots can be converted to successful slots. This capability reduces the losses from the collided slots. Moreover, modern RFID receivers have the capability to identify the type of slot and terminate it as soon as it recognizes that it is not a successful slot. This capability reduces the losses from the empty slots.

The main focus of this thesis is to optimize the DFSA anti-collision algorithm taking into consideration the PHY layer parameters, e.g., the collision recovery capability and the differences in slots durations. Thus, the thesis aims to establish and propose advanced algorithms to increase the performance of the system. Since the work is focused on passive UHF RFID systems, which employ simple tags with in-complex operations. Thus, the proposed changes and algorithms are performed on the reader side except in chapter 6, a new compatible changes of EPCglobal C1 G2 standard are proposed.

7.1 Conclusions

The advanced RFID readers, which are proposed in this thesis decrease the mean average of the FSA reading time. They incorporate different PHY layer parameters in order to efficiently optimize the MAC anti-collision protocols. The first three chapters give an introduction to the UHF RFID systems, where the motivation of the work is discussed. Chapter 4 presents a novel closed form solution for a collision recovery aware ML estimator, which considers the effects of the collision recovery probability of the RFID reader. The theoretical derivations lead to a new analytical estimator that can be easily implemented in RFID readers. Using the proposed formula, neither look-up tables nor numerical searching is used. Furthermore, the estimator gives more precise relative number of tags estimation error compared to the existing state-of-art proposals. Moreover, the proposed estimation algorithm reduces the total identification time by $\simeq 10\%$ compared to the existing state-of-the-art solutions.

With the sole optimization of number of tags estimation, there is still a room of improvement between the proposed algorithm and the theoretical lower identification time limit for the FSA by $\simeq 30\%$. In this regards, chapter 5 presents different proposals of FSA frame length optimization. The first proposal is called “Time aware frame length” frame length. In this proposal, the frame length considers only the difference in slots durations and no collision recovery effect is considered. A closed form solution for the optimum frame length is analytically derived. The proposed solution achieves 8% average saving in reading time compared to the conventional FSA with frame length $L = n$. The second proposal is called “Multiple collision recovery aware” frame length. This proposal considers the differences between the collision recovery coefficients. Thus, it considers that the collision recovery capability strongly depends on the number of the collided tags. However, this proposal assumes constant slots durations regardless the slot type. A closed form solution for the optimum frame length is analytically derived. The proposed solution results in 12% average saving in reading time compared to the conventional FSA with frame length $L = n$. The third proposal is “Time and constant collision recovery coefficients aware” frame length. In this proposal, the frame length considers the time differences in slots durations and the collision recovery capability of the receiver. However, it assumes that the receiver has a constant collision recovery capability regardless the number of collided tags. A closed form solution is analyzed for the frame length. The proposed solution results in 18% average saving in reading time compared to the conventional FSA with frame length $L = n$. Finally, the fourth proposal is “Time and multiple collision recovery aware” frame length. This proposal considers the differences in slots durations and the variable collision recovery coefficients. A closed form solution is analyzed for the frame length. The proposed solution results in 22% average saving

in reading time compared to the conventional FSA with frame length $L = n$. For the proposed systems, there is still $\simeq 10\%$ room of improvement between the best proposed system and the theoretical limit of the EPCglobal C1 G2 standard [11]. The main reason of this is that, the allowed optimization was only in the reader side. To follow the EPCglobal C1 G2 standard [11], the tags could not be modified.

In chapter 6, compatible improvements of the EPCglobal C1 G2 standard are proposed. It presents some modifications on the communication signal of Tag/reader. Using these modifications, the new system approaches the theoretical lower reading time limit of the EPCglobal C1 G2 standard. The proposed system is compatible with the EPCglobal C1 G2 standard, i.e. the proposed tags could be jointly operated with conventional tags and identified by conventional readers without affecting the performance. Additionally, conventional tags can also be operated together with the proposed tags and can be identified by the proposed reader.

7.2 Open Issues and Future Work

Despite the effort invested in this dissertation, there are still some remaining issues left that require further investigations. For instance, the influence of the initial frame length of the proposed system is neglected. However, it should be analyzed. In addition, the MAC layer knowledge of the current SNR should send a feedback signal to the PHY layer. In this signal, the MAC layer decides to start resolving the current collided slot either to a successful or unsuccessful slot, depending on the current value of the SNR. Thereby, if the current SNR value is below a certain threshold, it might be better to leave this slot to a normal collided slot. On the other hand, when the current value of the SNR is above this threshold, it would be better to resolve this collided slot to a successful slot. Finally, a practical assessment of the proposed work through measurements would be beneficial for a more comprehensive evaluation.

List of Abbreviations

ACK	Acknowledgment
CDMA	Code Division Multiple Access
CW	Continuous Wave
DFSA	Dynamic Frame Slotted ALOHA
EPC	Electronic Product Code
FDMA	Frequency Division Multiple Access
FSA	Framed Slotted ALOHA
FSA	Framed Slotted ALOHA
HF	High Frequency
LF	Low Frequency
MAC	Medium Access Control
ML	Maximum Likelihood
MMSE	Minimum Mean-Square Error
MSE	Minimum Squared Error
PER	Packet Error Rate
RFID	Radio Frequency Identification
RN16	Random Number 16
SA	Slotted ALOHA
SDMA	Space Division Multiple Access
SNR	Signal to Noise Ratio

100

TDMA	Time Division Multiple Access
UHF	Ultra High Frequency
USRP	Universal Software Defined Radio Peripheral
ZF	Zero Forcing

List of Symbols

α	Collision recovery probability
α_2	Second collision recovery coefficient
α_3	Third collision recovery coefficient
α_4	Fourth collision recovery coefficient
η_{TA}	Time-Aware reading efficiency
η_{conv}	Conventional FSA reading efficiency
η_{MCRC}	Multiple collision recovery aware reading efficiency
η_{TAMCRC}	Time and multiple collision recovery aware reading efficiency
η_{TCA}	Time and collision recovery aware reading efficiency
γ	Mean of Poisson random variable
\hat{n}	Estimated number of tags
ε_{conv}	Minimum squared error estimator
φ	Pseudo parallel factor
ζ	Mean reduction in number of slots
ζ_t	Mean reduction in reading time
BLF	Backscatter Link Frequency
C	Number of collided slots
c	Q-slot constant
c_1	Collided slot count selection constant
c_2	Empty slot count selection constant

C_b	Number of collided slots before the collision recovery
c_c	Collided Q-slot constant
c_e	Empty Q-slot constant
C_t	Slot duration constant
C_{exp}	Expected number of collided slots
C_{rate}	Estimated collision rate
DR	Divided Ratio
E	Number of empty slots
E_b	Number of empty slots before the collision recovery
E_{exp}	Expected number of empty slots
f_s	Sampling frequency
L	Frame Slotted ALOHA frame length
L_{MCRC}	Multiple collision recovery aware frame length
L_{opt}	Optimum FSA frame length
L_{TAMCRC}	Time and multiple collision recovery aware frame length
L_{TA}	Time aware frame length
L_{TCA}	Time and collision recovery aware frame length
M	Number of collided tags per slot
n	number of tags in the reading area
n_p	Number of pilot tones
$P(i)$	Probability of i tag rely per slot
$P(R)$	Probability that exactly R tags are active in one slot
P_c	Probability of collided slot
P_e	Probability of empty slot
P_s	Probability of successful slot

$P_{S_l}(R)$	Probability that scenario S_l happens
Q_{ini}	Slot count parameter
R_{sol}	Number of recovered tags
S	Number of successful slots
S_b	Number of successful slots before the collision recovery
S_{exp}	Expected number of successful slots
t_c	Collided slot durations
t_e	Empty slot durations
t_s	Successful slot durations
T_{EPC}	EPC time
T_{QRep}	Query repeat time
T_{RN16}	RN16 time

List of Own Publications

1. H. A. Ahmed, H. Salah, J. Robert, A. Heuberger, "A Closed-Form Solution for ALOHA Frame Length Optimizing Multiple Collision Recovery Coefficients' Reading Efficiency," in IEEE Systems Journal , IEEE Early Access Articles
2. H. Salah, H. A. Ahmed, J. Robert and A. Heuberger, "A Time and Capture Probability Aware Closed Form Frame Slotted ALOHA Frame Length Optimization," in IEEE Communications Letters, vol. 19, no. 11, pp. 2009-2012, Nov. 2015.
3. H. Salah, H. A. Ahmed, J. Robert and A. Heuberger, "Multi-Antenna UHF RFID Reader Utilizing Stimulated Rate Tolerance," in IEEE Journal of Radio Frequency Identification, vol. 1, no. 2, pp. 124-134, June 2017.
4. H. Salah, H. A. Ahmed, Joerg Ropert, and Albert Heuberger, "Performance Evaluation of Rate Estimation for UHF RFID Systems," in International Journal of RF Technologies, vol. 7, no. 2-3, pp. 87-104, Nov. 2016
5. H. A. Ahmed, H. Salah, J. Robert and A. Heuberger, "Time aware closed form frame slotted ALOHA frame length optimization," in IEEE Wireless Communications and Networking Conference, Doha, pp. 1-5, Oct. 2016.
6. H. A. Ahmed, H. Salah, J. Robert and A. Heuberger, "A closed form solution for frame slotted ALOHA utilizing time and multiple collision recovery coefficients," in IEEE Topical Conference on Wireless Sensors and Sensor Networks (WiSNet), Austin, TX, pp. 11-14, Apr 2016.
7. H. A. Ahmed, H. Salah, J. Robert and A. Heuberger, "An Efficient RFID Tag Estimation Method Using Biased Chebyshev Inequality for Dynamic Frame Slotted ALOHA," in Smart SysTech, European Conference on Smart Objects, Systems and Technologies, Dortmund, Germany, pp. 1-4, Sept 2014.

8. H. Salah, H. A. Ahmed, J. Robert and A. Heuberger, "A Study of Software Defined Radio Receivers for Passive RFID Systems," in Smart SysTech, European Conference on Smart Objects, Systems and Technologies, Dortmund, Germany, pp. 8-11, Sept 2014.
9. H. A. Ahmed, H. Salah, J. Robert and A. Heuberger, "A New Optimization Criteria For Frame Slotted ALOHA Utilizing Time And The Collision Recovery Coefficients," in Smart SysTech, European Conference on Smart Objects, Systems and Technologies, Aachen, Germany, pp. 1-4, Sept 2015.
10. H. Salah, H. A. Ahmed, J. Robert and A. Heuberger, "FFT Based Rate Estimation for UHF RFID Systems," in Smart SysTech, European Conference on Smart Objects, Systems and Technologies, Aachen, Germany, pp. 10-15, Sept 2015.
11. H. A. Ahmed, H. Salah, J. Robert and A. Heuberger, "Backwards compatible improvement of the EPCglobal class 1 gen 2 standard," in IEEE International Conference on RFID Technology and Applications (RFID-TA), Tokyo, pp. 114-119, Sept. 2015.
12. H. A. Ahmed, H. Salah, J. Robert and A. Heuberger, "A closed form solution for frame slotted ALOHA utilizing time and multiple collision recovery coefficients," in IEEE Topical Conference on Wireless Sensors and Sensor Networks (WiSNet), Austin, TX, pp. 11-14, Jan. 2016.
13. H. Salah, H. A. Ahmed, J. Robert and A. Heuberger, "Maximum Likelihood decoding for non-synchronized UHF RFID tags," in IEEE Topical Conference on Wireless Sensors and Sensor Networks (WiSNet), Austin, TX, pp. 89-92, Jan 2016.
14. H. A. Ahmed, H. Salah, J. Robert and A. Heuberger "A Closed Form Solution For Collision Recovery Aware Number of Tags Estimation", Submitted to IEEE Journal of Radio Frequency Identification.

Bibliography

- [1] R. Want, “An introduction to RFID technology,” *IEEE Pervasive Computing*, vol. 5, pp. 25–33, Jan 2006.
- [2] N. C. Karmakar, *RFID ReadersReview and Design*, pp. 83–121. Wiley-IEEE Press, Oct 2010.
- [3] N. Raza, V. Bradshaw, and M. Hague, “Applications of RFID technology,” in *IEE Colloquium on RFID Technology*, pp. 1–5, 1999.
- [4] S. Piramuthu and Y.-J. Tu, “Improving accuracy of RFID tag identification,” in *International Conference on Information and Communication Technology in Electrical Sciences*, pp. 692–696, Dec 2007.
- [5] H. E. Matbouly, K. Zannas, Y. Duroc, and S. Tedjini, “Analysis and Assessments of Time Delay Constraints for Passive RFID Tag-Sensor Communication Link: Application for Rotation Speed Sensing,” in *IEEE Sensors Journal*, vol. 17, pp. 2174–2181, Apr 2017.
- [6] A. Habib, M. A. Afzal, H. Sadia, Y. Amin, and H. Tenhunen, “Chipless RFID tag for IoT applications,” in *IEEE 59th International Midwest Symposium on Circuits and Systems*, pp. 1–4, Oct 2016.
- [7] H. Ma, Y. Wang, K. Wang, and Z. Ma, “The Optimization for Hyperbolic Positioning of UHF Passive RFID Tags,” in *IEEE Transactions on Automation Science and Engineering*, vol. 1, pp. 1–11, 2017.
- [8] N. Ayer and D. W. Engels, “Evaluation of ISO 18000-6C artifacts,” in *IEEE International Conference on RFID*, pp. 123–130, Apr 2009.
- [9] S. R. Aroor and D. D. Deavours, “Evaluation of the State of Passive UHF RFID: An Experimental Approach,” in *IEEE Systems Journal*, vol. 1, pp. 168–176, Dec 2007.
- [10] X. Yang, L. Meng, F. Yu, L. Yang, Q. Wu, J. Su, J. Lu, and G. Li, “Design and Test of a RFID UHF Tag,” in *Pacific-Asia Conference on Circuits, Communications and Systems*, pp. 346–349, May 2009.

- [11] “EPC radio-frequency protocols class-1 generation-2 UHF RFID protocol for communications at 860 MHz 960 MHz version 1.1.0 2006.”
- [12] S. q. Geng, D. m. Gao, C. Zhu, M. He, and W. c. Wu, “An improved dynamic framed slotted ALOHA algorithm for RFID anti-collision,” in *9th International Conference on Signal Processing*, pp. 2934–2937, Oct 2008.
- [13] S.-R. Lee, S.-D. Joo, and C.-W. Lee, “An enhanced dynamic framed slotted ALOHA algorithm for RFID tag identification,” in *The Second Annual International Conference on Mobile and Ubiquitous Systems: Networking and Services*, pp. 166–172, Jul 2005.
- [14] F. Ricciato and P. Castiglione, “Pseudo-Random ALOHA for Enhanced Collision-Recovery in RFID,” in *IEEE Communications Letters*, vol. 17, pp. 608–611, Mar 2013.
- [15] L. Fu, L. Liu, M. Li, and J. Wang, “Collision recovery receiver for EPC Gen2 RFID systems,” in *3rd IEEE International Conference on the Internet of Things*, pp. 114–118, Oct 2012.
- [16] D. D. Donno, V. Lakafosis, L. Tarricone, and M. M. Tentzeris, “Increasing performance of SDR-based collision-free RFID systems,” in *IEEE International Microwave Symposium Digest*, pp. 1–3, Jun 2012.
- [17] H. Mahdavifar and A. Vardy, “Coding for tag collision recovery,” in *IEEE International Conference on RFID*, pp. 9–16, Apr 2015.
- [18] D. Harris, “Radio transmission system with modulatable passive responder,” *US. Patent*, 2927321, 1960.
- [19] W. Charles, “Portable radio frequency emitting identifier,” *US. Patent* 4384288, 1973.
- [20] F. Vernon, “Applications of the microwave homodyne,” in *Journal of Transactions of the IRE Professional Group on Antennas and Propagation*, vol. 4, pp. 110–116., Oct 1952.
- [21] A. Cerino and W. P. Walsh, “Research and application of radio frequency identification (RFID) technology to enhance aviation security,” in *the IEEE National Aerospace and Electronics Conference*, pp. 127–135, 2000.
- [22] M. Kossel, H. Benedickter, and W. Baechtold, “An active tagging system using circular polarization modulation,” in *IEEE International Microwave Symposium Digest*, vol. 4, pp. 1595–1598, Jun 1999.

- [23] W. Che, Y. Yang, C. Xu, N. Yan, X. Tan, Q. Li, H. Min, and J. Tan, “Analysis, design and implementation of semi-passive Gen2 tag,” in *IEEE International Conference on RFID*, pp. 15–19, Apr 2009.
- [24] A. Janek, C. Steger, R. Weiss, J. Preishuber-Pfluegl, and M. Pistauer, “Lifetime extension of semi-passive UHF RFID tags using special power management techniques and energy harvesting devices,” in *AFRICON*, pp. 1–7, Sept 2007.
- [25] K. V. S. Rao, “An overview of backscattered radio frequency identification system (RFID),” in *Microwave Conference, Asia Pacific*, vol. 3, pp. 746–749, Oct 1999.
- [26] D. Friedman, H. Heinrich, and D. W. Duan, “A low-power CMOS integrated circuit for field-powered radio frequency identification tags,” in *IEEE International Solids-State Circuits Conference. Digest of Technical Papers*, pp. 294–295, Feb 1997.
- [27] J. Garcia, A. Arriola, F. Casado, X. Chen, J. I. Sancho, and D. Valderas, “Coverage and read range comparison of linearly and circularly polarised radio frequency identification ultra-high frequency tag antennas,” in *IET Microwaves, Antennas Propagation*, vol. 6, pp. 1070–1078, Jun 2012.
- [28] M. A. Islam and N. Karmakar, “A linearly polarized (LP) reader antenna for LP and orientation insensitive (OI) chipless RFID tags,” in *9th International Conference on Electrical and Computer Engineering*, pp. 431–434, Dec 2016.
- [29] L. Shafai and K. Antoszkiewicz, “Circular polarized antennas employing linearly polarized radiators,” in *Symposium on Antenna Technology and Applied Electromagnetics*, pp. 1–4, Aug 1988.
- [30] N. Usami and A. Hirose, “Proposal of wideband reconfigurable circular-polarized single-port antenna,” in *Asia-Pacific Microwave Conference*, pp. 34–36, Nov 2014.
- [31] T. Jiayin, H. Yan, and M. Hao, “A novel baseband-processor for LF RFID tag,” in *7th International Conference on ASIC*, pp. 870–873, Oct 2007.
- [32] M.-W. Seo, Y.-C. Choi, Y.-H. Kim, and H.-J. Yoo, “A 13.56MHz receiver SoC for multi-standard RFID reader,” in *IEEE International Conference on Electron Devices and Solid-State Circuits*, pp. 1–4, Dec 2008.
- [33] M. Hirvonen, N. Pesonen, O. Vermesan, C. Rusu, and P. Enoksson, “Multi-system, multi-band RFID antenna: Bridging the gap between HF- and

- UHF-based RFID applications,” in *European Conference on Wireless Technology*, pp. 346–349, Oct 2008.
- [34] D. W. Engels and S. E. Sarma, “The reader collision problem,” in *IEEE International Conference on Systems, Man and Cybernetics*, vol. 3, pp. 6–9, Oct 2002.
 - [35] J. Waldrop, D. W. Engels, and S. E. Sarma, “Colorwave: an anticollision algorithm for the reader collision problem,” in *IEEE International Conference on Communications*, vol. 2, pp. 1206–1210, May 2003.
 - [36] D. Wang, J. Wang, and Y. Zhao, “A Novel Solution to the Reader Collision Problem in RFID System,” in *International Conference on Wireless Communications, Networking and Mobile Computing*, pp. 1–4, Sept 2006.
 - [37] J. Ho, D. W. Engels, and S. E. Sarma, “HiQ: a hierarchical Q-learning algorithm to solve the reader collision problem,” in *International Symposium on Applications and the Internet Workshops*, pp. 4–9, Jan 2006.
 - [38] N. Li, X. Duan, Y. Wu, S. Hua, and B. Jiao, “An Anti-Collision Algorithm for Active RFID,” in *International Conference on Wireless Communications, Networking and Mobile Computing*, pp. 1–4, Sept 2006.
 - [39] V. Pillai, R. Martinez, J. Bleichner, K. Elliot, S. Ramamurthy, and K. V. S. Rao, “A technique for simultaneous multiple tag identification,” in *Fourth IEEE Workshop on Automatic Identification Advanced Technologies*, pp. 35–38, Oct 2005.
 - [40] L. C. Wang and H. C. Liu, “A Novel Anti-Collision Algorithm for EPC Gen2 RFID Systems,” in *3rd International Symposium on Wireless Communication Systems*, pp. 761–765, Sept 2006.
 - [41] L. Liu and S. Lai, “ALOHA-Based Anti-Collision Algorithms Used in RFID System,” in *International Conference on Wireless Communications, Networking and Mobile Computing*, pp. 1–4, Sept 2006.
 - [42] H. C. Liu and J.-P. Ciou, “Performance analysis of multi-carrier RFID systems,” in *International Symposium on Performance Evaluation of Computer Telecommunication Systems*, vol. 41, pp. 112–116, Jul 2009.
 - [43] J. Yu, K. Liu, and G. Yan, “A Novel RFID Anti-Collision Algorithm Based on SDMA,” in *4th International Conference on Wireless Communications, Networking and Mobile Computing*, pp. 1–4, Oct 2008.
 - [44] L. C. Wuu, Y. J. Chen, C. H. Hung, and W. C. Kuo, “Zero-Collision RFID Tags Identification Based on CDMA,” in *Fifth International Conference on Information Assurance and Security*, vol. 1, pp. 513–516, Aug 2009.

- [45] C. Zhai, Z. Zou, Q. Chen, L. Zheng, and H. Tenhunen, “Optimization on guard time and synchronization cycle for TDMA-based deterministic RFID system,” in *IEEE International Conference on RFID Technology and Applications*, pp. 71–75, Sept 2015.
- [46] J. Myung, W. Lee, J. Srivastava, and T. Shih, “Tag-Splitting: Adaptive Collision Arbitration Protocols for RFID Tag Identification,” in *IEEE Transactions on Parallel and Distributed Systems*, vol. 18, pp. 763–775, Oct 2007.
- [47] R. Hush and C. Wood, “Analysis of Tree Algorithms for RFID Arbitration,” in *IEEE International Symposium on Information Theory*, pp. 44–47, Oct 1998.
- [48] A. E. M.Jacomet and U. Gehrig, “Contactless identification device with anticollision algorithm,” in *IEEE Computer Society, Conference on Circuits, Systems, Computers and Communications*, Sept 1999.
- [49] J. Park, M. Y. Chung, and T.-J. Lee, “Identification of RFID Tags in Framed-Slotted ALOHA with Tag Estimation and Binary Splitting,” in *First International Conference on Communications and Electronics*, pp. 368–372, Sept 2006.
- [50] A. Leon-Garcia and I. Widjaja, *Communication Networks: Fundamental Concepts and Key Architectures*. McGraw-Hill Press, Boston, 1996.
- [51] J. E. Wieselthier, A. Ephremides, and L. A. Michaels, “An exact analysis and performance evaluation of framed ALOHA with capture,” in *IEEE Transactions on Communications*, vol. 37, pp. 125–137, Feb 1989.
- [52] F. Schoute, “Dynamic Frame Length ALOHA,” in *IEEE Transactions on Communications*, vol. 31, pp. 565–568, Apr 1983.
- [53] A. Zanella, “Estimating Collision Set Size in Framed Slotted Aloha Wireless Networks and RFID Systems,” in *IEEE Communications Letters*, vol. 16, pp. 300–303, Mar 2012.
- [54] H. Vogt, “Efficient object identification with passive RFID tags,” in *International Conference on Pervasive Computing*, Zürich, pp. 18–21, Aug 2002.
- [55] L. Zhu and T. Yum, “Optimal Framed Aloha Based Anti-Collision Algorithms for RFID Systems,” in *IEEE Transactions on Communications*, vol. 58, pp. 3583–3592, Dec 2010.

- [56] H. Vogt, "Multiple object identification with passive RFID tags," in *IEEE International Conference on Systems, Man and Cybernetics*, vol. 3, pp. 6–9, Oct 2002.
- [57] X. Yang, H. Wu, Y. Zeng, and F. Gao, "Capture-Aware Estimation for the Number of RFID Tags with Lower Complexity," in *IEEE Communications Letters*, vol. 17, pp. 1873–1876, Oct 2013.
- [58] B. Li and J. Wang, "Efficient Anti-Collision Algorithm Utilizing the Capture Effect for ISO 18000-6C RFID Protocol," *Communications Letters, IEEE*, vol. 15, pp. 352–354, Mar 2011.
- [59] D. Donno, L. Tarricone, L. Catarinucci, V. Lakafosis, and M. Tentzeris, "Performance enhancement of the RFID epc gen2 protocol by exploiting collision recovery," in *Electromagnetics Research Progress*, vol. 43, pp. 53–72, Sept 2012.
- [60] A. Bui, C. Nguyen, T. Hoang and A. Pham, "Tweaked query tree algorithm to cope with capture effect and detection error in RFID systems," in *International Conference on Communications, Management and Telecommunications*, pp. 46–51, Dec 2015.
- [61] M. Nemati, H. Takshi, and V. Shah-Mansouri, "Tag estimation in RFID systems with capture effect," in *23rd Iranian Conference on Electrical Engineering*, pp. 368–373, May 2015.
- [62] S. Choi, J. Choi, and J. Yoo, "An efficient anti-collision protocol for tag identification in RFID systems with capture effect," in *Fourth International Conference on Ubiquitous and Future Networks*, pp. 482–483, Jul 2012.
- [63] Ettus Research, "USRP B210." <http://www.ettus.com/product/details/UB210-KIT>, retrieved Oct. 2015.
- [64] I. Joe and J. Lee, "A novel anti-collision algorithm with optimal frame size for rfid system," in *International Conference on Software Engineering Research, Management Applications*, pp. 424–428, Aug 2007.
- [65] D. Lee, K. Kim, and W. Lee, ""q+-algorithm: An enhanced rfid tag collision arbitration algorithm", in *International conference of RFID*, pp. 23–32, Dec 2007.
- [66] M. Daneshmand, C. Wang, and K. Sohraby, "A New Slot-Count Selection Algorithm for RFID Protocol," in *Second International Conference on communications and Networking in China*, pp. 926–930, Aug 2007.

- [67] C. Floerkemeier, "Transmission control scheme for RFID object identification," in *Pervasive Wireless Networking Workshop*, pp. 44–47, Oct 2006.
- [68] J.-R. Cha and J.-H. Kim, "Novel Anti-collision Algorithms for Fast Object Identification in RFID System," in *11th International Conference on Parallel and Distributed Systems*, vol. 2, pp. 63–67, Jul 2005.
- [69] J.-R. Cha and J.-H. Kim, "Dynamic framed slotted ALOHA algorithms using fast tag estimation method for RFID system," in *Consumer Communications and Networking Conference*, vol. 772, pp. 314–317, 2006.
- [70] B. S. Wang, Q. S. Zhang, D. K. Yang, and J. S. Di, "Transmission Control Solutions Using Interval Estimation Method for EPC C1G2 RFID Tag Identification," in *International Conference on Wireless Communications, Networking and Mobile Computing*, pp. 2105–2108, Sept 2007.
- [71] W.-T. Chen, "An Accurate Tag Estimate Method for Improving the Performance of an RFID Anticollision Algorithm Based on Dynamic Frame Length ALOHA," in *IEEE Transactions on Automation Science and Engineering*, vol. 6, pp. 9–15, Jan 2009.
- [72] E. Vahedi, V. Wong, I. Blake, and R. Ward, "Probabilistic analysis and correction of chen's tag estimate method," in *IEEE Transactions on Automation Science and Engineering*, vol. 8, pp. 659–663, Jul 2011.
- [73] M. Kodialam and T. Nandagopal, "Fast and reliable estimation schemes in RFID systems," in *12th annual international conference on Mobile computing and networking*, pp. 322–333, Apr 2006.
- [74] P. Solic, J. Radic, and N. Rozic, "Linearized combinatorial model for optimal frame selection in gen2 rfid system," in *IEEE International Conference on RFID*, pp. 89–94, Apr 2012.
- [75] P. Harremoes, "Binomial and Poisson distributions as maximum entropy distributions," in *IEEE Transactions on Information Theory*, vol. 47, pp. 2039–2041, Jul 2001.
- [76] G. V. Weinberg, "Bit error rate approximations using Poisson and negative binomial sampling distributions," in *Electronics Letters*, vol. 44, pp. 217–219, Jan 2008.
- [77] H. Salah, H. Ahmed, J. Robert, and A. Heuberger, "A Time and Capture Probability Aware Closed Form Frame Slotted ALOHA Frame Length Optimization," in *IEEE Communications Letters*, vol. 19, pp. 2009–2012, Nov 2015.

- [78] D. Struik, *A Source Book in Mathematics 1200-1800*. Princeton University Press, 1986.
- [79] C. Angerer, R. Langwieser, and M. Rupp, “RFID Reader Receivers for Physical Layer Collision Recovery,” in *IEEE Transactions on Communications*, vol. 58, pp. 3526–3537, Dec 2010.
- [80] T. Sansanayuth, P. Suksompong, C. Chareonlarpnopparut, and A. Taparugssanagorn, “RFID 2D-localization improvement using modified LANDMARC with linear MMSE estimation,” in *13th International Symposium on Communications and Information Technologies*, pp. 133–137, Sept 2013.
- [81] H. Wu and Y. Zeng, “Bayesian Tag Estimate and Optimal Frame Length for Anti-Collision Aloha RFID System,” in *IEEE Transactions on Automation Science and Engineering*, vol. 7, pp. 963–969, Oct 2010.
- [82] W. J. Shin and J. G. Kim, “A capture-aware access control method for enhanced RFID anti-collision performance,” *IEEE Communications Letters*, vol. 13, pp. 354–356, May 2009.
- [83] X. Xu, L. Gu, J. Wang, G. Xing, and S.-C. Cheung, “Read More with Less: An Adaptive Approach to Energy-Efficient RFID Systems,” in *IEEE Journal on Selected Areas in Communications*, vol. 29, pp. 1684–1697, Sept 2011.
- [84] J. Alcaraz, J. Vales-Alonso, E. Egea-Lopez, and J. Garcia-Haro, “A Stochastic Shortest Path Model to Minimize the Reading Time in DFSA-Based RFID Systems,” in *IEEE Communications Letters*, vol. 17, pp. 341–344, Feb 2013.
- [85] G. Khandelwal, A. Yener, K. Lee, and S. Serbetli, “ASAP : A MAC Protocol for Dense and Time Constrained RFID Systems,” in *IEEE International Conference on Communications, 2006. ICC '06.*, vol. 9, pp. 4028–4033, June 2006.
- [86] A. Zanella, “Adaptive batch resolution algorithm with deferred feedback for wireless systems,” in *IEEE Transactions on Wireless Communications*, vol. 11, pp. 3528–3539, Oct 2012.
- [87] D. Liu, Z. Wang, J. Tan, H. Min, and J. Wang, “ALOHA algorithm considering the slot duration difference in RFID system,” in *IEEE International Conference on RFID*, pp. 56–63, Apr 2009.
- [88] H. Wu and Y. Zeng, “Passive RFID Tag Anticollision Algorithm for Capture Effect,” in *IEEE Sensors Journal*, vol. 15, pp. 218–226, Jan 2015.

- [89] A. Mokhtari, mehregan mahdavi, R. E. Atani, and M. Maghsoodi, "Using Capture Effect in DFSA Anti-collision Protocol in RFID Systems According to ISO18000-6C Standard," in *Journal of Mechatronic Systems*, vol. 1, pp. 33–38, Oct 2012.
- [90] J. Kaitovic, R. Langwieser, and M. Rupp, "A smart collision recovery receiver for RFIDs," *EURASIP Journal on Embedded Systems*, no. 1, 2013.
- [91] M. Abramowitz and I. A. Stegun, *Solutions of Quartic Equations*. New York: Dover, 1972.
- [92] J. Kaitovic, M. Simko, R. Langwieser, and M. Rupp, "Channel estimation in tag collision scenarios," in *IEEE International Conference on RFID*, pp. 74–80, Apr 2012.
- [93] Sensor Systems Laboratory. <http://sensor.cs.washington.edu/WISP.html>, retrieved Oct. 2015.
- [94] M. Nabeel, A. Najam, Y. Duroc, and F. Rasool, "Multi-tone carrier technique for signal recovery from collisions in UHF RFID with multiple acknowledgments in a slot," in *9th IEEE International Conference on Emerging Technologies*, pp. 1–5, Dec 2013.